Enclosure 8

Serco Technical Consulting Services,
"A Survey of Steel and Zircaloy Corrosion Data for Use in the SMOGG Gas Generation Model,"
Report No. SA/ENV-0841, Issue 3, August 2010.
(1 paper copy)

serco

bringing service to life

A Survey of Steel and Zircaloy Corrosion Data for Use in the SMOGG Gas Generation Model

Report to the NDA RWMD

Our Reference: SA/ENV–0841 Issue 3

Date: August 2010

Title	A Survey of Steel and Zircaloy Corrosion Data for Use in the SMOGG Gas Generation Model
Customer	NDA RWMD
Customer reference	–
Confidentiality, copyright and reproduction	
File Reference	SMOGG_SteelsCorrosionReport_i3.doc
Report Number	SA/ENV–0841
Report Status	Issue 3

Serco Technical Consulting Services
Culham Science Centre
Abingdon
Oxfordshire
OX14 3ED

Telephone 01635 280385
Facsimile 01635 280389

www.serco.com/technicalservices

Technical Consulting Services is part of Serco Defence, Science and Nuclear, a division of Serco Ltd.

In the areas where this work would be performed, Technical Consulting Services is certified to ISO 9001 (2000) and ISO 14001

	Name	Signature	Date
Author	N.R. Smart and A.R. Hoch	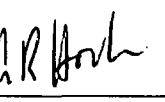	27/08/2010
Reviewed by	B.T. Swift	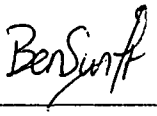	27/08/2010
Approved by	D. Holton		27/08/2010

This report has been prepared by Serco under contract to Nirex and forms part of an ongoing programme of research commissioned by Nirex to underpin the long-term safety of a geological disposal facility for higher-activity radioactive wastes. Before it was published Nirex was subsumed into the NDA.

The report has been reviewed by NDA. However, references to Nirex in the text have been retained as they are appropriate for the period when this research was being performed. The views expressed and the conclusions drawn in this report are those of Serco and do not necessarily represent those of Nirex or the NDA.

Conditions of Publication

Bibliography

If you would like to see other reports available from NDA, a complete listing can be viewed at our website www.nda.gov.uk, or please write to the Library at the address below.

Feedback

Readers are invited to provide feedback to the NDA on the contents, clarity and presentation of this report and on the means of improving the range of NDA reports published. Feedback should be addressed to:

John Dalton,
Head of Communications,
Nuclear Decommissioning Authority (Radioactive Waste Management Directorate),
Curie Avenue,
Harwell Science and Innovation Campus,
Didcot,
Oxon.,
OX11 0RH, UK.

The potential for gas generation from waste packages forms part of the assessment of the safety of geological disposal of intermediate-level and certain low-level radioactive wastes. Gas is expected to be produced by corrosion of metals, radiolysis of materials containing hydrogen (*e.g.* water), and microbial degradation of organic materials.

To address this issue, United Kingdom Nirex Limited commissioned Serco to develop a modelling tool for use in packaging proposal and safety assessment studies. The tool is called SMOGG (Simplified Model of Gas Generation), and considers gas generation from radioactive wastes in the UK National Inventory.

To carry out realistic calculations with SMOGG, it is necessary to parameterise the model with appropriate data for the corrosion rates of metals.

This report identifies the various environments that could be experienced by both containers and cement encapsulated metal wastes during their long-term management and, for each environment, compiles relevant corrosion rate data for carbon steel, stainless steel and Zircaloy from the literature. Where appropriate, these experimental data are used to calibrate the SMOGG corrosion model. Finally, parameters recommended for use in the SMOGG corrosion model for carbon steel, stainless steel and Zircaloy are selected and tabulated.

Executive Summary

The potential for gas generation from waste packages forms part of the assessment of the safety of geological disposal of intermediate-level and certain low-level radioactive wastes. Gas is expected to be produced by corrosion of metals, radiolysis of materials containing hydrogen (*e.g.* water), and microbial degradation of organic materials.

To address this issue, Nirex commissioned Serco to develop a modelling tool for use in packaging proposal and safety assessment studies. The tool is called SMOGG (Simplified Model of Gas Generation), and considers gas generation from radioactive wastes in the UK National Inventory.

To carry out realistic calculations with SMOGG, it is necessary to parameterise the model with appropriate data for the corrosion rates of metals.

Carbon steel, stainless steel and Zircaloy may be present in some cement encapsulated wastes, and containers may be manufactured from stainless steel. These metals will corrode under aerobic and anaerobic alkaline conditions, and will generate hydrogen under anaerobic conditions.

This report identifies the various environments that could be experienced by these encapsulated metal wastes during their long-term management (*i.e.* during surface storage and transportation, and then in a geological repository, both before and after resaturation with a groundwater that could have a high chloride concentration). For each environment, relevant corrosion rate data for carbon steel, stainless steel and Zircaloy were compiled from the literature and reviewed critically. The literature survey focused on metal loss and gas generation as a result of general corrosion rather than localised corrosion (the latter is unlikely to contribute significantly to gas generation). The effects on the corrosion rates of a number of variables (including oxygen concentration, temperature and chloride concentration) were considered.

The main conclusions from this work are as follows:

(a) The possible environmental conditions during radioactive waste management for which corrosion data are required include:
- (humid) gaseous atmospheres, and neutral and alkaline solutions;
- aerobic and anaerobic conditions;
- a range of chloride concentration (up to tens of thousands ppm); and
- a range of temperatures (up to 80°C).

(b) For these environmental conditions, there are corrosion rate data in the literature. However, only a small amount of data is available:
- for all of the metals under atmospheric conditions at elevated temperature; and
- for Zircaloy under all conditions.

(c) Interpretation of the corrosion rate data is required to parameterise a SMOGG model. SMOGG has been calibrated for carbon steel under anaerobic conditions, providing directly applicable parameter values for use in the model. For carbon steel under aerobic conditions, and for stainless steel and Zircaloy, a calibration was not possible. In these cases, parameter values for use in SMOGG were selected based on a direct interpretation of the literature data.

Parameters recommended for use in the SMOGG corrosion model for carbon steel, stainless steel and Zircaloy have been selected and are tabulated.

Tables

1 Introduction

The potential for gas generation from waste packages forms part of the assessment of the safety of geological disposal of intermediate-level (ILW) and certain low-level (LLW) radioactive wastes [1, 2]. Gas is expected to be produced by corrosion of metals, radiolysis of materials containing hydrogen (*e.g.* water), and microbial degradation of organic materials.

To address this issue, United Kingdom Nirex Limited commissioned Serco to develop a modelling tool for use in packaging proposal and safety assessment studies. The tool is called SMOGG (Simplified Model of Gas Generation) [3, 4], and considers gas generation from radioactive wastes in the UK National Inventory.

To carry out realistic calculations with SMOGG, it is necessary to parameterise the model with appropriate data for the corrosion rates of metals.

Carbon steel, stainless steel and Zircaloy may be present in some cement encapsulated wastes, and containers may be manufactured from stainless steel. These metals will corrode under aerobic and anaerobic[1] alkaline conditions, and will generate hydrogen under anaerobic conditions.

This report identifies the various environments that could be experienced by both containers and encapsulated metal wastes during their long-term management (*i.e.* during surface storage and transportation, and then in a geological repository, both before and after re-saturation with a groundwater that could have a high chloride concentration). For each environment, relevant corrosion rate data for carbon steel, stainless steel and Zircaloy were compiled from the literature. The literature survey focused on metal loss and gas generation as a result of general corrosion rather than localised corrosion (the latter is unlikely to contribute significantly to gas generation). The effects on the corrosion rates of a number of variables (including oxygen concentration, temperature and chloride concentration) were considered.

The experimental data are reviewed critically, and, where appropriate, are used to calibrate the SMOGG corrosion model. From this information, parameters recommended for use in the SMOGG corrosion model for carbon steel, stainless steel and Zircaloy are selected.

Section 2 of this report describes the SMOGG corrosion model. The following six sections discuss the corrosion of carbon steel, stainless steel and Zircaloy. Sections 3, 5 and 7 review the corrosion rate data for carbon steel, stainless steel and Zircaloy respectively. Within each of these main sections there are sub-sections giving:

- A summary of information about the corrosion mechanisms for the metal; and
- Corrosion rate data under a range of relevant conditions.

Sections 4, 6 and 8 select the parameters recommended for use in the SMOGG corrosion model for carbon steel, stainless steel and Zircaloy respectively. Where appropriate, the experimental data are used to calibrate the SMOGG corrosion model. Finally, Section 9 summarises the parameters. (A companion report identifies the corrosion rates of the reactive metals Magnox, aluminium and uranium [5].)

This work was prepared by Serco Technical Consulting Services under contract to United Kingdom Nirex Limited (Nirex). The main technical work reported here was carried out initially in the period 1993 to 1997, but the literature review was updated and the data were reassessed in

---

[1] In this report, the terms "aerobic" and "anaerobic" are used interchangeably with "oxic" and "anoxic" respectively.

the period January 2006 to March 2006. The work forms part of the Nirex research programme. The information has been verified under arrangements established by Serco Technical Consulting Services. These arrangements have been approved by Nirex and are consistent with ISO 9001.

The views expressed and the conclusions reached are those of Serco Technical Consulting Services and do not necessarily represent those of Nirex or the NDA.

2 Corrosion Models for Long-term Corrosion

This section begins (see Subsection 2.1) by describing the SMOGG corrosion model for carbon steel, stainless steel and Zircaloy. Next, Subsection 2.2 identifies the various corrosive environments that could be experienced by these metal wastes during their long-term management. Finally, Subsection 2.3 provides a general overview of the literature review described in the subsequent sections.

2.1 SMOGG model

2.1.1 Corrosion reaction stoichiometries

The corrosion reactions for carbon steel, stainless steel and Zircaloy included in SMOGG [3, 4] are listed below.

The metal wastes contain both carbon steel and stainless steel. For the purpose of modelling gas generation these are assumed to corrode according to the same reactions, but at different rates. The simplified reaction[2] stoichiometries considered are:

Aerobic corrosion: $3Fe + 2O_2 \Rightarrow Fe_3O_4$ (2.1)

Anaerobic corrosion: $3Fe + 4H_2O \Rightarrow Fe_3O_4 + 4H_2$ (2.2)

Under some circumstances the final transformation to magnetite (Fe_3O_4) may be kinetically inhibited, and the end product of anaerobic corrosion may be ferrous hydroxide ($Fe(OH)_2$). This subtlety is ignored in SMOGG, as it has only a small effect on the amount of hydrogen released.

Aerobic corrosion of Zircaloy is likely to be slow because Zircaloy forms a strongly adherent oxide layer. Therefore, although it is possible that some corrosion of Zircaloy will take place under aerobic conditions, this is neglected in SMOGG. Zircaloy corrodes under anaerobic conditions. The reaction for zirconium, the main component of Zircaloy, is:

Anaerobic corrosion: $Zr + 2H_2O \Rightarrow ZrO_2 + 2H_2$ (2.3)

2.1.2 Corrosion model

A common feature exhibited by metal corrosion is a relatively high initial corrosion rate, which reduces over time to a long-term steady or slightly decreasing rate. The first phase may be considered as a period of "acute" corrosion and the long-term slower rate of corrosion as a period of "chronic" corrosion. The model implemented in SMOGG [3, 4] allows separate rates of corrosion to be specified for the acute and chronic phases.

---

[2] It is recognised that a range of corrosion products can form on iron under aerated conditions, but for the purposes of the SMOGG model it is not necessary to take these into account because they do not affect the gas generation rate during the subsequent anaerobic corrosion processes.

The rate of movement of the position, s [m], of the surface of the metal is specified as:

$$\frac{ds}{dt} = -k_a e^{-\frac{t}{t_a}} - k_c e^{-\frac{t}{t_c}} \tag{2.4}$$

where

t	is the time during which corrosion is occurring [yr];
k_a	is the initial acute corrosion rate [m yr^{-1}];
t_a	is a characteristic time for the acute corrosion [yr];
k_c	is the initial chronic corrosion rate [m yr^{-1}];
t_c	is a characteristic time for the chronic corrosion [yr].

This formulation provides a smooth transition between the two types of corrosion. Setting the characteristic time for either type of corrosion very large makes the rate for that type of corrosion effectively constant, and of course either rate can be set to zero if only a single rate is required. Note that, formally in the model, acute and chronic corrosion occur simultaneously at all times, but it is expected that the parameters will be chosen such that acute corrosion dominates at short times and chronic corrosion at long times.

Two characteristic metal shapes are allowed, spheres or plates. So s corresponds either to a sphere radius, r, or to a plate surface position, h, taken to be the distance from the mid-plane of the plate. For these two cases, the rates of change of metal volume are

$$\frac{dV_s}{dt} = V_s \frac{3}{r}\frac{dr}{dt} = 4\pi n_s r^2 \frac{dr}{dt} \tag{2.5}$$

and, taking account of the fact that there are two corroding surfaces on a plate,

$$\frac{dV_p}{dt} = A_p\left(\frac{dh_1}{dt} + \frac{dh_2}{dt}\right) \tag{2.6}$$

where

V_s, V_p	are the volumes of metal as spheres and plates respectively [m^3];
n_s	is the number of metal spheres [-];
A_p	is the area of the plane of a metal plate [m^2];
h_1, h_2	are the distances of the two surfaces of the plate from the mid-plane of the plate [m].

A separate category of steel plate is used to represent the stainless steel from which the containers may be manufactured. This is necessary because, during surface storage and transportation, the exterior surface of the containers may be subject to a different environment to the interior; the exterior may be open to the atmosphere at approximately neutral pH, while the interior typically will be exposed to the high pH environment created by an encapsulation grout. Hence different corrosion rates may apply on the outer and inner surfaces of the containers.

The rate of production of hydrogen gas, q_H, is:

$$q_H = -\eta_H \zeta\left(\frac{dV_s}{dt} + \frac{dV_p}{dt}\right) \tag{2.7}$$

where

η_H is a stoichiometric coefficient giving the number of moles of hydrogen produced per mole of the metal corroded;

ζ is the molar density of the metal [mol m^{-3}].

There are equations analogous to Equation (2.7) for the consumption of:

- Oxygen, in the case of carbon steel and stainless steel, during aerobic corrosion; and
- Water during anaerobic corrosion.

During the transport and storage stages of the waste-package lifetime, it is assumed that the waste environment is aerobic. At closure there is a specified amount of oxygen in the vault atmosphere ensuring initially aerobic conditions. Conditions become anaerobic when this is exhausted.

Treatment of the effect of temperature on metal corrosion requires specification of (a) the variation of the temperature over the duration of the calculation, and (b) the dependence of the corrosion rates on temperature. The former is specified by the user in the form of a list of temperature values at a series of successive times. The latter, the temperature dependence of the corrosion rates, is also specified by the user in the form of input tables of corrosion rate versus temperature. Corrosion rates at particular temperatures are obtained by linear interpolation of the data in these tables. The characteristic times are treated as not temperature dependent.

2.1.3 Oxygen and water availability

The corrosion reactions for carbon steel, stainless steel and Zircaloy consume oxygen or water.

The consumption of oxygen is important because its exhaustion controls the transition from aerobic to anaerobic conditions, and the onset of hydrogen production from the less-reactive metals. The corrosion processes also consume or depend on the presence of water. For vented containers (considered to be all ILW and LLW containers), water will be freely available (both inside and outside the container) after resaturation, but in early phases there will be uncertainty about the availability of water.

During transport and storage SMOGG assumes that air flow through the vent ensures the environment in waste containers remains aerobic. This is probably an oversimplification, as it is possible that anaerobic niches may be present in these circumstances. However, as long as the niches are small in size relative to the waste volumes, the assumption of aerobic conditions during these phases is a reasonable assumption overall. Post-closure, when the wastes are isolated from the atmosphere, the oxygen remaining in the vaults at closure has to be consumed before the conditions become anaerobic.

During transport and storage, some water may be present in packages from the initial creation of the waste form. Some water vapour may also diffuse into packages through the vent. Following repository closure, there will be a period of intermediate water saturation in the vaults, en route to full resaturation. During the period of partial saturation, the vault humidity may be at 100%, but it is not clear to what extent gas generating processes in packages into which liquid water has not yet percolated will be inhibited by water shortages. While conditions are aerobic, SMOGG assumes sufficient humidity will be available for the less-reactive metals to corrode. Post-closure, when the oxygen in the vaults is consumed, SMOGG assumes water flows at a constant rate into a package and its associated backfill until they are fully saturated. Water availability is checked during this period of resaturation, and the corrosion reactions are scaled back if consumption exceeds availability.

2.2 Environmental conditions

In order to identify the environments for which corrosion data are required, a summary of the conditions expected to occur on the exterior surface and in the interior of a waste package [6] is given below. The various environments affecting the waste package can be divided into:

- Those pre-backfilling (including filling, storage, transport and emplacement in the repository); and
- Those post-backfilling (including repository closure).

A further distinction is drawn between atmospheric and aqueous (i.e. fully saturated) exposure, since corrosion is different for these two environments.

2.2.1 Conditions pre-backfilling

Atmospheric exposure

The ambient temperature of the atmosphere in contact with the waste container during fabrication, filling, above-ground storage, transport and underground storage will probably be in the range 5°C to 35°C. The internal temperature of the package will be determined by the external temperature and the small amount of heat generated by the waste form. Temperature cycling during storage may cause condensation / evaporation cycles, but radiation-induced heating will tend to counteract this effect. The relative humidity inside the package will be a function of the water content of the wasteform and, if the container is vented, the external relative humidity.

Aqueous exposure

If a concrete liner or internal grout is used, the interior surface of the container, and the waste if it is encapsulated, will be subjected to an aerobic, alkaline, cementitious environment. If a concrete liner and internal grout are not used, and if water is present in the waste, the interior of the package may be exposed to an aerobic, near-neutral[3] environment (or to an aerobic, acidic environment if acidic residues are present in the waste). The pH and chloride concentration will depend on the composition of the waste. During this stage, corrosion will depend on the availability of water. It is possible that localised regions of anoxic conditions could develop within the wasteform as a result of corrosion or microbial activity, although it seems likely that most of the wasteform will remain oxic[4] assuming air can enter through a container vent.

2.2.2 Conditions post-backfilling

After placement, the containers may be surrounded with Nirex Reference Vault Backfill (NRVB), which is an Ordinary Portland Cement (OPC)-based material. When the repository is full the remaining tunnels will be backfilled and the repository closed. In the early years after closure the temperature within some parts of the repository may rise to 80°C, mainly due to chemical reactions such as curing of the backfill. After closure, groundwater will flow back into the repository, resaturating all the excavated and backfilled spaces. The rate of resaturation will depend on the way the repository has been operated, the backfill and the host rock permeabilities, and the regional head gradient. The groundwater is expected to contain very low concentrations of oxygen and therefore will impose anaerobic conditions within the repository. Corrosion and microbial activity also will reduce the oxygen concentration in the repository. The

---

[3] Throughout this report near-neutral/neutral pH refers to a pH in the range 6–8, *i.e.* it does not refer to a pH of exactly 7.

[4] Grouts containing blast furnace slag can develop internal reducing conditions.

inflowing groundwater may contain significant concentrations of chloride ions (up to tens of thousands ppm).

Atmospheric exposure

Initially regions of the package could be exposed to an aerobic atmosphere, from air trapped in voids. These voids will become anaerobic as a result of corrosion or microbial activity.

Aqueous exposure

If a concrete liner or internal grout is used, the interior surface of the container, and the waste if it is encapsulated, will be exposed initially (i.e. after backfilling, but before resaturation) to an aerobic, alkaline (pH 12.5–13) aqueous phase, which may contain chloride. The initial chloride concentration of any aqueous phase will depend on the chloride content of the waste. If a concrete liner and internal grout are not used, and if the waste is not dry, neutral or even acidic solutions could be present initially.

After resaturation, the interior of the package will be exposed to aerobic, alkaline (pH 12.5–13) porewater which has mixed with groundwater. The chloride concentration may increase as the repository resaturates and groundwater enters the container via a gas vent or a corrosion-induced penetration. Eventually the solution will become anaerobic. Once the repository is completely resaturated and anaerobic, the interior of the package will be exposed to an anaerobic, high pH, aqueous phase that may contain high concentrations of chloride ions and a mixture of other inorganic salts.

2.2.3 Summary

In summary, data for the corrosion of carbon steel, stainless steel and Zircaloy are required in:

- Aerobic and anaerobic atmospheric conditions for various chloride deposition rates and temperatures (up to 80°C).
- Aerobic and anaerobic fully immersed conditions for ranges of pH (neutral and alkaline; this report does not consider corrosion at pH values less than 6), chloride concentration and temperature (up to 80°C).

2.3 Introduction to the review of corrosion data

For the purposes of the literature survey only general corrosion has been considered. Localised forms of corrosion, such as pitting and stress corrosion cracking, have largely been ignored, since they are unlikely to contribute significantly to total metal loss or gas generation (although they may result in small areas of corrosion that may lead, for example, to perforation of a container). However carbon steel often exhibits broad, shallow pitting (a type of "localised general corrosion"), which can result in significant metal loss; therefore these data have been included in the review.

Apart from the material properties (*e.g.* composition, metallurgical state, *etc.*) and the presence of moisture, the primary factors determining the corrosion rates of metals are the oxygen concentration and pH at the metal surface. The oxygen concentration at the metal surface depends on the rate of diffusion of oxygen through the surrounding media and whether there are any other restrictions or factors controlling the supply of oxygen (*e.g.* convection currents).

Many other variables affect the corrosion rate of metals under water saturated conditions. These include: the time of exposure, temperature, the concentrations of anions and cations (particularly chloride), the previous history of the surface (*e.g.* whether it is freshly prepared, pre-corroded, or still covered with the mill scale produced during metal production), the formation of surface scale, the physical and chemical properties of the cementitious materials used to encapsulate the waste,

hydrodynamic conditions, the concentrations of dissolved gases (*e.g.* CO_2, H_2S), differential aeration and radiation levels. For atmospheric corrosion, the important parameters include: relative humidity, frequency of wetting (or "time of wetness") and the presence of chloride particulates and sulphur dioxide in the atmosphere.

Some of these variables are interconnected. For example, the solubility of oxygen in a chloride solution depends on the temperature, the chloride concentration, the atmospheric pressure and the concentration of oxygen in the gaseous phase. Furthermore, the corrosion process itself may change the environment at the metal surface, leading to a subsequent change in corrosion rate (*e.g.* corrosion consumes oxygen and changes the pH due to the reduction of oxygen to form hydroxide, and as a result the corrosion rate decreases).

In view of the large number of interconnected variables that could affect the corrosion rate, there will be a range of possible values for each stage of the model. A best-estimate value is selected that is ju dged to relate most closely to the conditions expected in a repository.

Extensive literature searches were carried out in several bibliographic databases (*e.g.* INIS and Corrosion Abstracts). The Dechema corrosion handbooks [7] also contained useful bibliographies, as did some standard text books and reviews [8- 12].

In the literature, corrosion rate data are derived from investigations using both instantaneous and integrated techniques. Instantaneous techniques give a measure of the corrosion rate at any particular time, and include electrochemical methods such as: linear polarisation resistance; Tafel-slope extrapolation; and passive current measurement. They provide a value for the corrosion rate at the time of the measurement. Descriptions of instantaneous techniques may be found in a number of texts, *e.g.* [13] and [14]. Integrated techniques include measurements of dimensional change, weight loss (*e.g.* [15]) or hydrogen evolution (*e.g.* [16, 17]). The total change over a period of time is used to derive the corrosion rate. Instantaneous measurements may give misleadingly high corrosion rates, particularly in systems where a steady corrosion rate is achieved only after a long time.

In general terms, the corrosion rate of carbon steel is higher in acidic solutions and lower in alkaline solutions. This is shown for aerobic conditions in Figure 1. Discussion of the corrosion rates for carbon steel will be subdivided into neutral (Subsection 3.2) and alkaline (Subsection 3.3) solutions, and further subdivided into aerobic and anaerobic conditions.

3.1 Corrosion processes

The following reactions [9] are assumed to occur in oxygenated conditions:

$$4Fe + 6H_2O + 3O_2 \Rightarrow 4Fe(OH)_3$$
$$4Fe + 3O_2 \Rightarrow 2Fe_2O_3 \qquad (3.1)$$

In anaerobic conditions, corrosion is thought to occur according to the reactions [18, 19]:

$$Fe + 2H_2O \Rightarrow Fe(OH)_2 + H_2$$
$$3Fe + 4H_2O \Rightarrow Fe_3O_4 + 4H_2$$
$$3Fe(OH)_2 \Rightarrow Fe_3O_4 + 2H_2O + H_2 \quad \text{(at higher temperatures)} \qquad (3.2)$$

These equations are a simplified view of the complex array of reactions that are likely to occur in practice. A range of corrosion products would be formed under the many combinations of pH, chloride concentration and temperature that would occur during waste management. The remainder of this subsection discusses the composition of the films that are likely to form in the various phases of waste management. The discussion applies to stainless steel as well as to carbon steel. The composition of corrosion products and passive films has been the subject of a large number of publications (*e.g.* [20, 21]) and it is not the intention to provide a comprehensive review here.

An indication of the complex range of oxides and hydroxides that can arise through corrosion in neutral water is shown in Figure 2 [20]. According to this diagram the final reaction product from slow oxidation of iron in aerobic, neutral solutions is magnetite, Fe_3O_4. A multi-layer film containing iron in a range of oxidation states (*e.g.* FeO, Fe_3O_4 and Fe_2O_3) is often found [9]. Measurements by Kalashnikova [22] showed that the stoichiometry of the magnetite corrosion product changed with immersion time in seawater. At higher temperatures both Fe_2O_3 and Fe_3O_4 are formed. Using Mössbauer spectroscopy, Peev [23] identified FeOCl, β-FeOOH and γ-FeOOH in the corrosion products of steel in seawater. Chen [24] also identified green rust ($Fe(OH)_2/Fe(OH)_3$), $Fe(OH)_2$ and $Fe_2(OH)_3Cl$. Sagoe-Crentsil [25] has constructed a stability diagram for iron in cement at pH 12 and temperature 25°C, as a function of chloride concentration (Figure 3). Similarly, Refait [26] has produced a Pourbaix diagram for iron in the presence of chloride, taking account of the green rust phases (Figure 4). Since many groundwaters contain some carbonate alkalinity, it is possible that corrosion product films containing carbonate would also be formed, although, if grout is present, it is likely that most of the carbonate would precipitate out as calcium carbonate before the groundwater reaches the metal surface. Jelinek [18] reported that a two-layer corrosion product formed on iron in de-aerated water. The outer layer was friable and the inner layer was adherent and compact. X-ray diffraction (XRD) analysis identified Fe_3O_4, but there were several other unidentified peaks. Mass spectroscopy of the gas released while heating the corrosion product revealed that hydrogen was trapped in it.

The detailed composition and structure of the passive films formed in alkaline solutions are still a matter of debate, despite much research. It is generally agreed that Fe_2O_3 is a major component, in which Fe_3O_4 and bound water may also be present. The film may have a multi-layer structure, the exact composition of which depends on the electrochemical potential [9, 27]. Several workers

have investigated the reduction of the oxide films using electrochemical techniques. Riley [28], for example, used a galvanostatic technique to reduce the film formed on a NiCrMoV steel at pH 9.2 in de-aerated carbonate-bicarbonate solution at 70°C. By using a ring-disc electrode it was possible to monitor the products of the film reduction in solution. The results supported the concept of a two-layer film composed of an inner layer of Fe_3O_4 and an outer layer of Fe_2O_3. In some experiments the "auto reduction" of the passive film was observed, *i.e.* the film formed in the passive region was allowed to "float" without potential control and the film was observed to dissolve. The following reaction was postulated:

$$Fe \Rightarrow Fe^{2+} + 2e^-$$
$$\gamma\text{-}Fe_2O_3 + 6H^+ + 2e^- \Rightarrow 2Fe^{2+} + 3H_2O \qquad (3.3)$$

Fe^{2+} dissolved from the metal lattice provides electrons that can reduce the ferric ion in the outer layer of the oxide. The "auto reduction" or "reductive dissolution" of a film that had been grown at +0.2V (SCE) took approximately 1 minute and the final rest potential was approximately -0.8V (SCE).

Long-term atmospheric corrosion tests for iron produce corrosion products composed of a range of iron oxides and hydroxides, including α-, β- and γ-FeOOH, γ -Fe_2O_3 and Fe_3O_4 [20]. During wet cycles, the anodic dissolution of iron provides electrons for the reduction of Fe(III) oxides, *viz.*

$$Fe \Rightarrow Fe^{2+} + 2e^-$$
$$Fe^{2+} + 8FeOOH + 2e^- \Rightarrow 3Fe_3O_4 + 4H_2O \qquad (3.4)$$

During dry cycles, when oxygen can permeate the porous corrosion product, the magnetite (Fe_3O_4) is re-oxidised to FeOOH. These reactions involve complex solid-state processes [29, 30]. It should be noted that the dry, re-oxidation step would not be possible in an anaerobic environment.

Reductive dissolution of the oxide film, *i.e.* conversion of Fe(III) oxide to Fe(II) oxide, has been observed in the laboratory for passive films that have been produced by maintaining a positive potential using a potentiostat, and for air-formed films (*e.g.* [31, 32]), but it is not clear whether such reactions can occur for the films formed under repository conditions and, if so, what the kinetics of reaction would be. In some cases, for example corrosion in aerobic neutral conditions or wet atmospheric conditions, the corrosion product may already be in the reduced state, *i.e.* Fe_3O_4.

Research has also been carried out in the Nirex Safety Assessment Research Programme (NSARP) to determine how films formed under one set of conditions affect the corrosion behaviour under a subsequent set of conditions. For example, films formed in the aerobic stage at neutral pH, with low chloride concentrations, may subsequently be exposed under anaerobic conditions to high pH, high chloride conditions as resaturation of the grout occurs. Most published corrosion rate data refer to the corrosion behaviour of freshly prepared metal surfaces. Experiments in the NSARP have shown that aerobically-formed films can delay the onset of hydrogen evolution; this may reflect the time required to allow film reduction to occur.

3.2 Neutral solutions

3.2.1 Aerobic neutral solutions

A summary of data relating to the corrosion of carbon steel in aerobic neutral solutions is given in Table 2; some of the information is shown graphically in Figure 5 to Figure 14.

Considerable bodies of work have been published on corrosion in drinking water, seawater and hot concentrated brines (particularly in relation to the corrosion of HLW waste packaging

materials in hot geological brines, *e.g.* Q-brine, Germany, and Yucca mountain brines, U.S.A.). Other papers report corrosion rate data for a variety of chloride solutions, including simple chloride solutions, minewaters and groundwaters. For comparison the compositions of seawater and other brines for which significant amounts of data have been published are given in Table 1. (It can be seen that the composition of the groundwater from Sellafield Borehole 2 is similar to that of seawater.)

The following subsections review how the corrosion rate depends on the main environmental variables.

(a) Effect of temperature

The temperature can affect the corrosion rate in two main ways. Firstly, an increase in chemical reaction rates, and hence corrosion rate, is to be expected if the temperature is raised. Secondly, the temperature affects the solubility of oxygen and consequently the access of oxygen to the surface. Temperature differentials produce convection currents and so also influence the access of oxygen to the surface. In general the corrosion rate increases up to about 80°C, after which the corrosion rate declines as a result of the effect of reduced oxygen solubility at higher temperatures dominating over the increased electrochemical reaction rates and oxygen diffusion rate. This behaviour is shown in Figure 10 [8]; Figure 10 also shows that in a closed system the corrosion rate does not pass through a peak, but continues to rise with temperature because the oxygen is not allowed to escape.

(b) Effect of oxygen concentration

In seawater the corrosion rate is normally directly proportional to the oxygen concentration. This can be seen by examining the corrosion rate of steel as a function of depth in the sea (Figure 13), and the results of corrosion tests over a range of oxygen concentrations (Figure 14). This implies that in a repository, the corrosion rate would fall as the oxygen is consumed by corrosion, and that the approach to anaerobic conditions would decelerate.

The aerobic corrosion rate would be controlled by the supply of oxygen to the metal surfaces of the containers and waste, which in turn would depend on restrictions to the oxygen supply and the diffusion rate of oxygen through the surrounding media. As the oxygen concentration drops, the corrosion potential of iron would fall until eventually the potential at which hydrogen generation can occur would be reached, and anaerobic corrosion, by the reduction of water, would begin.

It is important to distinguish between data from experiments in which the test solution is static and those where a rotating electrode is used to fix the mass transport rate of oxygen to the surface. In controlled mass transport rotating electrode experiments (*e.g.* [33-35]) the corrosion rate is under anodic control and is proportional to the oxygen and chloride concentrations, and temperature (see Figure 7 to Figure 9). At high oxygen concentrations, oxygen has a passivating effect [9]. However, in static experiments the corrosion rate is under cathodic control and is governed by the rate of diffusion of oxygen to the surface. In some experiments reported in the literature the test solution was actively sparged with either air or oxygen, which has the effect of stirring the solution and increasing the oxygen supply to the surface, so increasing the corrosion rate. The data from static immersion tests and real life exposure, for example in seawater, are the most relevant to carbon steel in the waste repository.

It is possible that hydrogen would be generated under aerobic conditions. For example, Hara *et al.* [36] measured the production of hydrogen from carbon steel as a function of the oxygen concentration in seawater at 80°C. The hydrogen production increased with increasing oxygen concentration, although the proportion of the corrosion rate due to hydrogen production decreased with increasing oxygen concentration. The most likely explanation for this behaviour is that acidification had occurred within regions of localised corrosion, leading to hydrogen production.

(c) Effect of chloride concentration

In stagnant conditions the corrosion rate of steel in chloride solutions reaches a maximum at a chloride concentration of approximately 0.5M NaCl (Figure 5). At low chloride concentrations the corrosion rate is increased by increasing the concentration of chloride, because the conductivity of the solution increases, but at higher concentrations the corrosion rate falls because the oxygen solubility is reduced. The corrosion rate is also different for different cations in chloride solutions (Figure 5).

(d) Effect of dissolved gases

Dissolved carbon dioxide increases the corrosion rate of iron in water [8, 37, 38] by decreasing the pH of the water and hence increasing the current due to hydrogen ion reduction. Similarly, dissolved H_2S can increase the corrosion rate of metals by reducing the pH [8].

(e) Effect of surface condition

The condition of the surface, *e.g.* whether the surface is freshly prepared, pre-corroded, or covered with mill scale, affects the subsequent corrosion rate. It is possible that the presence of some types of iron oxide would prevent the potential of the specimen becoming sufficiently negative to allow hydrogen generation by anaerobic corrosion.

(f) Effect of radiation

Gamma radiation fields can cause an increase, and sometimes a decrease, in the corrosion rate. This is due to the production of oxidising agents in solution, such as free radicals and hydrogen peroxide. Some authors (*e.g.* [39]) have allowed for this by experimentally determining multiplier factors, which should be applied to the corrosion rate measured in the absence of a radiation field.

As an example of the dose rate required to affect the corrosion rate, anaerobic corrosion rate experiments [40] observed an increase in the corrosion rate at a dose rate of 11 Gy hr^{-1}. However, it is not possible to generalise about the effect of radiation on corrosion, and it is necessary to consider each case on its own merits.

(g) Effect of hydrodynamics

The corrosion rate of many materials is increased if the corrosive medium is flowing [41], because (i) diffusion restrictions on the supply of oxygen to the surface are reduced (see Subsection 3.2.1 (b)), and (ii) the flow can exert a mechanical effect on the oxide surface, removing protective oxide films. In static solutions the corrosion rate is determined by the diffusion of oxygen to the surface, and is hence under cathodic control, whereas in flowing solutions the corrosion rate may be under mixed or anodic control [33, 34].

(h) Effect of corrosion product build up and scaling

As corrosion proceeds, a layer of corrosion product forms on the surface. If it is tightly adherent and highly protective it is usually referred to as a passive film. A passive film forms a barrier layer on the metal surface and reduces the corrosion rate. A passive film starts forming immediately and is protective rapidly (*i.e.* within a few days; carbon steel is likely to passivate more slowly than stainless steel). Similarly, the deposition of a mineral scale from the water can reduce the corrosion rate. Scale deposition can be caused by (i) a change in pressure, (ii) a change in temperature, or (iii) mixing waters of different composition. For example, if Sellafield groundwater were to be mixed with grout porewater, a number of magnesium / calcium hydroxides and carbonates would be expected to be deposited. If this were to occur at the metal surface, a

protective scale could develop. On the other hand, the formation of a scale can also lead to under-deposit corrosion, by producing a crevice at the metal surface [42].

3.2.2 Anaerobic neutral solutions

A summary of the data relating to the corrosion of carbon steel in anaerobic neutral solutions is given in Table 3; some of the data are summarised in Figure 15 to Figure 20.

Diercks [43,44] has published a compilation of literature corrosion rate data for anaerobic and aerobic acid chloride solutions (Figure 15 and Figure 16), such as might occur in HLW repositories with concentrated brines at high temperatures. An Arrhenius relationship can be used to describe the data, with an activation energy, E_a, of 32 kJ mole^{-1} (see Figure 15). A compilation of corrosion rates for mild steel in aerobic and anaerobic neutral solutions over a range of temperatures, also taken from Diercks, is shown in Figure 17. At temperatures below 100°C the corrosion rates fall in the range 1 to 100 µm yr^{-1}. Figure 18 shows schematically the various types of hydrogen evolution curves observed by Simpson *et al.* [45] for mild steel in groundwaters in the pH range 7-10. The hydrogen evolution rates as a function of pH and chloride are summarised in Figure 19 and Figure 20.

Examination of the data in Table 3 shows that instantaneous electrochemical measurements give much higher corrosion rates than long-term weight loss and hydrogen evolution measurements. This is illustrated in Figure 21 and Figure 22, which show the corrosion rates measured using instantaneous and integrated techniques, as a function of temperature, for all chloride concentrations. The corrosion rate in anaerobic neutral conditions is insensitive to temperature, in agreement with Jelinek [18]. Corrosion under neutral, anaerobic conditions has recently been reviewed by Platts *et al.* [46].

3.3 Alkaline solutions

3.3.1 Aerobic alkaline solutions

A summary of the data relating to the corrosion of carbon steel in aerobic alkaline solutions is given in Table 4.

Akolzin's results [47] (Figure 23 and Figure 24) show that the higher the concentration of $Ca(OH)_2$ the lower the corrosion rate. For passive mild steel, corrosion rates in the range 1-10 µm yr^{-1} have been reported for ambient temperatures. At high temperatures at pH above 14 the corrosion rate is very high, for example Yasuda [48] (Figure 25) recorded 4,000 µm yr^{-1} at 117°C in 30% NaOH. There is a lack of information for intermediate temperatures.
Grubitsch [49] has shown that the rate of corrosion in $Ca(OH)_2$ increases with increasing chloride concentration.

3.3.2 Corrosion in concrete

The corrosion of steel reinforcement bars in concrete is analogous to the corrosion of waste and containers in cementitious grout. The general features of corrosion in concrete have been described in a number of publications (*e.g.* [50-58]). The important parameters in determining the corrosion rate are the relative humidity [59, 60] of the surrounding atmosphere, the rate of movement of the carbonation front through the concrete and whether it has resulted in a fall in pH at the steel-concrete interface, concrete porosity, cement type, chloride concentration, the OH^-/Cl^- concentration ratio at the metal interface and the rate of diffusion of oxygen through the concrete. The existence of cracks in the mortar can also affect the corrosion rate. Table 5 provides examples of corrosion rates for steel in concrete.

Flis' work [61] illustrates the range of corrosion rates that can occur in real structures. In constructions where chloride had not penetrated the concrete and the carbonation front had not

reached the reinforcement bar, corrosion rates as low as 0.08 μm yr^{-1} were recorded. At the other extreme, reinforcement in concrete immersed in marine environments experienced corrosion rates up to 350 μm yr^{-1}. Tuuti [52] has also reported data from real structures; in the worst case the corrosion rate in a chloride-containing concrete reached 500 μm yr^{-1}. The likelihood of corrosion in concrete increases with temperature [62].

In de-aerated mortars without added chloride, corrosion rates in the range 0.23 to 1.44 μm yr^{-1} have been observed [63-67], although it was noted that these probably represented maximum values.

3.3.3 Anaerobic alkaline solutions

A summary of the data relating to the corrosion of carbon steel in anaerobic alkaline solutions is given in Table 6.

The most relevant data are those generated over very long periods by hydrogen evolution experiments [16, 17, 68]. These experiments show that the corrosion rate may fall as low as 0.07 nm yr^{-1} at 20°C. This is a reflection of the very low solubility of iron oxides at high pH and the low concentration of H^+ at high pH.

In the NSARP, the hydrogen evolution rate for carbon steel and stainless steel was measured for a range of conditions; the data obtained have been summarised in reference [69]. The data for carbon steel are given in Table 7 and are shown graphically in Figure 26. Some of the data for carbon steel in alkaline conditions were used to calibrate the SMOGG model as described in Subsection 4.2. If the material is pickled initially to remove the air-formed film there is an initial peak in corrosion rate, which then decrease with time to a low value as a layer of corrosion product builds up, which is predominantly magnetite in the tests carried out by Serco. This general form of the curve relating hydrogen evolution rate or corrosion to time has been observed both in strongly alkaline conditions, which are relevant to the Nirex repository concept [69], and in weakly alkaline conditions, which are relevant to the SKB programme (*i.e.* in bentonite or bentonite porewater simulant [70- 72]). As for the work in strongly alkaline solutions carried out in the NSARP, the experiments within the SKB programme showed that the corrosion rates in aqueous conditions were initially higher at higher temperature; the long-term rates were higher in the lower pH solution used in the SKB programme than in the highly alkaline solutions used for the NSARP.

Japanese workers have reported the results from hydrogen generation rate corrosion measurements [73]; they obtained anaerobic corrosion rate data for carbon steel, stainless steel and Zircaloy in alkaline solutions under low oxygen conditions. The corrosion rates for carbon steel, stainless steel and Zircaloy were given as 10^{-1} μm yr^{-1}, 10^{-2} μm yr^{-1} and 10^{-3} μm yr^{-1} respectively. In further work [74], the rate of hydrogen gas generation was measured in a solution of $Ca(OH)_2$ with 5,000 ppm chloride at pH 12.4. In these experiments the long-term corrosion rates for carbon steel and stainless steel were ~2×10^{-2} μm yr^{-1} after 900 days and 650 days respectively. The corrosion rate for Zircaloy was ~1×10^{-2} μm yr^{-1} after 650 days.

3.4 Atmospheric corrosion

During storage and subsequently the operational phase of a repository, carbon steel in the waste may be exposed to the ambient atmosphere, rather than be fully immersed in an aqueous phase. In this situation corrosion may arise as a result of the presence of a thin layer of moisture on the metal surface, which may contain chloride if the material is in a marine environment, and/or sulphur oxides in an industrial environment. The corrosion rate is therefore highly dependent on the exact atmospheric conditions. Typical atmospheric corrosion data in the literature are summarised in Table 8. In unpolluted, rural atmospheres the corrosion rates are typically in the range 10-50 μm yr^{-1}, but in humid marine atmospheres corrosion rates up to 1200 μm yr^{-1} may be experienced. A clear relationship exists between the deposition rate for chloride particulates and

the corrosion rate, as shown by Figure 27. There is a lack of atmospheric corrosion rate data for temperatures greater than about 30°C.

From the information summarised in Section 3, corrosion of carbon steel will generate hydrogen once conditions have become anaerobic. Therefore a model for corrosion of carbon steel is included in SMOGG.

4.1 SMOGG model

The model implemented in SMOGG [3, 4] specifies the corrosion rate of carbon steel as:

$$\frac{ds}{dt} = -k_a e^{-\frac{t}{t_a}} f_a(T) - k_c e^{-\frac{t}{t_c}} f_c(T) \tag{4.1}$$

where

s	is the position of the surface of the carbon steel [m];
t	is the time during which corrosion is occurring [yr];
k_a	is the initial acute corrosion rate (defined at a reference temperature, T_{ref}, for which f_a = 1) [m yr^{-1}];
t_a	is a characteristic time for the acute corrosion [yr];
f_a	is a factor that specifies the dependence of the acute corrosion rate on temperature [-];
T	is the temperature [K];
k_c	is the initial chronic corrosion rate(defined at a reference temperature, T_{ref}, for which f_c = 1) [m yr^{-1}];
t_c	is a characteristic time for the chronic corrosion [yr];
f_c	is a factor that specifies the dependence of the chronic corrosion rate on temperature [-].

This formulation allows separate corrosion rates to be specified for an initial "acute" phase and a later "chronic" phase.

Furthermore, for the purpose of this study the model is simplified by assuming the corrosion rates increase with temperature according to an Arrhenius relationship. That is:

$$f_a(T) = \exp\left[-\frac{E_a}{R}\left(\frac{1}{T} - \frac{1}{T_{ref}}\right)\right] \tag{4.2}$$

and

$$f_c(T) = \exp\left[-\frac{E_c}{R}\left(\frac{1}{T} - \frac{1}{T_{ref}}\right)\right] \tag{4.3}$$

where

E_a	is the activation energy for the acute corrosion [J mol^{-1}];

R is the gas constant [J $mol^{-1}K^{-1}$];
T_{ref} is a reference temperature at which k_a and k_c are defined [K];
E_c is the activation energy for the chronic corrosion [J mol^{-1}].

Hence, a total of six parameters must be specified to define the corrosion rate of carbon steel for a particular corrosive environment:

- Two rate constants (k_a and k_c, giving the base corrosion rates);
- Two characteristic times (t_a and t_c, defining the decrease with time); and
- Two activation energies (E_a and E_c, defining the effect of temperature).

Carbon steel corrodes under aerobic conditions to produce iron oxides according to:

$$3Fe + 2O_2 \Rightarrow Fe_3O_4 \quad (4.4)$$

Although this reaction occurs without the production of gas, it is included in SMOGG because it may reduce the inventory of carbon steel available for the subsequent production of gas under the anaerobic conditions that will develop after repository closure.

Under anaerobic conditions, carbon steel corrodes to produce hydrogen according to:

$$3Fe + 4H_2O \Rightarrow Fe_3O_4 + 4H_2 \quad (4.5)$$

It is anticipated that the carbon steel waste generally will be encapsulated in cement in metal containers to form stable and easily movable packages. The conditioned waste then will be transported to a deep underground repository and at an appropriate time surrounded by a cement-based backfill. Therefore the corrosive environments of interest are:

- An aerobic, cementitious (*i.e.* alkaline) environment;
- An anaerobic, cementitious environment; and
- After resaturation, an alkaline (pH 12.5–13) porewater which has mixed with groundwater containing chloride ions and various other inorganic salts.

To summarise, the environments which have to be considered in SMOGG are:

Conditions	Carbon steel
Atmospheric corrosion	Not considered
Aerobic corrosion in grout, low chloride	Required
Anaerobic corrosion, high pH, low chloride	Required
Anaerobic corrosion, high pH, high chloride	Required

4.2 Calibration

To calibrate all the parameters in the SMOGG corrosion model (see Subsection 4.1) requires experimental data for a given set of conditions covering timescales from a few days to a number of years, with a sufficient frequency of measurements to capture accurately the variations in the

corrosion rate. For carbon steel in anaerobic conditions, the series of experiments using gas cell measurements summarised by Smart *et al.* [69] provide appropriate data at several temperatures. However, for other conditions the available data are not sufficiently detailed to allow a proper calibration.

Therefore the parameters selected for the aerobic corrosion of carbon steel in Subsection 4.4 are estimated from limited experimental data. The calibrations of the SMOGG corrosion parameters described in this subsection are for only the anaerobic corrosion of carbon steel.

The gas cell experiments on carbon steel [69] were performed for a number of conditions. These included experiments at high pH in solutions of NaOH and $Ca(OH)_2$ and in NRVB, with and without additions of NaCl in each case, and experiments at neutral and low pH. SMOGG calculations will generally require data for corrosion in cement grouts, so the most relevant results are those at high pH. A total of sixteen experiments from this series (numbered 5, 9, 14, 15, 18, 19, 23, 24, 25, 26, 27, 28, 37, 39, 51 and 53), all with high pH conditions, have been used in the calibrations.

Examination of the cumulative gas generation and the gas generation rates from the sixteen experiments suggests that experiments differing only in the addition of NaCl produce qualitatively similar results with only limited quantitative differences. The largest differences between such results are: a factor of 2 variation in the total gas generated after a number of years; and in some cases a slightly lower gas generation rate at earlier times for the experiment including NaCl. The experiments in saturated $Ca(OH)_2$ solution with and without the addition of NaOH showed similar variations. Given this it was decided to calibrate SMOGG for the following six sets of conditions:

- Saturated $Ca(OH)_2$ solution at 30°C (with added NaOH, with and without addition of NaCl);
- Saturated $Ca(OH)_2$ solution at 50°C (with and without addition of NaOH and/or NaCl);
- NaOH solution at 30°C (with and without addition of NaCl);
- NaOH solution at 50°C (with and without addition of NaCl);
- NaOH solution at 80°C (with and without addition of NaCl);
- NRVB at 50°C (with and without addition of Cl^-).

For each condition the gas generation rate was initially rapid but reduced (in most cases within a year) to a near constant value. The exception was that for NaOH at 30°C the gas generation rate continued to reduce slowly after the initial rapid reduction. For $Ca(OH)_2$ at 30°C the rapid reduction in gas generation rate was preceded by a period in which the gas generation rate was more constant. With the exception of initial constant gas generation rate, these characteristics fit the SMOGG corrosion model (Equation (4.1)) of a period of acute corrosion followed by chronic corrosion at a slower rate well. Therefore SMOGG was calibrated by adjusting the parameters to improve the fit to all the experimental data except the initial period of constant gas generation rate for $Ca(OH)_2$ at 30°C.

For all the experiments, the carbon steel consisted of 1 mm diameter wires with a surface area of 0.1 m^2. The largest quantity of hydrogen evolved was 0.376 mol m^{-2}. This corresponds to a total depth of corrosion of only 2 μm. Since the fraction of the wires corroded is small in all experiments the area of the surface of the un-corroded metal will be virtually constant. Therefore the wires were represented as plates in SMOGG, and the total mass and thickness were chosen to achieve the required surface area of 0.1 m^2.

The SMOGG calculations also required several other quantities as input. The mass of water was set to be large enough that there was sufficient to corrode all the metal. The calculations were performed for a period of 15 years, with "repository closure" at the start of the calculation so that anaerobic corrosion would be modelled. In SMOGG the corrosion rate after "repository closure" varies with groundwater saturation. This variation is not required for the calibrations, so was

removed by ensuring that the two sets of rate parameters for the corrosion were the same. In this case the choice of values for the parameters controlling the resaturation is not important. Intermediate times were chosen to ensure the calculated results captured the characteristics of the gas generation. Since the calculations were for anaerobic corrosion no oxygen was required. However, this is not a valid input for SMOGG so a very small value was chosen so that it would be consumed rapidly by corrosion of the metal and would not affect the gas generation results calculated (except that the initial rate would be zero).

Using this input data the SMOGG results were fitted to the experimental data for the corresponding conditions by varying the rate constants and characteristic times for the acute and chronic anaerobic corrosion of carbon steel. The calibrated[5] corrosion parameter values for each of the sets of conditions are listed in Table 9. The resulting cumulative gas generation and gas generation rates calculated by SMOGG are plotted with the corresponding experimental results in Figure 28 to Figure 33. (Note that a number of the gas generation rate values determined from the experiments were negative; these are plotted at the minimum value to allow some account to be taken of these in calibrating the parameters in SMOGG.)

In general good fits of the SMOGG results to the experimental results, or to averages of them where there was some variation, were obtained. Considering each set of conditions in turn, the following, more detailed observations can be made:

- **For saturated $Ca(OH)_2$ solution at 30°C:** The initial period of more constant corrosion made calibration of parameters more difficult, although the fit obtained is considered reasonable. To improve the fit, a constant corrosion rate of 0.1–0.2 μm yr^{-1} for the first 2 years would be required.

- **For saturated $Ca(OH)_2$ solution at 50°C:** There is a significant variation in the quantity of gas generated over the first 0.5 years, but the rate at longer times appears to be reasonably consistent (although the large fraction of negative rates makes this difficult to determine with certainty). The calibrated parameters fit the average, so it is expected that adjustment of the acute corrosion rate constant or characteristic time by up to ±50% would allow reasonable fits to the individual experimental results.

- **For NaOH solution at 30°C:** There was a substantial variation between the results obtained from the four experiments. The differences do not appear to correspond to any differences in conditions (i.e. whether NaCl was added) between the experiments. The evolution of the gas generation for Cells 5 and 9 appears to be more consistent with that seen in most of the experiments under other conditions, so the SMOGG parameters have been calibrated using the results of these experiments only. As noted above, a feature of these experiments not seen in other experiments is that the gas generation rate continues to decrease in the long term. This is reflected in the much smaller value required for the chronic corrosion characteristic time. It is possible that a constant value would eventually be reached, in which case the calibrated chronic corrosion values would actually represent an intermediate-term corrosion regime. The gas generation rate for the other two experiments appears to be more constant, or at least reduce over a much longer time period. However, it is useful to note that the rate of this corrosion is approximately the same as the calibrated initial chronic corrosion rate, so that a reasonable fit may be obtained with the same rate constants by reducing and increasing only the acute and chronic corrosion characteristic times respectively.

- **For NaOH solution at 50°C:** The experimental results do not show as clear an evolution of the gas generation as the results for other conditions. The calibration is therefore only approximate and should be treated with caution. There appears to be virtually no corrosion in the experiments after 1.5 years. In practice corrosion is likely to continue at a very slow rate so the parameters for chronic corrosion have been set to reflect this.

---

[5] The calibration involved an approximate (*i.e.* "by eye") fit of the SMOGG results to the experimental data.

- **For NaOH solution at 80°C:** An accurate calibration was possible for the first year, but the accuracy of the calibrated chronic corrosion parameters may be less, due to the difficulty in interpreting the large fraction of negative gas generation rate values determined from the experiments.

- **For NRVB at 50°C:** The quantity of gas generated over the first 0.5 years and the rate at times greater than 1 year are reasonably consistent, but there is a significant variation in the quantity of gas generated over the period from 0.5 to 1 year. The calibrated parameters fit the average, so it is expected that adjustment of the acute corrosion characteristic time by ±20% would allow reasonable fits to the individual experimental results.

Overall, the calibrations show that the acute corrosion rate constant increases with temperature and with changing from NRVB to $Ca(OH)_2$ solution to NaOH solution. The only result that does not fit this pattern is that for NaOH at 50°C, but the calibration for these conditions is questionable. The acute corrosion characteristic time decreases as the acute corrosion rate constant increases, so that the quantity of metal corroded during the acute phase remains approximately constant. The exception is that significantly more metal is corroded during the acute phase for corrosion in NaOH at 80°C.

In contrast, the calibrated chronic corrosion parameters are virtually independent of the conditions, the rate constant being around 0.005 μm yr^{-1} and the characteristic time being very large, so that the corrosion rate in the long term is constant. The significant exception to this is for NaOH at 30°C, where there is a substantial decrease in the gas generation rate and therefore corrosion rate over a number of years. However, this could be an intermediate corrosion phase, and the corrosion rate could become constant with a similar value to that for the other conditions in the very long term. Indeed, with the calibrated parameters the chronic corrosion rate reduces to 0.005 μm yr^{-1} after approximately 7 years, and, from the plot of the hydrogen generation rate in Figure 30, it is possible that the calibrated result is underestimating the gas generation for times after around 7 years.

Since corrosion data for a range of temperatures may be required for use in SMOGG it is useful to determine the relationship between the corrosion model parameters and temperature. It is noted that the chronic corrosion appears to be independent of temperature, so only the acute corrosion requires consideration. Commonly there is an Arrhenius relationship between corrosion rate and temperature so it is appropriate to examine this possibility. An Arrhenius relationship is of the form

$$\text{Rate} \propto e^{-\frac{E}{RT}} \tag{4.6}$$

where

E is an activation energy [J mol^{-1}];
R is the gas constant [J $mol^{-1}K^{-1}$];
T is the absolute temperature [K].

Therefore the logarithms of the rates are plotted against the reciprocals of the absolute temperatures in Figure 34, where the rates are the calibrated acute corrosion rate constants. With only six data points, and given that there is some difference in rate constants between $Ca(OH)_2$, NaOH and NRVB cases, the validity of the relationship is not clear. However, the line of best fit does appear reasonable, and, assuming the relationship is valid, gives an activation energy of 56 kJ mol^{-1}.

4.3 Focussed review of corrosion data

The data requirements for SMOGG are summarised in Subsection 4.1. For each phase, consideration needs to be given to whether there is any difference between the acute (*i.e.* over a short period) corrosion rate and the chronic (*i.e.* long-term) corrosion rate. It is also necessary to

take account of the characteristic time for the acute and chronic phases and possible effects of temperature, as described in Subsection 4.1.

Having reviewed the available literature on the corrosion of carbon steel, the most relevant data for each stage of the SMOGG model have been selected. Data were chosen by examining the corrosion rate summary tables (*i.e.* Table 2 to Table 8). For the purposes of making calculations with SMOGG, it is necessary to choose single values for the initial corrosion rate in the acute and chronic stages of the model. In reality, it is likely that the carbon steel will experience a range of corrosion rates, depending on the exact nature of the chemical environment produced by the specific waste stream. It was therefore necessary to use expert judgement to choose the most appropriate corrosion rates for the model. The corrosion rates chosen are listed in Subsection 4.4 and the reasons for the choice of these values are discussed below.

(a) Aerobic corrosion in grout, low chloride

There are not very many data relating to the acute corrosion rate of carbon steel; however Arya has reported electrochemical data as a function of time [75], showing an exponential decrease with time for a number of different cement mixes containing 1% or 3% chloride. The initial acute corrosion rate was of the order of 200 μm yr^{-1}. The decay in corrosion rate probably reflects both the reduction in the availability of water during curing and the passivation of the steel surface. The passivation was more rapid in 1% chloride tests, where passivation was typically complete within 20 days, compared to 80 days with 3% chloride present. In the absence of chloride it is probable that passivation would be complete within a few hours. The precise corrosion rate will depend on the chemistry of the specific cement type and wastestream, but for the purposes of the SMOGG model an acute initial corrosion rate of 200 μm yr^{-1} at ambient temperature and a characteristic time of 0.003 years (~1 day) have been selected.

In the absence of chloride and carbonation effects, the corrosion rate of carbon steel in cementitious environments is very low because of the protection offered by the passive film formed in alkaline conditions (Table 5). For the purposes of defining a single corrosion rate for use in SMOGG it will be assumed that the chloride concentrations and degree of carbonation during this stage will be insignificant. Consequently a long-term initial chronic corrosion rate of 0.1 μm yr^{-1} at ambient temperature is selected and it is assumed that this stays constant with time (i.e. in the SMOGG model the characteristic time is infinite).

There is a limited amount of data relating to the effect of temperature on the corrosion rate in concrete; most experimental work has been carried out at ambient temperature. However, Liu and Weyers [76] carried out a systematic 5-year study of the corrosion rate of steel in concrete as a function of temperature (0-35°C), concrete ohmic resistance and chloride content. They developed a model for predicting the corrosion rate in concrete and included the following relationship for the effect of temperature on the corrosion rate of steel in concrete:

$$i_2 = i_1 e^{2283\left(\frac{1}{T_1}-\frac{1}{T_2}\right)} \qquad (4.7)$$

where

T_1, T_2 are temperatures [K];
i_1 is the corrosion current at temperature T_1 [A];
i_2 is the corrosion current at temperature T_2 [A].

It should be noted that changes in temperature will also affect other interacting factors which could influence corrosion rate, such as oxygen diffusion rate and the electrical resistance of the concrete. The relationship defined by Equation (4.7) is applicable for describing the effect of temperature on the chronic corrosion rate, but in the absence of any data to describe the effect of temperature on the short-term corrosion rate it will also be used for the acute stage of aerobic corrosion in grout.

(b) Anaerobic corrosion, low chloride

For pre-corroded materials, there will probably be an incubation period before anaerobic corrosion initiates, as shown in the NSARP [69] and Fujisawa work [77]. If any uncorroded carbon steel is present, the initial corrosion rate will depend on the temperature; there is an Arrhenius type relationship between the acute corrosion rate and temperature [69]. For pre-corroded material it is reasonable to assume that eventually anaerobic corrosion will initiate at a low level, although it is likely that there will not be an initial peak in the corrosion rate (*i.e.* there will be no acute phase).

Figure 34 shows the Arrhenius relationship for the initial (acute) corrosion rates obtained from the calibration in Subsection 4.2. This plot gives a rate of approximately 0.5 μm yr^{-1} at a temperature of 30°C and so this value has been chosen as the base acute anaerobic corrosion rate constant. The activation energy given in Subsection 4.4 is also derived from Figure 34. The data in reference [69] show that although the initial anaerobic corrosion rates of carbon steel are higher at 50°C and 80°C, the corrosion rate falls more rapidly at higher temperatures, i.e. the characteristic time for the acute phase varies as a function of temperature. However, since it is not possible to take this into account in the SMOGG model, a conservative characteristic time of 0.5 years, based on the calibrated 50°C data (Subsection 4.2), has been chosen.

The most relevant data for the long-term anaerobic corrosion rate of carbon steel is the gas evolution data obtained in the NSARP (Table 7) and in recent Japanese work [73,74,77]. On the basis of the data in Table 7 and the calibration calculations carried out (Subsection 4.2), a single long-term chronic anaerobic corrosion rate of 0.005 μm yr^{-1} has been selected, as this value gave a good fit in the calibration calculations. There does not appear to be any effect of temperature on the long-term anaerobic corrosion rate of carbon steel. On the basis of the available data it is not possible to conclude that the corrosion rate will fall below a value of 0.005 μm yr^{-1} with time, so the characteristic time is set at infinity.

(c) Anaerobic corrosion, high chloride

The anaerobic corrosion rate of carbon steel appears to be only weakly affected by the presence of chloride [69] and it is therefore suggested that the same SMOGG parameters should be used for this stage as for the low chloride phase. However, there may be no acute phase if long-term corrosion has taken place previously in low chloride, anaerobic conditions.

4.4 Selection of data recommended for use in SMOGG

The objective of this study was to parameterise the corrosion model for carbon steel that has been implemented in SMOGG, as given by Equations (4.1) – (4.3). In Subsections 4.2–3, the available data have been identified and interpreted, as far as possible, to give values for the various parameters.

The set of parameters for carbon steel corrosion recommended for use in SMOGG is summarised in the following table.

Stage in SMOGG model		Carbon steel
Atmospheric	acute	Not required
	chronic	Not required
Aerobic, grout, low chloride	acute	k_a = 200 μm yr^{-1} at 20°C t_a = 0.003 years Arrhenius variation of k_a: activation energy E_a = 19 kJ mol^{-1}
	chronic	k_c = 0.1 μm yr^{-1} at 20°C, $t_c \sim \infty$ [1] Arrhenius variation of k_c: activation energy E_c = 19 kJ mol^{-1}
Anaerobic, low chloride	acute	k_a = 0.5 μm yr^{-1} at 30°C, t_a = 0.5 years Arrhenius variation of k_a: activation energy E_a = 56 kJ mol^{-1}
	chronic	k_c = 0.005 μm yr^{-1} $t_c \sim \infty$ [1] No temperature dependence: activation energy E_c = 0 kJ mol^{-1}
Anaerobic, high chloride	acute	k_a = 0.5 μm yr^{-1} at 30°C, t_a = 0.5 years Arrhenius variation of k_a: activation energy E_a = 56 kJ mol^{-1}
	chronic	k_c = 0.005 μm yr^{-1} $t_c \sim \infty$ [1] No temperature dependence: activation energy E_c = 0 kJ mol^{-1}

[1] In using the SMOGG model a finite value is required; a value much greater than the duration of the calculation should be used (e.g. 10^8 years).

Note that:

- Under aerobic conditions, the corrosion rate at 20°C increases with temperature according to an Arrhenius relationship:

$$f_a(T) = f_c(T) = \exp\left[-\frac{19000}{8.314472}\left(\frac{1}{T} - \frac{1}{293.15}\right)\right] \tag{4.8}$$

where T is the temperature [K]. For example, at the temperatures listed below the corrosion rate at 20°C should be scaled by the corresponding factors:

Temperature, T	20°C	35°C	50°C	80°C
Factor, f_a or f_c	1.000	1.461	2.062	3.760

- Under anaerobic conditions, the acute corrosion rate at 30°C increases with temperature according to an Arrhenius relationship:

$$f_a(T) = \exp\left[-\frac{56000}{8.314472}\left(\frac{1}{T} - \frac{1}{303.15}\right)\right] \tag{4.9}$$

where T is the temperature [K]. For example, at the temperatures listed below the acute corrosion rate at 30°C should be scaled by the corresponding factors:

Temperature, T	20°C	35°C	50°C	80°C
Factor, f_a	0.469	1.434	3.955	23.234

Calculations of gas generation performed with SMOGG might include variant cases intended to scope the effect of uncertainties in the model parameters. From the experimental results examined here, it has not been possible to determine ranges of values for the parameters in the carbon steel corrosion model.

4.5 Discussion

Having derived a parameterisation of the SMOGG model for the corrosion rate of carbon steel (Subsection 4.4), it is useful to compare the resulting values with the corrosion rates used previously. Because the earlier models did not account for the temporal variation of the corrosion rate, it is possible to compare only the chronic behaviours.

An early assessment of gas generation in repositories [78], for Nirex, noted that "there appears to be a lot of uncertainty about the corrosion behaviour of mild and stainless steels", and assumed in the worst case corrosion rates at high pH would be in the range 0.1 μm yr^{-1} to 1 μm yr^{-1}.

A later NSARP Reference Document on Gas Generation and Migration [79] recommended: an aerobic corrosion rate of 100 μm yr^{-1}; an anaerobic (chronic) corrosion rate at neutral pH in the range 1 μm yr^{-1} to 10 μm yr^{-1}, with a preferred value of 5 μm yr^{-1}; and an anaerobic (chronic) corrosion rate at high pH in the range 0.1 μm yr^{-1} to 1 μm yr^{-1}, with a preferred value of 0.5 μm yr^{-1}.

In the *Nirex 97* assessment of gas generation from radioactive wastes [80], the carbon steel (chronic) corrosion rate was assumed to be: 1 μm yr^{-1} under aerobic conditions; and 0.1 μm yr^{-1} under anaerobic conditions.

Subsequently, a temperature-dependence for the aerobic corrosion rate of carbon steel was derived [81] by making the following assumptions:

- The aerobic (chronic) corrosion rate in the *Nirex 97* assessment, 1 μm yr^{-1}, is for a temperature of 40°C;
- Based on a consideration of unpublished experimental data obtained in the NSARP [82], the aerobic corrosion rate scales by the factors 1 : 4 : 22 as the temperature increases from 30°C : 50°C : 80°C; and
- The variation of the aerobic corrosion rate with temperature is given by an approximate form of the Arrhenius equation., *i.e.*

$$\text{Rate}\,(T) = \text{Rate}\,(T_{ref}) \times \exp\left[-\frac{E}{R}\left(\frac{1}{T}-\frac{1}{T_{ref}}\right)\right] \approx \text{Rate}\,(T_{ref}) \times \exp\left(\alpha\left(T - T_{ref}\right)\right)$$

Hence, the aerobic (chronic) corrosion rate of carbon steel was calculated to be:

Temperature, T	20°C	35°C	50°C	80°C
Corrosion rate	0.3 μm yr^{-1}	0.7 μm yr^{-1}	1.9 μm yr^{-1}	11.9 μm yr^{-1}
Factor, f_c	1.000	2.528	6.389	40.823

The anaerobic (chronic) corrosion rate of carbon steel was still assumed to be 0.1 μm yr^{-1}.

Subsequent assessments of gas generation from radioactive waste, such as the Generic Post-closure Performance Assessment (GPA) [2], generally reused this parameterisation.

Comparing the numbers listed above with the (chronic) corrosion rates given in Subsection 4.4, it can be seen that:

- In the GPA the long-term aerobic corrosion rate at 20°C, *i.e.* 0.3 μm yr^{-1}, is similar to the value now being recommended, *i.e.* 0.1 μm yr^{-1}.

- However, in the GPA the long-term aerobic corrosion rate increases more rapidly with temperature than is now being recommended.

  The activation energy measured by Liu and Weyers [76] is preferred to the value estimated from the NSARP data for the following reasons: the former data were obtained from long-term (*i.e.* 5 year) exposure tests which used both electrochemical and weight loss techniques on real concrete samples, whereas the NSARP data were obtained from long-term passive current measurements on solutions, and were not corroborated by weight loss measurements.

- The long-term anaerobic corrosion rate used in some earlier assessments of gas generation in repositories, *i.e.* 0.1 μm yr^{-1}, was chosen conservatively, and is more than an order of magnitude larger than the value now being recommended, *i.e.* 0.005 μm yr^{-1}.

5.1 Corrosion processes

The corrosion processes for stainless steel are similar to those for carbon steel, discussed in Subsection 3.1.

5.2 Neutral solutions

The general corrosion rate of stainless steels is very low, but localised corrosion can occur in stagnant solutions and therefore most literature has concentrated on the localised corrosion of stainless steel. A summary of the data relating to the aerobic corrosion of stainless steels in neutral solutions is given in Table 10 and Table 11, and some of the data are shown in Figure 35 and Figure 36. Weight loss experiments give corrosion rates of 0.1 to 0.5 μm yr^{-1} at <30°C, but 130 μm yr^{-1} at 90°C [83]. The high rate at 90°C was probably due mainly to pitting attack rather than general corrosion. There is a lack of data for intermediate temperatures. Only one reference in the open literature has been found for corrosion of stainless steel in anoxic neutral conditions (see Table 11).

5.3 Alkaline solutions

A summary of the data relating to the corrosion of stainless steel in aerobic and anaerobic alkali solutions is given in Table 12 and Table 13. At ambient temperature in aerobic solutions, the corrosion rate is <0.3 μm yr^{-1}, but at high temperatures in concentrated alkali solutions the corrosion rate may exceed 760 μm yr^{-1} (Figure 37). For anaerobic conditions, at ambient temperature, the corrosion rate determined by passive current measurements was found to be of the order of 0.4 μm yr^{-1} [84]. However, later passive current measurements on stainless steel in the Nirex Safety Assessment Research Programme (NSARP) [85] have yielded values as low as 0.05 μm yr^{-1}. At high temperatures and high concentrations of alkali the corrosion rate increases (*e.g.* 30 μm yr^{-1} in 30% NaOH at 117°C) [48], but it is not as high as in aerobic conditions at the same temperature.

Stainless steel is becoming more common as a material for use as reinforcing bar in concrete structures; indeed there is practical experience of its use for over 75 years (*e.g.* [86, 87]). In general the corrosion rates of stainless steel in concrete are very low, with a high resistance to chloride. In fact the threshold chloride concentrations probably exceed the solubility limit for chloride in cementitious porewater [88].

Bertolini *et al.* [89] investigated the corrosion resistance of a range of stainless steels in chloride contaminated and carbonated concrete. In the absence of chloride the corrosion rates of 304L[6] and 316L, measured by linear polarisation resistance (LPR), were both of the order of 0.05 μm yr^{-1} for the test duration of ~28 months. This applied to tests both at ambient temperature when exposed outdoors and at 40°C at 95-98% RH. Both stainless steels exhibited similar corrosion rates in carbonated concrete and concrete containing up to 6% chloride by mass of cement, under ambient / external exposure conditions and 40°C at 95-98% RH. In carbonated

[6] Steel grades, such as 302, 304, 304L, 316 and 316L, are used to classify various steels by their composition and physical properties. Type 304 is the most common grade; the classic 18/8 stainless steel. Type 316 is the second most common grade; alloy addition of molybdenum prevents specific forms of corrosion. Type 316 is also known as marine grade stainless steel due to its increased resistance to chloride corrosion compared to Type 304.

concrete containing up to 4% chloride by mass of cement the corrosion rate of 304L and 316L was ~0.06 μm yr^{-1} under ambient / external exposure conditions and 0.1 μm yr^{-1} at 40°C at 95-98% RH. The presence of a high temperature scale (*e.g.* from welding) on the surface of the 304L increased the corrosion rate in high chloride conditions (*e.g.* 1 μm yr^{-1} in 4wt% chloride) but 316L was unaffected by a heat tint surface film.

Treadaway *et al.* [90] measured weight loss from a range of steels including 302, 315 and 316L stainless steel in concrete containing chloride at a range of concentrations, with two different cement : aggregate ratios (8:1 and 6:1) and cover thicknesses (10 mm and 20 mm) for periods up to 9.5 years. Corrosion rates were measured by weight loss. The results for the 302 and 315 austenitic stainless steels, together with their compositions, are summarised in Table 14; the data for 316L were only expressed as percentage annual weight loss (which was fairly constant irrespective of chloride content at ~0.008% yr^{-1}; it was not possible to convert this value to a corrosion rate because the initial specimen dimensions are not given in the paper). Table 14 shows the range of the mean corrosion rates for the two different cement : aggregate ratios and cover thicknesses; there was no clear effect of either of these two parameters on the corrosion rate. No visible corrosion attack was visible on any of the austenitic stainless steels, apart from slight micro-pitting on the 302 stainless steel. It is possible that some of the weight loss measured was due to the cleaning process when the specimens were removed from the test for examination, although the authors claim to have taken this effect into account.

Attempts have been made in the Nirex research programme to measure the gas generated by the anaerobic corrosion of stainless steels in alkaline solutions, by monitoring gas cells over a period of over ten years [69]. During these measurements it was not possible to measure any hydrogen generation, indicating that the anaerobic corrosion rate of stainless steel was less than the detection limit for the gas cell technique, which was estimated to be less than 0.01 μm yr^{-1}. Japanese workers have also reported the anaerobic corrosion rate of stainless steel to be 0.01 μm yr^{-1} [73], based on gas evolution measurements using a mass spectroscopy technique to measure the amount of hydrogen evolved. Interestingly, this corrosion rate is similar to that measured in long-term aerobic corrosion experiments in concrete (Table 14), suggesting that the long-term corrosion rate in alkaline conditions is determined by the properties of the passive film (*e.g.* very low solubility of chromium oxyhydroxides), rather than the nature of the cathodic reactant (*i.e.* oxygen in aerated conditions and water in de-aerated conditions). Other work has suggested that the passive film is able to reform if it is disrupted by reaction with the surrounding water [91], even in the absence of oxygen. It is worth noting that a corrosion rate as low as 0.01 μm yr^{-1} corresponds to only a few unit cells of an oxide film thickness per year.

5.4 Atmospheric corrosion

The very thin passive film formed on stainless steels is essentially composed of hydrated chromium oxy-hydroxide [92]. The exact composition and structure depend on the material and the environment. Atmospheric corrosion data for stainless steels are summarised in Table 15. Atmospheric attack is minimal; 2.8 μm yr^{-1} was reported for marine atmosphere exposure, but it may be as low as 0.03 μm yr^{-1}. No data were found for atmospheric corrosion at elevated temperatures or in anoxic conditions.

There are very few data for the uniform corrosion rate of stainless steels, because the corrosion rates are so low that most authors have concentrated on the depths of pits that are formed. It is assumed that the depth of pitting is not important for the SMOGG model since the bulk loss of metal is the important factor in determining the possible rate of gas generation from subsequent anaerobic corrosion in the model, although pit propagation rates are important in determining the point of first penetration of a stainless steel waste container [93]. However, Wallinder *et al.* [94] have measured the actual release rates of chromium and nickel from stainless steels exposed to rainwater during atmospheric exposure; this work was carried out because of environmental concerns about the release of chromium and nickel, rather than to determine the corrosion rate for engineering reasons. The annual release rates during atmospheric exposure in Stockholm, Sweden for 304 were 0.25-0.3 mg Cr m^{-2} and 0.3-0.4 mg Ni m^{-2} and for 316 they were 0.35-0.4 mg Cr m^{-2} and 0.7-0.8 mg Ni m^{-2}. The iron release rates were not measured. For

comparison, a value of 1 mg Ni $m^{-2}yr^{-1}$ corresponds to a corrosion rate of 1.1 10^{-4} μm yr^{-1}. Other work has shown that the iron dissolution rate is 2-3 orders of magnitude higher [95], giving an overall corrosion rate, which is predominantly due to the loss of iron, of the order of 0.01-0.1 μm yr^{-1}.

From the information summarised in Section 5, corrosion of stainless steel will generate hydrogen once conditions have become anaerobic. Therefore a model for corrosion of stainless steel is included in SMOGG.

6.1 SMOGG model

The corrosion model for stainless steel is similar to that for carbon steel, discussed in Subsection 4.1.

A total of six parameters must be specified to define the corrosion rate of stainless steel for a particular corrosive environment:

- Two rate constants (k_a and k_c, giving the base corrosion rates);
- Two characteristic times (t_a and t_c, defining the decrease with time); and
- Two activation energies (E_a and E_c, defining the effect of temperature).

Stainless steel corrodes under aerobic conditions to produce iron oxides according to:

$$3Fe + 2O_2 \Rightarrow Fe_3O_4 \qquad (6.1)$$

Although this reaction occurs without the production of gas, it is included in SMOGG because it may reduce the inventory of stainless steel available for the subsequent production of gas under the anaerobic conditions that will develop after repository closure.

Under anaerobic conditions, stainless steel corrodes to produce hydrogen according to:

$$3Fe + 4H_2O \Rightarrow Fe_3O_4 + 4H_2 \qquad (6.2)$$

It is anticipated that the stainless steel waste generally will be encapsulated in cement in metal containers to form stable and easily movable packages. The conditioned waste then will be transported to a deep underground repository and at an appropriate time surrounded by a cement-based backfill. Therefore the corrosive environments of interest are:

- An aerobic, cementitious (*i.e.* alkaline) environment;
- An anaerobic, cementitious environment; and
- After resaturation, an alkaline (pH 12.5–13) porewater which has mixed with groundwater containing chloride ions and various other inorganic salts.

The containers themselves, which generally will be fabricated from stainless steel, have to be considered separately. That is because, during transport and storage, the exterior of a container could be subject to a different environment to the interior (the exterior will be exposed to the atmosphere at neutral pH, until after backfilling; the interior could be exposed to either neutral or high pH conditions, depending on the time and the material of encapsulation). Hence, a different corrosion rate could apply on the outer surface of a container.

To summarise, the environments which have to be considered in SMOGG are:

Conditions	Stainless steel
Atmospheric corrosion	Required: uniform corrosion only considered
Aerobic corrosion in grout, low chloride	Required
Anaerobic corrosion, high pH, low chloride	Required
Anaerobic corrosion, high pH, high chloride	Required

6.2 Focussed review of corrosion data

The data requirements for SMOGG are summarised in Subsection 6.1. For each phase, consideration needs to be given to whether there is any difference between the acute (*i.e.* over a short period) corrosion rate and the chronic (i.e. long-term) corrosion rate. It is also necessary to take account of the characteristic time for the acute and chronic phases and possible effects of temperature.

Since stainless steel repassivates rapidly if the passive film is disrupted [91], it is anticipated that there will not be a distinct period of acute corrosion. Hence, in SMOGG it is assumed that the acute corrosion rate of stainless steel is zero for all conditions.

Having reviewed the available literature on the corrosion of stainless steel, the most relevant data for each stage of the SMOGG model have been selected. Data were chosen by examining the corrosion rate summary tables (*i.e.* Table 10 to Table 15). (Note: the data for stainless steel are not sufficiently detailed to allow a calibration.) The corrosion rates chosen are listed in Subsection 6.3 and the reasons for the choice of these values are discussed below.

(a) Atmospheric corrosion

The main concern is the rate of metal loss rather than the risk of localised corrosion. There is a lack of atmospheric corrosion data for stainless steel indoors because the corrosion rate is so low. On the basis of the data in Table 15 and the data reported by Wallinder [94], and the fact that the stainless steel will experience an indoor environment where the time of wetness will be short, a uniform corrosion rate of 0.03 $\mu m\ yr^{-1}$ is selected. This is probably conservatively high. It is unlikely that this corrosion rate will change with time so the characteristic time is infinite. There are no relevant data relating to the effect of temperature on the atmospheric corrosion rate of stainless steel, but there is unlikely to be any significant effect of temperature on the atmospheric corrosion rate within the range expected during storage or repository operation (*e.g.* 0-50°C).

(b) Aerobic corrosion in grout, low chloride

The aerobic corrosion rate of stainless steel in concrete will be very low, even if the chloride content increases, for example if a high chloride waste is grouted. On the basis of long-term weight loss data reported by Treadaway [90] a corrosion rate for stainless steel in aerated grout of 0.02 $\mu m\ yr^{-1}$ is selected. Bertolini's data [89] gave slightly higher values, but the measurements were made electrochemically and these types of measurements are likely to over-estimate the measured corrosion rates. The corrosion rate is likely to remain constant with time so the characteristic time is infinite.

In relation to the effect of temperature on corrosion rate, passive current densities measured for stainless steel in alkaline simulated porewater within the NSARP [85] gave the following data for

30, 50 and 80°C respectively: 0.05, 0.15 and 0.8 μm yr^{-1}. Figure 38 shows that this data follows an Arrhenius relationship. Based on the line of best fit, the activation energy is 50 kJ mol^{-1}. Treadaway's data are preferred to the NSARP electrochemical measurements for a general measure of long-term corrosion rate, as they are based on measurement of weight loss and hence require fewer assumptions to be made in calculating corrosion rate.

(c) Anaerobic corrosion, low chloride

On the basis of the NSARP measurements in anaerobic alkaline conditions [69] and the comparable, independent Japanese work [73,102] a corrosion rate of 0.01 μm yr^{-1} is selected. The corrosion rate is likely to remain constant in the long term, so an infinite characteristic time has been selected. There are currently very few data on the effect of temperature on the anaerobic corrosion rate of stainless steel; experiments were carried out in the NSARP at 30°C and 50°C and there was no discernible difference between the two temperatures. It has been assumed here that there is no acute phase; however, there is some indication of an acute phase in recent Japanese studies [73,74] and further analysis of translations of these papers is required to confirm this.

(d) Anaerobic corrosion, high chloride

Chloride is unlikely to affect the corrosion rate under anaerobic conditions, and so the same parameters have been chosen as for the low chloride situation.

6.3 Selection of data recommended for use in SMOGG

The objective of this study was to parameterise the corrosion model for stainless steel that has been implemented in SMOGG. In Subsection 6.2, the available data have been identified and interpreted, as far as possible, to give values for the various parameters.

The set of parameters for stainless steel corrosion recommended for use in SMOGG is summarised in the following table.

Stage in SMOGG model		Stainless steel
Atmospheric	acute	No acute stage
	chronic	k_c = 0.03 μm yr^{-1} $t_c = \infty$ [1] No temperature dependence: activation energy E_c = 0 kJ mol^{-1}
Aerobic, grout, low chloride	acute	No acute stage
	chronic	k_c = 0.02 μm yr^{-1} at 20°C $t_c = \infty$ [1] Arrhenius variation of k_c: activation energy E_c = 50 kJ mol^{-1}
Anaerobic, low chloride	acute	No acute stage
	chronic	k_c = 0.01 μm yr^{-1} $t_c = \infty$ [1] No temperature dependence: activation energy E_c = 0 kJ mol^{-1}
Anaerobic, high chloride	acute	No acute stage
	chronic	k_c = 0.01 μm yr^{-1} $t_c = \infty$ [1] No temperature dependence: activation energy E_c = 0 kJ mol^{-1}

[1] In using the SMOGG model a finite value is required; a value much greater than the duration of the calculation should be used (e.g. 10^6 years).

Note that:

- Under aerobic conditions, the chronic corrosion rate at 20°C increases with temperature according to an Arrhenius relationship:

$$f_c(T) = \exp\left[-\frac{50000}{8.314472}\left(\frac{1}{T} - \frac{1}{293.15}\right)\right] \tag{6.3}$$

where T is the temperature [K]. For example, at the temperatures listed below the corrosion rate at 20°C should be scaled by the corresponding factors:

Temperature, T	20°C	35°C	50°C	80°C
Factor, f_c	1.000	2.714	6.716	32.632

6.4 Discussion

Having derived a parameterisation of the SMOGG model for the corrosion rate of stainless steel (Subsection 6.3), it is useful to compare the resulting values with the corrosion rates used previously. Because the acute corrosion rate of stainless steel is assumed to be zero for all conditions, it is possible to compare only the chronic behaviours.

An NSARP Reference Document on Gas Generation and Migration [79] recommended: an aerobic corrosion rate of 0.1 μm yr^{-1}; an anaerobic (chronic) corrosion rate at neutral pH of 0.03 μm yr^{-1}; and an anaerobic (chronic) corrosion rate at high pH of 0.03 μm yr^{-1}.

These corrosion rates were used unchanged in the *Nirex 97* assessment of gas generation from radioactive wastes [80].

Subsequently, a temperature-dependence for the aerobic corrosion rate of stainless steel was derived [81] by making the following assumptions:

- The aerobic (chronic) corrosion rate is 0.05 μm yr^{-1} at a temperature of 30°C;
- Based on a consideration of unpublished experimental data obtained in the NSARP [82][7], the aerobic corrosion rate scales by the factors 1 : 3 : 16 as the temperature increases from 30°C : 50°C : 80°C;
- The variation of the aerobic corrosion rate with temperature is given by an approximate form of the Arrhenius equation., *i.e.*

$$\text{Rate}\,(T) = \text{Rate}\,(T_{ref}) \times \exp\left[-\frac{E}{R}\left(\frac{1}{T}-\frac{1}{T_{ref}}\right)\right] \approx \text{Rate}\,(T_{ref}) \times \exp\left(\alpha\left(T - T_{ref}\right)\right)$$

Hence, the aerobic (chronic) corrosion rate of stainless steel was calculated to be:

Temperature, T	20°C	35°C	50°C	80°C
Corrosion rate	0.029 μm yr^{-1}	0.066 μm yr^{-1}	0.150 μm yr^{-1}	0.782 μm yr^{-1}
Factor, f_c	1.000	2.282	5.207	27.113

The anaerobic (chronic) corrosion rate of stainless steel was still assumed to be 0.03 μm yr^{-1}.

Subsequent assessments of gas generation from radioactive waste, such as the Generic Post-closure Performance Assessment (GPA) [2], generally reused this parameterisation.

Comparing the numbers listed above with the (chronic) corrosion rates given in Subsection 6.3, it can be seen that:

- In the GPA the long-term aerobic corrosion rate at 20°C, *i.e.* about 0.03 μm yr^{-1}, is similar to the value now being recommended, *i.e.* 0.02 μm yr^{-1}.
- In the GPA the long-term aerobic corrosion rate varies with temperature in almost the same way as is now being recommended. That is not surprising, because both analyses of the effect of temperature on the long-term aerobic corrosion rate relied on the same data from the NSARP.

[7] These are the same data referred to in Subsection 6.2, when quantifying the effect of temperature on the long-term aerobic corrosion rate.

- The long-term anaerobic corrosion rate used in earlier assessments of gas generation in repositories, *i.e.* 0.03 μm yr^{-1}, is similar to the value now being recommended, *i.e.* 0.01 μm yr^{-1}.

7.4 Corrosion of Zircaloy

Although zirconium is a reactive metal, Zircaloy is highly resistant to both general and localised corrosion in neutral and alkaline, aqueous chloride solutions, as a result of its tenacious oxide film [96-98]. It is able to passivate even in highly alkaline, anaerobic, chloride-containing environments [7]. The corrosion product of Zircaloy consists of a tightly adherent passive film composed of ZrO_2, which is believed to form by the following sequence of reactions:

$$Zr + 3H_2O \Rightarrow ZrO^{2+} + 2H_2 + 2OH^-$$
$$ZrO^{2+} + H_2O \Rightarrow ZrO_2 + 2H^+ \qquad (7.1)$$

Reference [98] gives the corrosion rate in both potassium and sodium hydroxide as less than 25 μm yr^{-1}. The corrosion behaviour of Zircaloy 2 in de-aerated synthetic pore water was investigated by Hansson [64] and it was found to be passive at all values of pH and electrochemical potential investigated. The passive corrosion rate was <0.01 μm yr^{-1} and it is probable that a similarly low corrosion rate would apply in neutral conditions and aerobic conditions. It is unlikely that the corrosion rate would increase significantly at temperatures up to 80°C. Other workers have reported the corrosion rate as being in the range 0.06-0.17 μm yr^{-1} [99]. On the basis of hydrogen evolution experiments, Mihara [73] reports corrosion rates of 0.001 μm yr^{-1} (full experimental details are not currently available). Hietanen [100] measured the corrosion rate of Zircaloy in concrete as 0.003-0.05 μm yr^{-1}. A corrosion rate of 0.001 μm yr^{-1} is equivalent to a rate of removal of approximately 1 unit layer of ZrO_2 per year; this is a reflection of the very low solubility of ZrO_2.

Kurashige *et al.* [101] reported data for the rate of hydrogen gas generation for Zircaloy in alkaline synthetic groundwater (pH 10.8 and pH 12.5) at 30°C and 45°C. At pH 10.8 and 30°C the gas generation rate was equivalent to a corrosion rate of 0.006 μm yr^{-1}, averaged over the first 100 days and 0.001 μm yr^{-1} averaged over 500 days. In the long-term there was little difference between the two temperatures and two pH values examined, but the acute rate was higher at the higher temperature, for both pH values. Similarly, Wada *et al.* [102] have carried out gas evolution experiments on Zircaloy at pH 10 and pH 12.5, and temperatures of 30°C and 50°C, and obtained decreasing corrosion rates over a period of 300 days. The long-term corrosion rates at pH 12.5 were 2×10^{-4} μm yr^{-1} and 3×10^{-4} μm yr^{-1} at 30°C and 50°C respectively.

From the information summarised in Section 7, corrosion of Zircaloy will generate hydrogen once conditions have become anaerobic. Therefore a model for corrosion of Zircaloy is included in SMOGG.

8.1 SMOGG model

The corrosion model for Zircaloy is similar to that for carbon steel, discussed in Subsection 4.1.

A total of six parameters must be specified to define the corrosion rate of Zircaloy for a particular corrosive environment:

- Two rate constants (k_a and k_c, giving the base corrosion rates);
- Two characteristic times (t_a and t_c, defining the decrease with time); and
- Two activation energies (E_a and E_c, defining the effect of temperature).

Aerobic corrosion of Zircaloy is expected to be slow, because Zircaloy forms a strongly adherent oxide layer. Therefore, although some Zircaloy will corrode under aerobic conditions, that is neglected in the SMOGG model.

Under anaerobic conditions, stainless steel corrodes to produce hydrogen according to:

$$Zr + 2H_2O \Rightarrow ZrO_2 + 2H_2 \qquad (8.1)$$

It is anticipated that the Zircaloy waste generally will be encapsulated in cement in metal containers to form stable and easily movable packages. The conditioned waste then will be transported to a deep underground repository and at an appropriate time surrounded by a cement-based backfill. Therefore the corrosive environments of interest are:

- An anaerobic, cementitious environment; and
- After resaturation, an alkaline (pH 12.5–13) porewater which has mixed with groundwater containing chloride ions and various other inorganic salts.

To summarise, the environments which have to be considered in SMOGG are:

Conditions	Zircaloy
Atmospheric corrosion	Not required
Aerobic corrosion in grout, low chloride	Not required
Anaerobic corrosion, low chloride	Required
Anaerobic corrosion, high chloride	Required

8.2 Focussed review of corrosion data

The data requirements for SMOGG are summarised in Subsection 8.1. For each phase, consideration needs to be given to whether there is any difference between the acute (*i.e.* over a short period) corrosion rate and the chronic or long-term corrosion rate. It is also necessary to take account of the characteristic time for the acute and chronic phases and possible effects of temperature.

Having reviewed the available literature on the corrosion of Zircaloy, the most relevant data for each stage of the SMOGG model have been selected. The corrosion rates chosen are listed in Subsection 8.3 and the reasons for the choice of these values are discussed below.

(a) Anaerobic corrosion, low chloride

Although Zircaloy is a highly passive material, the work by Kurashige [101] and Wada [102] indicates that there is a higher corrosion rate initially under anaerobic conditions, which gradually falls with time. Measurements showed a higher corrosion rate during the first 100 days and so a characteristic time of 0.1 years has been selected for the acute phase. From this characteristic time and the average corrosion rate over 100 days, the acute rate constant for SMOGG is calculated from Equation (4.1) as 0.02 μm yr^{-1}. There is a temperature dependence during the acute phase, with the corrosion rate being higher at higher temperature (*i.e.* there is an increase of a factor of ~3 from 30°C to 45°C), but there are insufficient data to be able to derive an activation energy.

The corrosion rate in the long term is virtually constant, at least within the timescales that are achievable experimentally. A rate constant of 0.001 μm yr^{-1} and an infinite characteristic time have been selected. This is consistent with the electrochemical measurements made by Hansson [64] and the gas generation experiments of Mihara [73]. Wada's work suggests that the corrosion rate may fall to even lower values in the long-term, so choosing an infinite characteristic time represents a conservative approach. The long-term rate is independent of temperature.

(b) Anaerobic corrosion, high chloride

Chloride is not expected to affect the anaerobic corrosion behaviour significantly, so the parameters in SMOGG will be the same as for the low chloride case.

8.3 Selection of data recommended for use in SMOGG

The objective of this study was to parameterise the corrosion model for Zircaloy that has been implemented in SMOGG. In Subsection 8.2, the available data have been identified and interpreted, as far as possible, to give values for the various parameters.

The set of parameters for Zircaloy corrosion recommended for use in SMOGG is summarised in the following table.

Stage in SMOGG model		Zircaloy
Atmospheric	acute	No acute stage
	chronic	Not required
Aerobic, grout, low chloride	acute	No acute stage
	chronic	Not required
Anaerobic, low chloride	acute	k_a = 0.02 μm yr^{-1} at 30°C k_a = 0.06 μm yr^{-1} at 45°C t_a = 0.1 years
	chronic	k_c = 0.001 μm yr^{-1} $t_c = \infty$ [1] No temperature dependence
Anaerobic, high chloride	acute	k_a = 0.02 μm yr^{-1} at 30°C k_a = 0.06 μm yr^{-1} at 45°C t_a = 0.1 years
	chronic	k_c = 0.001 μm yr^{-1} $t_c = \infty$ [1] No temperature dependence

[1] In using the SMOGG model a finite value is required; a value much greater than the duration of the calculation should be used (e.g. 10^6 years).

8.4 Discussion

Having derived a parameterisation of the SMOGG model for the corrosion rate of Zircaloy (Subsection 8.3), it is useful to compare the resulting values with the corrosion rates used previously.

In all earlier assessments of gas generation in repositories for Nirex, it has been assumed that the Zircaloy could be combined with the stainless steel. (See Subsection 6.4 for more details on the corrosion rate of stainless steel).

In the *Nirex 97* assessment of gas generation from radioactive wastes [80], the Zircaloy (chronic) corrosion rate was assumed to be: 0.1 μm yr^{-1} under aerobic conditions; and 0.03 μm yr^{-1} under anaerobic conditions.

Subsequently, a temperature-dependence for the aerobic (chronic) corrosion rate of Zircaloy was derived:

Temperature, T	20°C	35°C	50°C	80°C
Corrosion rate	0.029 μm yr^{-1}	0.066 μm yr^{-1}	0.150 μm yr^{-1}	0.782 μm yr^{-1}
Factor, f_c	1.000	2.282	5.207	27.113

The anaerobic (chronic) corrosion rate of Zircaloy was still assumed to be 0.03 μm yr^{-1}.

Subsequent assessments of gas generation from radioactive waste, such as the Generic Post-closure Performance Assessment (GPA) [2], generally reused this parameterisation.

Comparing the numbers listed above with the (chronic) corrosion rates given in Subsection 8.3, it can be seen that:

- In the GPA the long-term aerobic corrosion rate at 20°C, *i.e.* about 0.03 μm yr^{-1}, is different to the assumption made in SMOGG, *i.e.* 0.0 μm yr^{-1}.

- The long-term anaerobic corrosion rate used in earlier assessments of gas generation in repositories, *i.e.* 0.03 μm yr^{-1}, is more than an order of magnitude larger than the value now being recommended, *i.e.* 0.001 μm yr^{-1}.

In conclusion, the assumption that Zircaloy would behave like stainless steel appears to be conservative.

The less-reactive metals (*i.e.* carbon steel, stainless steel and Zircaloy) may be present in some cement encapsulated wastes, and will corrode under aerobic and anaerobic alkaline conditions. Under anaerobic conditions the metals will corrode to form hydrogen.

This report identifies the various corrosive environments that could be experienced by these encapsulated metal wastes during their long-term management (*i.e.* during surface storage and transportation, and then in a deep geological repository, both before and after resaturation with a groundwater that could have a high chloride concentration). For each environment, relevant corrosion rate data for carbon steel, stainless steel and Zircaloy have been compiled from the literature. The literature survey has focused on metal loss and gas generation as a result of general corrosion rather than localised corrosion (the latter is unlikely to contribute significantly to gas generation). The effects on the corrosion rates of a number of variables (including oxygen concentration, temperature and chloride concentration) have been considered.

These experimental data have been reviewed critically, and, where appropriate, used to calibrate the SMOGG corrosion model. From this information, parameters which should be used in the SMOGG corrosion model for the less-reactive metals (*i.e.* carbon steel, stainless steel and Zircaloy) have been selected.

The main conclusions from this work are as follows:

(a) In general, corrosion rate data for carbon steel, stainless steel and Zircaloy are required for neutral and alkaline solutions, and gaseous atmospheres, under aerobic and anaerobic conditions, over a range of chloride concentrations and temperatures, to fully describe the possible range of conditions during radioactive waste management.

(b) Most of the data for the required conditions are available in the literature, although there is only a small amount of information available for Zircaloy in all conditions and for atmospheric corrosion of steels at elevated temperature.

(c) Interpretation of the corrosion rate data identified is required to parameterise the SMOGG model. SMOGG has been calibrated for carbon steel under anaerobic conditions, providing directly applicable values for use in the model. For aerobic conditions and for stainless steels and Zircaloy a detailed calibration was not possible, so parameter values for SMOGG were selected based on direct interpretation of literature data.

(d) A database has been collated providing all the parameter values for corrosion of steels and Zircaloy recommended for performing gas generation calculations using SMOGG (see the summary table below).

Selected corrosion data for use in SMOGG, based on assessment of literature and calibration

Stage in SMOGG model		Carbon steel	Stainless steel	Zircaloy
Atmospheric	acute	Not required	No acute stage	No acute stage
	chronic	Not required	k_c = 0.03 μm yr^{-1} t_c = ∞ [1] No temperature dependence (0–50°C)	Not required
Aerobic, grout, low chloride	acute	k_a = 200 μm yr^{-1} at 20°C t_a = 0.003 years Activation energy E_a = 19 kJ mol^{-1}	No acute stage	No acute stage
	chronic	k_c = 0.1 μm yr^{-1} at 20°C t_c ~ ∞ [1] Activation energy E_c = 19 kJ mol^{-1}	k_c = 0.02 μm yr^{-1} at 20°C t_c = ∞ [1] Activation energy E_c = 50 kJ mol^{-1}	Not required
Anaerobic, low chloride	acute	k_a = 0.5 μm yr^{-1} at 30°C t_a = 0.5 years Activation energy E_a = 56 kJ mol^{-1}	No acute stage	k_a = 0.02 μm yr^{-1} at 30°C k_a = 0.06 μm yr^{-1} at 45°C t_a = 0.1 years
	chronic	k_c = 0.005 μm yr^{-1} t_c = ∞ [1] No temperature dependence	k_c = 0.01 μm yr^{-1} t_c = ∞ [1] No temperature dependence	k_c = 0.001 μm yr^{-1} t_c = ∞ [1] No temperature dependence
Anaerobic, high chloride	acute	k_a = 0.5 μm yr^{-1} at 30°C t_a = 0.5 years Activation energy E_a = 56 kJ mol^{-1}	No acute stage	k_a = 0.02 μm yr^{-1} at 30°C k_a = 0.06 μm yr^{-1} at 45°C t_a = 0.1 years
	chronic	k_c = 0.005 μm yr^{-1} t_c = ∞ [1] No temperature dependence	k_c = 0.01 μm yr^{-1} t_c = ∞ [1] No temperature dependence	k_c = 0.001 μm yr^{-1} t_c = ∞ [1] No temperature dependence

Notes:

[1] In using the SMOGG model a finite value is required. A value much greater than the period of the calculation should be used (e.g. 10^6 years).

1 W.R. Rodwell, A.W. Harris, S.T. Horseman, P. Lalieux, W. Müller, L. Ortiz Amaya and K. Pruess, *Gas Migration and Two-phase Flow through Engineered and Geological Barriers for a Deep repository for Radioactive Waste (A Joint EC/NEA Status Report)*, European Commission Report EUR 19122 EN, 1999.

2 *Generic Repository Studies. Generic Post-closure Performance Assessment*, Nirex Report N/080, July 2003.

3 W.R. Rodwell, *Specification for SMOGG Version 4.0: a Simplified Model of Gas Generation from Radioactive Wastes*, Serco Assurance Report SERCO/ERRA-0452, Version 5, 2005.

4 B.T. Swift, *SMOGG (Version 4.0): a Simplified Model of Gas Generation from Radioactive Wastes: User Guide*, Serco Assurance Report SA/ENV-0511, Version 5, 2005.

5 A.R. Hoch, N.R. Smart and B. Reddy, *A Survey of Reactive Metal Corrosion Data for Use in the SMOGG Gas Generation Model*, SA/ENV-0895, 2007.

6 C.C. Naish, N.R. Smart and M.J. Longster, *Corrosion Principles for the Assessment of Containers for Intermediate and Low Level Radioactive Waste*, AEA-ESD-0066, Issue B, 1996.

7 *DECHEMA Corrosion Handbook: Corrosive Agents and their Interaction with Materials*, Volume 1 Potassium Hydroxide (1987), Volume 2 Sodium Hydroxide (1988), Volume 3 Lithium Hydroxide (1988), Volume 5 Alkaline Earth Hydroxides (1989), Volume 7 Atmosphere (1990), Volume 10 Drinking water (1991), Volume 11 Seawater (1992), eds. D.Behrens (vols. 1-9), G.Kreysa (vols. 10 and 11) and R.Eckerman (vols. 10 and 11).

8 F.N. Speller, *Corrosion: Causes and Prevention*, McGraw-Hill, 1951.

9 H.H. Uhlig, *Corrosion and Corrosion Control*, J. Wiley, 1971.

10 H.H. Uhlig, *The Corrosion Handbook*, J. Wiley, 1948.

11 M. Schumaker (ed.), *Seawater Corrosion Handbook*, Noyes Data Corporation, 1979.

12 N. Sridhar, G.A. Cragnolino, D.S. Dunn and H.K. Manaktala, *Review of Degradation Modes of Alternate Container Designs and Materials*, SWI Report CNWRA 94-010, 1994.

13 G.C. Moran and P. Labine (eds.), *Corrosion Monitoring in Industrial Plants*, ASTM STP 908, 1986.

14 G.S. Haynes and R. Baboian, *Laboratory Corrosion Tests and Standards*, ASTM STP 866, 1983.

15 G.P. Marsh, A.H. Harker and K.J. Taylor, *Corrosion of Carbon Steel Nuclear Waste Containers in Marine Sediment*, Corrosion **45**(7), 579, 1989.

16 R. Grauer, B. Knecht, P. Kreis and J.P. Simpson, *The Long Term Corrosion Rate of Passive Iron in Anaerobic Alkaline Solutions*, Werkstoffe und Korrosion **42**, 637, 1991.

17 R. Grauer, B. Knecht, P. Kreis and J.P. Simpson, *Hydrogen Evolution from Corrosion of Iron and Steel in Intermediate Level Waste Repositories*, p. 295 in Scientific Basis for Nuclear Waste Management **XIV**, T.A.Abrajano and L.H.Johnson (eds.), 1991.

18 J. Jelinek and P. Neufeld, *Kinetics of Hydrogen Formation from Mild Steel in Water under Anaerobic Conditions*, Corrosion **38**(2), 99, 1982.

19 U.R. Evans and J.N. Wanklyn, *Evolution of Hydrogen from Ferrous Hydroxide*, Nature **162**, 27, 1948.

20 A. Vértes and I. Czako-Nagy, *Mössbauer Spectroscopy and its Application to Corrosion Studies*, Electrochimica Acta **34**(6), 721, 1989.

21 R.P. Frankenthal and J. Kruger, *Passivity of Metals*, The Electrochemical Society, 1978.

22 I. Kalashnikova, L. Nunez and F. Corvo, *Corrosion Behaviour of Metallic Materials in the Cuban Caribbean Sea*, Corrosion Reviews **13**(2-4), 261, 1995.

23 T. Peev, M.K. Georgieva, S. Nagy and A. Vértes, *Mössbauer Study of Corrosion Products Formed on α-Iron in Sea Water,* Radiochem. Radioanal. Lett. **33**, 265, 1978.

24 J. Chen, Z. Cai, Z. Wang and H. Zhang, *A Study of the Barrier Layer Rust Formed on Low Alloy Steels in Sea water by Conversion Electron Mössbauer Spectroscopy*, Proceedings of ICAME, Jaipur, India, 264, 1981.

25 K.K. Sagoe-Crentsil and F.P. Glasser, *Constitution of Green Rust and Its Significance to the Corrosion of Steel in Portland Cement*, Corrosion **49**(6), 457, 1993.

26 P. Refait and J.-M.R. Genin, *The Oxidation of Ferrous Hydroxide in Chloride-Containing Aqueous Media and Pourbaix Diagrams of Green Rust One*, Corrosion Science **34**(5), 797, 1993.

27 S. Haupt and H.H. Strehblow, *Corrosion, Layer Formation, and Oxide Reduction of Passive Iron in Alkaline Solution: A Combined Electrochemical and Surface Analytical Study*, Langmuir **3**, 873, 1987.

28 A.M. Riley and J.M. Sykes, *The Cathodic Reduction of Passive Films on Low-Alloy Steel in Carbonate Solutions*, Corrosion Science **28**(8), 799, 1988.

29 E.R. Vago and E.J. Calvo, *Electrocatalysis of Oxygen Reduction at Fe_3O_4 Oxide Electrodes In Alkaline Solutions*, J.Electroanal. Chem. **339**, 41, 1992.

30 S. Nasrazadani and A. Raman, *Formation and Transformation of Magnetite (Fe_3O_4) on Steel Surfaces under Continuous and Cyclic Water Fog Testing*, Corrosion **49**(4), 294, 1993.

31 H. Konno, M. Kawai and M. Nagayama, *The Mechanism of Spontaneous Dissolution of the Air-Formed Oxide Film on Iron in a Deaerated Neutral Phosphate Solution*, Surface Technology **24**, 259, 1985.

32 D. Gilroy and J.E.O. Mayne, *The Breakdown of the Air-Formed Oxide Film on Iron Upon Immersion in Solutions of pH 6-13*, British Corrosion Journal **1**, 102, 1965.

33 P.E. Francis and A.D. Mercer, *Corrosion of a Mild Steel in Distilled Water and Chloride Solutions: Development of a Test Method*, p. 184 in 'Laboratory Corrosion Tests and Standards', ASTM STP 866, G.S.Haynes and R.Baboian (eds.), 1985.

34 A. Higginson, *The Effect of Physical and Chemical Factors on the Corrosivity of a Synthetic Minewater*, MINTEK Report M140, 1984.

35 A.D. Mercer and E.A. Lumbard, *Corrosion of Mild Steel in Water*, British Corrosion Journal **30**(1), 43, 1995.

36 K. Hara, H. Ishikawa, A. Honda and N. Sasaki, *Influence of Dissolved Oxygen on the Generation Rate of Hydrogen Gas with Corrosion of Carbon Steel*, Proc. Workshop on Gas Generation and Release from Radioactive Waste Repositories, Aix-en-Provence, September 1991, p. 121, OECD, 1992.

37 K. Videm and A. Dugstad, *Corrosion of Carbon Steel in an Aqueous Carbon Dioxide Environment Part 1: Solution Effects*, Materials Performance p. 63, March 1989.

38 K. Videm and A. Dugstad, *Corrosion of Carbon Steel in an Aqueous Carbon Dioxide Environment Part 2: Film Formation*, Materials Performance, p. 46, April 1989.

39 D.H. Lester, R.T. Stula and B.E. Kirstein, *Waste Package Performance Evaluation*, ONWI-302, 1983.

40 N.R. Smart, A.P. Rance and L.O. Werme, *The Effect of Radiation on the Anaerobic Corrosion of Steel*, Journal of Nuclear Materials **379**, 97, 2008.

41 A.J. Sedriks, *Corrosion of Stainless Steels*, John Wiley, second edition, pg. 211,1996.

42 F.L. Laque, *Marine Corrosion. Causes and Prevention*, J. Wiley, 1975.

43 D.R. Diercks, A.B. Hull and T.F. Kassner, *Analysis of Corrosion Data for Carbon Steels in Simulated Salt Repository Brines and Acid Chloride Solutions at High Temperatures*, Conf-880377-3, DE88-012030, Joint US/FRG Technical Exchange Workshop, Albuquerque, March 1988.

44 D.R. Diercks and T.F. Kassner, *Analysis of the Corrosion of Carbon Steels in Simulated Salt Repository Brines and Acid Chloride Solutions at High Temperatures*, ANL/PPRNT-90-207, DE90 009164, 1988.

45 J.P. Simpson and J. Weber, *Hydrogen Evolution from Corrosion in Nuclear Waste Repositories*, UK Corrosion '88, p. 33, 1988.

46 N. Platts, D.J. Blackwood and C.C. Naish, *Anaerobic Oxidation of Carbon Steel in Granitic Groundwaters: A Review of the Relevant Literature*, AEA-InTec-1413, 1994.

47 A.P. Akolzin, P. Ghosh and Y.Y. Kharitonov, *Application and Peculiarity of $Ca(OH)_2$ as Inhibitor in Presence of Corrosion Activators*, British Corrosion Journal **20**(1), 32, 1985.

48 M. Yasuda, K. Fukumoto, H. Koizumi, Y. Ogata and F. Hine, *On the Active Dissolution of Metals and Alloys in Hot Concentrated Caustic Soda*, Corrosion **43**(8), 492, 1987.

49 H. Grubitsch, L. Binder and F. Hilbert, *The Influence of Various Concentrations of Chloride Ions on the Active-Passive Corrosion Susceptibility of Steel in Saturated Calcium Hydroxide Solution*, Werkstoffe und Korrosion **30**(4), 241, 1979.

50 N. Kudo, *Corrosion and Its Prevention of Reinforcement in Concrete*, Corrosion Engineering **42**(7), 565, 1993.

51 A.P. Crane (ed.), *Corrosion of Reinforcement in Concrete Construction*, Ellis Horwood, 1983.

52 K. Tuuti, *Corrosion of Steel in Concrete*, Swedish Cement and Concrete Research Institute, 1982.

53 J.E. Slater, *Corrosion of Metals in Association with Concrete*, ASTM STP 818, 1983.

54 A. Alonso and C. Andrade, *Life Time of Rebars in Carbonated Concrete*, in 'Progress in the Understanding and Prevention of Corrosion', J.M.Costa and A.D.Mercer (eds.), Institute of Materials, p. 634, 1993.

55 H. Arup, *The Mechanisms of the Protection of Steel by Concrete,* p. 151 in 'Corrosion of Reinforcement in Concrete Construction', A.P.Crane (ed.), Ellis Horwood, 1983.

56 E. Escalante, T. Oka and U. Bertocci, *Effect of Oxygen Transport and Resistivity of the Environment on the Corrosion of Steel*, p. 287 in Scientific Basis for Nuclear Waste Management **XIV**, Materials Research Society Symposium proceedings Volume 212, T.A.Abrajano, L.H.Johnson (eds.) 1991.

57 C.M. Preece, F.O. Grønwold and T. Frølund, *The Influence of Cement Type on the Electrochemical Behaviour of Steel in Concrete*, p. 393 in Corrosion of Reinforcement in Concrete Construction, London, SCI, 1983.

58 A. Seghal, Y.T. Kho, K. Osseo-Asare and H.W. Pickering, *Comparison of Corrosion Rate-Measuring Devices for Determining Corrosion Rate of Steel-in-Concrete Systems*, Corrosion, **48**(10), 871, 1992.

59 J.A. Gonzalez, W. Lopez and P. Rodriguez, *Effects of Moisture Availability on Corrosion Kinetics of Steel Embedded In Concrete*, Corrosion **49**(12), 1004-1010, 1993.

60 J.N. Enevoldsen, C.M. Hansson and B.B. Hope, *The Influence Of Internal Relative Humidity On The Rate Of Corrosion Of Steel Embedded In Concrete And Mortar*, Cement and Concrete Research, **24**(7), 1373-1382, 1994.

61 J. Flis, S. Sabol, H.W. Pickering, A. Seghal, K. Osseo-Asare and P.D. Cady, *Electrochemical Measurements on Concrete Bridges for Evaluation of Reinforcement Corrosion Rates*, Corrosion **49**(7), 601, 1993.

62 S.E. Benjamin and J.M. Sykes, *Chloride Induced Pitting Corrosion of Swedish Iron in Ordinary Portland Cement Mortars and Alkaline Solutions: The Effect of Temperature*, p. 59 in 'Corrosion of Reinforcement in Concrete', C.L. Page, K.W.J. Treadaway, P.B. Bamforth (eds.), Elsevier, 1990.

63 C.M. Hansson, *Hydrogen Evolution in Anaerobic Concrete Resulting From Corrosion of Steel Reinforcement*, SKB-1984-11-28, 1984.

64 C.M. Hansson, *The Corrosion of Steel and Zirconium in Anaerobic Concrete*, pg. 475 in Scientific Basis for Nuclear Waste Management IX, L. Werme (ed.), **50**, 475, 1985.

65 C.M. Hansson, *The Corrosion of Steel in Anaerobic Concrete and the Associated Evolution of Hydrogen*, SKB report SFR 87-02, 1987.

66 C.C. Naish, P.H. Balkwill, T.M. O'Brien, K.J. Taylor and G.P. Marsh, *The Anaerobic Corrosion of Carbon Steel in Concrete*, Nirex Report NSS/R273, 1990.

67 C.C. Naish, P.H. Balkwill, T.M. O'Brien, K.J. Taylor and G.P. Marsh, *The Anaerobic Corrosion of Carbon Steel in Concrete*, EUR 13663, 1991.

68 R. Grauer, *The Corrosion Behaviour of Carbon Steel in Portland Cement*, NAGRA Technical Report 88-02E, 1988.

69 N.R. Smart, D.J. Blackwood, G.P. Marsh, C.C. Naish, T.M. O'Brien, A.P. Rance and M.I. Thomas, *The Anaerobic Corrosion of Carbon and Stainless Steels in Simulated Cementitious Repository Environments: A Summary Review of Nirex Research*, AEAT/ERRA-0313, 2004.

70 N.R. Smart, D.J. Blackwood and L. Werme, *The Anaerobic Corrosion of Carbon Steel and Cast Iron in Artificial Groundwaters*, SKB Report TR-01-22, 2001.

71 N.R. Smart, D.J. Blackwood and L. Werme, *Anaerobic Corrosion of Carbon Steel and Cast Iron in Artificial Groundwaters: Part 1–Electrochemical Aspects*, Corrosion **58**(7), 547, 2002.

72 N.R. Smart, D.J. Blackwood and L. Werme, *Anaerobic Corrosion of Carbon Steel and Cast Iron in Artificial Groundwaters: Part 2-Gas Generation*, Corrosion **58**(8), 627, 2002.

73 M. Mihara, T. Nishimura, R. Wada and A. Honda, *Estimation on Gas Generation and Corrosion Rates of Carbon Steel, Stainless Steel and Zircaloy In Alkaline Solutions Under Low Oxygen Condition* (in Japanese), Saikuru Kiko Giho **15**, 91-101, Jun 2002.

74 T. Nishimura, R. Wada and K. Fujiwara, *Evaluation of Gas Generation Rates Caused by Metal Corrosion Under the Geological Repository Conditions* (in Japanese), R and D Kobe Seiko Giho **53**(3), 78-83, Dec 2003.

75 C. Arya and Y. Xu, *Effect of Cement Type on Chloride Binding and Corrosion of Steel in Concrete*, Cement and Concrete Research **25**(4), 893-902, 1995.

76 T. Liu and R.W. Weyers, *Modeling the Dynamic Corrosion Process in Chloride Contaminated Concrete Structures*, Cement and Concrete Research **28**(3), 365-379, 1998.

77 R. Fujisawa, T. Cho, K. Sugahara, Y. Takizawa, Y. Horikawa, T. Shiomi and M. Hironaga, *The Corrosion Behaviour of Iron and Aluminum Under Waste Disposal Conditions*, Mat. Res. Soc. Symp. Proc. **465**, 675, 1997.

78 P. Biddle, D. McGahan, J.H. Rees and P.E. Rushbrook, *Gas Generation in Repositories*, UKAEA Report AERE R 12291, 1987.

79 P.J. Agg, A.D. Moreton, J.H. Rees, W.R. Rodwell and P.J. Sumner, *NSARP Reference Document: Gas Generation and Migration, January 1992*, Nirex Report NSS/G120, 1993.

80 A.J. Baker, D.A. Lever, J.H. Rees, M.C. Thorne, C.J. Tweed and R.S. Wikramaratna, *Nirex 97: An Assessment of the Post-closure Performance of a Deep Waste Repository at Sellafield. Volume 4: The Gas Pathway*, Nirex Science Report S/97/012, 1997.

81 M. Boath and W.M. Tearle, *Generic Assessment of Gas Generation from an ILW/LLW Repository*, AEA Technology Report AEAT-5649, 1999

82 N.R. Smart, *Temperature Limits - Corrosion Considerations*, AEA Technology Report for Nirex (customer reference: TEPT/2385), Draft, 1996.

83 S.M. Morsy, S.M. El-Raghy, A.A. Elsaed and A.E. El-Mehairy, *Effect of Cations on the Corrosion of Stainless Alloys in Saline Water at Elevated Temperatures*, Arab Republic of Egypt Atomic Energy Establishment Report 232, 1979.

84 S.M. Sharland and C.J. Newton, *The Long Term Prediction of Corrosion of Stainless Steel Nuclear Waste Canisters*, in Scientific Basis for Nuclear Waste Management **XII**, W. Lutze and R.C. Ewing (eds.), Materials Research Society Symposium Proceedings, **127**, p. 373, 1989 and Nirex Report NSS/R136, 1989.

85 D.J. Blackwood, C.C. Naish, S.M. Sharland and A.M. Thompson, *An Experimental and Modelling Study to Assess the Initiation of Crevice Corrosion in Stainless Steel Containers for Radioactive Waste*, AEA Technology Report AEAT/ERRA-0300, 2002.

86 J.F. McGurn and B.A. McKean, *Stainless Steel For Reinforcing Bar In Concrete*, in Environmentally Induced Cracking of Metals, 39th Annual Conference of Metallurgists of CIM; Ottawa, Ontario; Canada; 20-23 Aug. 2000, 253-263, 2000.

87 D.J. Cochrane, *Stainless Steel Reinforcement for Durability In Concrete Structures*, Nuclear Energy **37**(5), 331-5, 1998.

88 M.F. Hurley and J.R. Scully, *Threshold Chloride Concentrations of Selected Corrosion Resistant Rebar Materials Compared to Carbon Steel*, Corrosion/2005, paper 05259, 2005.

89 L. Bertolini, M. Gastaldi, T. Pastore, M.P. Pedeferri, *Corrosion Behaviour of Stainless Steels in Chloride Contaminated and Carbonated Concrete*, International Journal for Restoration of Buildings and Monuments **6**(3), 273-292, 2000.

90 K. W. J. Treadaway, R. N. Cox and B. L. Brown, *Durability of Corrosion Resisting Steel in Concrete*, Proc. Inst. Civ. Engrs., Part 1 **86**, 305-331, 1989.

91 N.R. Smart and N.J. Montgomery, *The Repassivation of Carbon Steel and Stainless Steel in Deaerated Alkaline Conditions: An Electrochemical and Surface Analytical Investigation*, AEA Technology Report AEAT/R/ENV/0232, 2001.

92 Z. Szklarska-Smialowska, *Pitting Corrosion of Metals*, National Association of Corrosion Engineers, 1986.

93 C.P. Jackson and N.R. Smart, *Assessment of Pit Propagation Rates in Stainless Steel*, SA/EIG/14921/C009, 2006.

94 I.O. Wallinder, J. Lu, S. Bertling and C. Leygraf, *Release Rates of Chromium and Nickel From 304 and 316 Stainless Steel During Urban Atmospheric Exposure - A Combined Field and Laboratory Study*, Corrosion Science **44**(10), 2303-2319, 2002.

95 J.S. Lu, I. Odneval and C. Leygraf, *Atmospheric Corrosion of 304 and 316 Stainless Steels*, Acta Metallurgica Sinica (English Letters) **12**(5), 958-961, 1999.

96 J.B. Cotton and B.H. Hanson, *Titanium and Zirconium*, chapter 5.4 in 'Corrosion', L.L. Shreir, R.A. Jarman and G.T. Burnstein (eds.), Butterworth-Heinemann, (1994).

97 T.Yau, *Corrosion Comparisons Between Zirconium and Titanium*, Werkstoffe und Korrosion, **43**(7), 358, (1992).

98 T.L. Yau, R.T. Webster, *Corrosion of Zirconium and Hafnium*, Metals handbook ninth edition. Volume 13. Corrosion, Gulf Publishing Company. pg 707, (1987).

99 Z.A. Munir, *An Assessment of the Long Term Storage of Zircaloy Fuel Rods in Water*, California Univ., Davis (USA). Dept. of Mechanical Engineering, report number CAEC-012, NTIS report PB-291 013, 1978.

100 S. Hietanen, K. Klemetti and P. Aaltonen, *Electrochemical Study On The Corrosion Of The Metal Waste Embedded In Concrete*, in Finnish, YJT-87-02, 1987.

101 T. Kurashige, R. Fujisawa, I. Inagaki and M. Senoo, *Gas Generation Behaviour of Zircaloy-4 Under Waste Disposal Conditions* in 7th International Conference Proceedings on Radioactive Waste Management and Environmental Remediation (ICEM'99), ASME, Nagoya, Japan, Sept 26-30, 1999.

102 R. Wada, T. Nishimura, K. Fujiwara, M. Tanabe and M. Mihara, *Experimental Study on Hydrogen Gas Generation Rate from Corrosion of Zircaloy and Stainless Steel Under Anaerobic Alkaline Condition*, in 7th International Conference Proceedings on Radioactive Waste Management and Environmental Remediation (ICEM'99), ASME, Nagoya, Japan, Sept 26-30, 1999.

103 K.A. Bond and C.J. Tweed, *Groundwater Compositions for the Borrowdale Volcanic Group, Boreholes 2,4 and RCF3, Sellafield, Evaluated Using Thermodynamic Modelling*, Nirex Report NSS/R397, 1995.

104 J.P. Simpson, R. Schenk and B. Knecht, *Corrosion Rate of Unalloyed Steels and Cast Irons In Reducing Granitic Groundwaters and Chloride Solutions*, p. 429 in Scientific Basis for Nuclear Waste Management **IX**, L.Werme (ed.), 1985.

105 C.W. Borgmann, *Initial Corrosion Rate of Mild Steel - Influence of the Cation*, Ind. Eng. Chem. **29**(7), 814, 1937.

106 W.R. Braithwaite and K.A. Lichti, *Surface Corrosion of Metals in Geothermal Fluids at Broadlands, New Zealand,* in 'Geothermal Scaling and Corrosion' ASTM STP 717 L.A. Casper and T.R. Pinchback (eds.), 1980.

107 W. Breckheimer and J. D'Ans, *Corrosion of Iron Influenced by Temperature Differences of the Attacking Electrolyte*, Werkst. Korros. **5**(2), 43, 1954.

108 F. Canadillas, E. Smailos and R. Koster, *Corrosion Studies on the Suitability of a Mild Steel for the Disposal of High Level Waste Products*, Kernforschunszentrum Karlsruhe, KfK 3549, 1983.

109 M.A. Elmorsi and R.M. Issa, *Corrosion of Metal Pipes in Ground Water*, Bulletin of Electrochemistry **4**(9), 785, 1988.

110 K.B. Gaonkar, P.K. Chauhan and H.S. Gadiyar, *Corrosion Behaviour of Mild Steel in Natural and Distilled Waters: Effect of Temperature and Addition of Various Chemicals,* Corrosion and Maintenance, July, 1983.

111 A. Hache, Rev. Métall. **1**, 76, 1956, taken from *DECHEMA Corrosion Handbook: Corrosive Agents and Their Interaction With Materials*, Volume 11 'Seawater', G.Kreysa and R.Eckerman (eds.), 1992.

112 K.H. Ho and S.K. Roy, *Corrosion of Steel in Tropical Sea Water*, British Corrosion Journal **29**(3), 233, 1994.

113 A. Honda, T. Teshima, K. Tsurudome, H. Ishikawa, Y. Yusa and N. Sasaki, *Effect of Compacted Bentonite on the Corrosion Behaviour of Carbon Steel as Geological Isolation Overpack Material*, p. 287 in Scientific Basis for Nuclear Waste Management **XIV**, T.A. Abrajano and L.H. Johnson (eds.) 1991.

114 E.R. Kennedy and J.S. Wilson, *New York Harbour Corrosion - Port of New York Authority Conducts Pile Survey*, Mater. Protection **6**, 53, 1967.

115 V.G. Kritsky, V.V. Morozov, A.F. Nechaev, Y.A. Khitrov, N.G. Petrik, N.N. Kalyazin and T.F. Makarchuk, *Material Corrosion Under Spent Nuclear Fuel Storage Conditions*, in 'Materials Reliability in the Backend of the Nuclear Cycle', IAEA-TECDOC-421, 1987.

116 D. Kuron, H. Grafen, H-P. Batroff, K. Fassler and R. Munster, *Influence of Chloride Content in Tap Water on the Corrosion of Unalloyed Steel*, Werkstoffe und Korrosion **36**, 68, 1985.

117 C.P. Larrabee, *Steel Has Low Corrosion Rate During Long Sea Water Exposure*, Materials Protection 95, Dec 1962.

118 R.D. McRight and H. Weiss, *Corrosion Behaviour of Carbon Steels under Tuff Repository Environmental Conditions*, p. 287 in Scientific Basis for Nuclear Waste Management **VIII**, C.M. Jantzen, J.A. Stone and R.C. Ewing (eds.), 1985.

119 M.D. Merz, *State-of-the-Art Report on Corrosion Data Pertaining to Metallic Barriers for Nuclear Waste Repositories*, Pacific Northwest Laboratory report, PNL-4474, 1982.

120 W. Nissing, W. Friehe and W. Schwenk, *Influence of Oxygen Content, pH and Flow Velocity under Corrosion of Hot-Dip Galvanised and Bare Piping of Unalloyed Steel in Potable Water*, Werkstoffe und Korrosion **33**(6), 346, 1982.

121 M.H. Peterson and L.J. Waldron, *Investigation of Mild Steel Corrosion Rate in San Diego Harbor*, Corrosion **17**, 114, 1961.

122 F.M. Reinhart, *Corrosion of Materials in Hydrospace*, U.S. Naval Civil Engineering Lab. Port Hueneme, California, Technical Report R504, 1966.

123 F.M. Reinhart, *Corrosion of Materials in Hydrospace - Part I. Irons, Steels, Cast Irons and Steel Products*, U.S.Naval Civil Engineering Lab. Port Hueneme, California, Technical Note N-900, 1967.

124 C.P. Larrabee, *Corrosion of Steels in Marine Atmospheres and in Sea Water*, Trans. Electrochem. Soc. **87**, 161, 1945.

125 W. Schwarzkopf, E. Smailos and R. Köster, *In-situ Corrosion Studies on Cast Steel For High-Level Waste Packaging in a Rock Salt Repository*, p. 411 in Scientific Basis for Nuclear Waste Management **XII**, W. Lutze and R.C. Ewing (eds.), 1989.

126 D.W. Shannon, *Economic Impact of Corrosion and Scaling Problems in Geothermal Energy Systems*, Battelle report, BNWL-1866, 1975.

127 J.P. Simpson and J. Weber, *Steel as a Container Material for Nuclear Waste Disposal,* p. 23 in 'Corrosion Problems Related to Nuclear Waste Disposal', European Federation of Corrosion Publication number 7, published by the Institute of Materials, 1992.

128 E. Smailos and R. Koster, *Corrosion Studies on Selected Packaging Materials for Disposal of High Level Wastes*, in 'Materials Reliability in the Backend of the Nuclear Cycle', IAEA-TECDOC-421, 1987.

129 E. Smailos, W. Schwarzkopf and R. Koster, *Corrosion Under Gamma Irradiation and Stress Corrosion Cracking Behaviour of Unalloyed Steels in a $MgCl_2$ Rich Brine*, Conf-880377-3, DE88-012030, Joint US/FRG Technical Exchange Workshop, Albuquerque, March, 1988.

130 E. Smailos, W. Schwarzkopf, R. Köster and B. Fiehn, *Gamma Irradiation and In-situ Studies On Unalloyed Steels for a High Level Waste Packaging in a Rock Salt Repository*, KfK 4529, 1989.

131 E. Smailos, W. Schwarzkopf, R. Köster and K.H. Gruenthaler, *Advanced Corrosion Studies on Selected Packaging Materials for Disposal of HLW Canisters in Rock Salt*, p. 23 in 'Corrosion Problems Related to Nuclear Waste Disposal', European Federation of Corrosion Publication number 7, published by the Institute of Materials, 1992.

132 C.R. Southwell and A.L. Alexander, *Corrosion of Metals in Tropical Waters. Structural Ferrous Materials*, Materials Protection **9**(1), 14, 1970.

133 J.H. White, A.E. Yaniv and H. Schick, *The Corrosion of Metals in the Water of the Dead Sea*, Corrosion Science **6**, 447, 1966.

134 D.J. Blackwood, A.R. Hoch, C.C. Naish, A.P. Rance and S.M. Sharland, *Research on Corrosion Aspects of the Advanced Cold Process Canister*, SKB Technical report 94-12, 1994.

135 A.M. Farvaque-Bera and S. Leistikow, *Electrochemical Studies of the Corrosion Behaviour of a Low-Carbon Steel in Aqueous Chloride Solutions Simulating Accident Conditions of Radioactive Waste Disposal*, Journal of Nuclear Materials **185**, 1, 1991.

136 M. Grassiani, *Corrosion of Carbon Steels in Hot Deaerated Seawater*, p. 260 in Materials Engineering Conference, Haifa, Israel, 1981.

137 J.H. Haberman, D.J. Frydrych and R.E. Westerman, *Corrosion and Hydrogen Permeation of A216 Grade WCA Steel in Hydrothermal Magnesium Containing Brines*, PNL/SRP-SA-15684, Conf-880377-1, DE88-012030, Presented at the Joint US/FRG Technical Exchange Workshop, Albuquerque, March 1988.

138 M. Helie and G. Plante, *HLW Container Corrosion in Geological Disposal Conditions*, p. 445 in Scientific Basis for Nuclear Waste Management **IX**, L.Werme (ed.), 1985.

139 P. Kreis, *Hydrogen Evolution from Corrosion of Iron and Steel in Low/Intermediate Level Waste Repositories*, NAGRA Technical Report 91-21, 1991.

140 P. Kreis and J.P. Simpson, *Hydrogen Gas Generation from the Corrosion of Iron in Cementitious Environments*, in Corrosion Problems Related to Nuclear Waste Disposal, European Federation of Corrosion Publication number 7, published by Institute of Materials, 1992.

141 F.A. Posey and A.A. Palko, *Corrosivity of Carbon Steel in Concentrated Chloride Solution*, Corrosion **35**(1), 38, 1979.

142 R.J. Reda, S.L.A. Hana and J.L. Kelly, *Intergranular Attack Observed in Radiation Enhanced Corrosion of Mild Steel*, Corrosion **44**(9), 632, 1988.

143 R. Schenk, *Untersuchungen Uber Die Wasserstoffbildung Durch Eisen Korrosion Unter Endlagerbdingungen*, NAGRA Technical Report 86-24, 1988.

144 J.P. Simpson and P.H. Vallotton, *Experiments on Container Materials for Swiss High-Level Waste Disposal Projects Part III*, NAGRA Technical report 86-25, 1986.

145 D.J. Smith and O.J. Van Der Schijff, *Corrosion of Galvanised Steel and Carbon Steel in Deaerated Aqueous Solutions of Industrial Fertiliser Chemicals*, British Corrosion Journal **24**(3), 189, 1989.

146 D. Stahl and N.E. Miller, *Long-Term Performance of Materials Used for High-Level Waste Packaging*, NUREG/CR-3427, 1984.

147 H.W. Tas, W. Debruyn and J. Dresselaers, *Compatibility of Candidate Overpack Materials with Deep Argillaceous HLW Disposal Environments*, IAEA-TECDOC-421, 1987.

148 R.E. Westerman, J.H. Haberman, S.G. Pitman, K.H. Pool, K.C. Rhoads and M.R. Telander, *Annual report - FY 1986, Corrosion Behaviour of A216 Grade WCA Mild Steel and Ti Grade 12 Alloy in Hydrothermal Brines*, Battelle report PNL/SRP-6221, 1988.

149 D.J. Blackwood, L.J. Gould, C.C. Naish, F.M.Porter, A.P. Rance, S.M. Sharland N.R. Smart, M.I. Thomas and T. Yates, *The Localised Corrosion of Carbon Steel and Stainless Steel in Simulated Repository Environments*, AEA Technology Report AEAT/ERRA-0318, In Preparation.

150 S.A. Byakova, V.F. Loskutov and I.S. Pogrebova, *Influence of Vanadising on the Corrosion Rate of Steels*, Zaschita Metallov **12**, 552, 1976.

151 D.M. Drazic and C.S. Hao, *Inhibition of Anodic Dissolution of Iron in Alkaline Solutions*, Corrosion Science **23**, 683, 1983.

152 M.A. Hubbe, *Polarisation Resistance Corrosivity Test with a Correction for Resistivity*, British Corrosion Journal **15**, 193, 1980.

153 P.K. Lesnikova and M.K. Frejd, *The Effect of Boriding on the Corrosion Resistance of Steels*, Zaschita Metallov **16**, 312, 1980.

154 W. Schwenk, *Some Aspects of the Corrosion of Iron in Alkaline Solutions and Associated Fundamental Questions*, Werkstoffe und Korrosion **34**, 287, 1983.

155 C. Andrade and C.M. Alonso, *Values of Corrosion Rate of Steel in Concrete to Predict Service Life of Concrete Structures*, in 'Application of Accelerated Corrosion Tests to Service Life Prediction of Materials, ASTM 1194, p. 282, 1994.

156 C. Andrade, C. Alonso and J.A. Gonzalez, *Results of Polarization Resistance and Impedance of Steel Bars Embedded in Carbonated Concrete Contaminated With Chlorides, in* Electrochemical methods in corrosion research (3rd international symposium), Zurich (Switzerland), 12-15 Jul 1988, Mater. Sci. Forum, **44-45,** 329-335, 1989.

157 M.A. Baccay, N. Otsuki, T. Nishida and S. Maruyama, *Influence of Cement Type and Temperature on the Rate of Corrosion of Steel In Concrete Exposed to Carbonation*, Corrosion/2005, Paper 05332, 2005.

158 H.T. Cao, L. Bucea and V. Sirivivatnanon, *Corrosion Rates of Steel Embedded in Cement Pastes*, Cement and Concrete Research **23**(6), 1273-1282, 1993.

159 W-J. Chitty, P. Dillmann, V. L'Hostis and C. Lombard, *Long-Term Corrosion Resistance of Metallic Reinforcements in Concrete A Study of Corrosion Mechanisms Based on Archaeological Artefacts*, Corrosion Science **47**(6), 1555-1581, 2005.

160 J.A. Gonzalez, W. Lopez and P. Rodriguez, *Effect of Moisture Availability on Corrosion Kinetics of Steel Embedded in Concrete*, Corrosion **49**(12), 1004, 1993.

161 T.J. Hakkarainen, *Corrosion Of Reinforcing Steel In Concrete - Electrochemical Laboratory Experiments*, Electrochemical Methods In Corrosion Research (3rd international symposium), Mater. Sci. Forum **44-45**, 347-356, 1989.

162 W. Hauser and R. Köster, *Corrosion Behaviour of Nodular Cast Iron Casks for Low and Intermediate Level Wastes*, p. 437 in Scientific Basis for Nuclear Waste Management **IX**, L.Werme (ed.), 1985.

163 D.J. Lee, *PETF Phase III Generic Studies. Generic Report on the Corrosion of Mild Steel in Contact with Cement Pastes,* CPDG(88)P019, PETF(88)P39, 1988.

164 D.K. Lysogorski, P. Cros, W.H. Hartt, *Performance of Corrosion Resistant Reinforcement as Assessed by Accelerated Testing and Long Term Exposure in Chloride Contaminated Concrete*, Corrosion/2005 , paper 05258, 2005.

165 H. Saito, Y. Miyata, H. Takazawa, K. Takai, G. Yamauchi, *Corrosion Rate Measurements Of Steel In Carbonated Concrete*, Corrosion`95, NACE, Paper 544, 1995.

166 R. Fujiwara, I. Yasutomi, K. Fukudome, T. Tateishi and K. Fujiwara, *Influence of Oxygen Concentration and Alkalinity on the Hydrogen Gas Generation by Corrosion of Carbon Steel*, Mat. Res. Soc. Symp. Proc. **663**, 497, 2001.

167 C.M. Hansson, *The Corrosion Rate of Mild Steel in Deaerated Synthetic Cement Pore Solution*, SKB-1984-11-14, 1984.

168 P. Kreis, *Wasserstoffentwicklung durch Korrosion von Eisen und Stahl in anaeroben, alkalischen Medien im Hinblick auf ein SMA-Endlager*, NAGRA-NTB-93-27, 1993.

169 F. Matsuda, R. Wada, K. Fujiwara, A. Fujiwara, *An Evaluation Of Hydrogen Evolution From Corrosion of Carbon Steel In Low/Intermediate Level Waste Repositories*, Scientific Basis for Nuclear Waste Management XVIII. Part I; Kyoto; Japan; 23-27 Oct. 1994. 719-726, 1994.

170 C.C. Naish, *Corrosion Aspects of the Proposed Sellafield Waste Repository*, U.K. Corrosion '93, 1993.

171 H.R. Ambler and A.A.J. Bain, *Corrosion of Metals in the Tropics*, J. Appl. Chem. **5**, 437, 1955.

172 A.A. Bragard and H.E. Bronnarens, *Prediction at Long Terms of the Atmospheric Corrosion of Structural Steels from Short Term Experimental Data*, p. 339 in 'Atmospheric Corrosion of Metals', ASTM STP 767, S.W. Dean and E.C. Rhea (eds.), 1980.

173 H.R. Copson, *Long-Time Atmospheric Corrosion Tests on Low Alloy Steels*, ASTM Proceedings **60**, 650, 1960.

174 S. Feliu, M. Morcillo and S. Feliu Jr., *The Prediction of Atmospheric Corrosion From Meteorological and Pollution Parameters I. Annual Corrosion*, Corrosion Science **34**(3), 403, 1993.

175 S. Feliu, M. Morcillo and S. Feliu Jr., *The Prediction of Atmospheric Corrosion from Meteorological and Pollution Parameters - II. Long-term Forecasts*, Corrosion Science **34**(3), 415, 1993.

176 D. Knotkova, K. Barton and B. Van Tu, *Atmospheric Corrosion in Maritime Industrial Atmospheres: Laboratory Research*, p. 290 in 'Degradation of Metals in the Atmosphere', ASTM STP 965, S.W. Dean and T.S. Lee (eds.), 1988.

177 C.R. Shastry, J.J. Friel and H.E. Townsend, *Sixteen Year Atmospheric Corrosion Performance of Weathering Steels in Marine, Rural and Industrial Environments*, pg. 5 in Degradation of Metals in the Atmosphere, ASTM STP 965, S.W. Dean and T.S. Lee (eds.), 1988.

178 A.L. Alexander, C.R. Southwell and B.W. Forgeson, *Corrosion of Metals in Tropical Environments, Part 5 - Stainless Steel*, Corrosion **17**(7), 345t, 1961.

179 B.J. Little and F.B. Mansfeld, *The Corrosion Behaviour of Stainless Steels and Copper Alloys Exposed to Natural Seawater*, Werkstoffe und Korrosion **42**, 331, 1991.

180 M.C. Juhas, R.D. McRight and R.E. Garrison, *Behaviour of Stressed and Unstressed 304L Specimens in Tuff Repository Environmental Conditions*, Lawrence Livermore report UCRL 91804, 1984.

181 J.R. Kearns, M.J. Johnson and I.A. Franson, *The Corrosion of Stainless Steels and Nickel Alloys in Caustic Solutions*, paper 146, Corrosion '84, NACE Houston, 1984.

182 D.B. McDonald, M.R. Sherman, D.W. Pfeifer and Y.P. Virmani, *Stainless Steel Reinforcing as Corrosion Protection*, reprint from Concrete International, supplied by Nickel Development Institute, reprint number 14034, May 1995.

183 E. Rabald, *Corrosion Guide*, p. 134, Elsevier, 1968.

184 F.I. Rubinshtejn, D.E. Lashchevskaya, E. Rubinshtejn, L.M. Mamontava and V.A. Gulyaev, *Accelerated Testing of the Corrosion Resistance of Chromium-Nickel Steels in Model Environments Simulating the Manufacturing Conditions of the Synthetic Resin KFE*, Lakokras Mat. Primen, Moskau, No.3, p. 59, 1977.

185 R.C. Scarberry, D.L. Graver and C.D. Stephens, *Alloying for Corrosion Control. Properties and Benefits of Alloy Materials*, Materials Protection **6**(6) 54, 1967.

186 A.J. Sedriks, J.W. Schultz and M.A. Cordovi, *Inconel Alloy 690 - A New Corrosion Resistant Material*, Boshoku Gijutsu **28**, 82, 1979.

187 B. Sorensen, P.B. Jensen and E. Maahn, *The Corrosion Properties of Stainless Steel Reinforcement*, p. 601 in 'Corrosion of Reinforcement in Concrete', C.L. Page, K.W.J. Treadaway, P.B. Bamforth (eds.), Elsevier, 1990.

188 R.K. Swandby, *Corrosion Charts: Guides to Materials Selection*, Chem. Eng. **69**, 186, 1962.

189 C.C. Naish, D.J. Blackwood, K.J. Taylor and M.I. Thomas, *The Anaerobic Corrosion of Stainless Steels in Simulated Repository Backfill Environments*, Nirex Report NSS/R307, 1995.

190 J.N. Wanklyn and D. Jones, *The Corrosion of Austenitic Stainless Steels Under Heat Transfer in High Temperature*, J. Nuc. Materials **2**, 154, 1959.

191 E.A. Baker and T.S. Lee, *Long-Term Atmospheric Corrosion Behaviour of Various Grades of Stainless Steel*, pg. 52 in Degradation of Metals in the Atmosphere, ASTM STP 965, S.W. Dean and T.S. Lee (eds.), 1988.

192 M.J. Johnson and P.J. Pavlik, *Atmospheric Corrosion of Stainless Steels*, p. 461 in 'Atmospheric Corrosion' W.H. Ailor (ed.), 1982.

193 J.R. Kearns, M.J. Johnson and P.J. Pavlik, *The Corrosion of Stainless Steels in the Atmosphere*, p. 35 in 'Degradation of Metals in the Atmosphere', ASTM STP 965, S.W. Dean and T.S. Lee (eds.), 1988.

194 W.G. Whitman, R.P. Russell and V.J. Altieri, *Effect of Hydrogen Ion Concentration on the Submerged Corrosion of Steel*, Ind. Eng. Chem. **16**, 665, 1924.

195 A. Hache, L. Barriety, J. Debyser, *Effect of Photosynthesis on the Corrosion of Steel in Seawater*, Werkstoffe und Korrosion **10**, 145, 1959.

Table 1. Typical compositions (mg l^{-1}) of Sellafield borehole groundwater and other waters for which corrosion rate data are available

	Sellafield Borehole 2 1587-1602m [103]	Seawater	MINTEK minewater [34]	Säckingen groundwater [104]	Böttstein groundwater [104]	Teddington drinking water [33]
Na	9120	10560		900-1070	4800	
K	187	380		75-86	54	
Ca	1490	400		124-158	1100	
Mg	136	1272		12-15	3	
Ba	0.288					
Fe	7.44					
Al	0.02					
Mn	1.88					
Sr	32.4					
Si	4.96					
Cl	17400	18980	1075	1480	8100	40
Br	30.3					62
SO_4^{2-}	1130	2649	1075	112-115	1820	
PO_4^{3-}						3
I	0.15					
F	2.61			2.3	3.8	0.15
Total Alkalinity (HCO_3 equivalent)	68.1	140				
Carbonate alkalinity (HCO_3)	62.0					276 (as $CaCO_3$)
pH	7.25	7.7	6.5			
Total inorganic carbon	12.4	18.6				

Table 2. Carbon steel corrosion rates in aerobic, neutral conditions

Reference	Environment	Temp (°C)	Corr. rate (μm yr^{-1})	Times	Remarks
Borgmann [105]	0 to 2M NaCl, KCl, LiCl, aerated	ambient	40-120	2 days	Corrosion rates measured by weight loss as a function of chloride concentrations (Figure 5).
Braithwaite [106]	geothermal condensates	10-20	18	1 year	Corrosion rates measured by weight loss. Incomplete analysis of condensate composition, but ~2 mMol H_2S present, low Cl.
Breckheimer [107]	0.001 to 3M KCl	25-85	50-250		Figure 6.
Canadillas [108]	Q-brine distilled water	35 55 90 35 55 90	25 25 62 67 62 41	75 & 148days	Weight loss experiments carried out in a closed system, so the oxygen would have been exhausted after a short period. In Q-brine "acid corrosion" occurs at higher temperatures so the corrosion rate increases.
Elmorsi [109]	groundwater	40	28-211	2-12 months	Corrosion rate was measured using a "corrosometer" in Egyptian well waters, with a wide range of compositions; TDS 150-731 ppm, ~2ppm H_2S present.
Francis [33] and Mercer [35]	forcibly aerated distilled water	40 60 70 80 90	93 120 160 230 324	up to 100 days	Corrosion rate was measured by weight loss measurements in static solutions. Corrosion rates were higher when the air was passed through the solution rather than over the surface. In static experiments the corrosion rate was independent of chloride concentration, because oxygen diffusion is the controlling parameter. In experiments using a rotating electrode (1 Hz) corrosion rate was related to oxygen concentration, temperature and chloride concentrations (Figure 7-Figure 9). Oxygen has a passivating effect at high concentrations.

Table 2 (contd.) Carbon steel corrosion rates in aerobic, neutral conditions

Reference	Environment	Temp (°C)	Corr. rate (μm yr^{-1})	Times	Remarks
Gaonkar [110]	distilled water & drinking water	25 40 60 70 80	90 222 324 340 334	up to 5 days.	The corrosion rate was measured by weight loss measurements over the temperature range 25-100°C. The maximum corrosion rate occurred at about 70°C. The shape of the curve was very similar to Figure 10. Chloride concentration 6 ppm.
Hache [111]	3% NaCl	0-80	See Figure 11.		
Higginson [34]	Mintek minewater (see Table 1)	25	200	14 days	The corrosion rate in static solutions (0.03M chloride, pH 6.5), measured by weight loss, became constant after an initial period of rapid corrosion. Corrosion rate was also measured as a function of temperature, oxygen concentration and chloride concentration using a rotating electrode to control mass transport of oxygen to surface.
Ho [112]	tropical seawater	28	350-530	2, 12 months	Weight loss measurements after immersion in natural seawater. In laboratory tests corrosion rate increased with temperature. Corrosion rate also affected by surface preparation and carbon content.
Honda [113]	seawater and distilled water mixed with compacted bentonite slurry	50-150	10-20	up to 180 days	Specimens were mounted between layers of bentonite and immersed in test solution. The corrosion rate was determined from weight loss.
Kalashnikova [22]	Cuban Caribbean seawater	23-29	50-280	24 months	Weight loss and electrochemical measurements. Corrosion decreased over test period and reached a plateau after ~18 months.
Kennedy [114]	harbour seawater	ambient	60-130	35 years	The thickness of sheet metal pilings in New York Harbour were measured using an ultrasonic thickness probe.
Kritsky [115]	spent nuclear fuel pond water	ambient	40-80	340 days	Corrosion rate measured by weight loss measurements in pond water containing ~2 ppm dissolved salts at pH 5 to 9.
Kuron [116]	tap water with 0.28-15.5M chloride added	ambient	~45	10000 hours	Corrosion rate was measured using rotating disks and pipe. The chloride concentration did not affect corrosion rate. The figures given refer to zero flow experiments.

Table 2 (contd.) Carbon steel corrosion rates in aerobic, neutral conditions

Reference	Environment	Temp (°C)	Corr. rate (μm yr^{-1})	Times	Remarks
Larrabee [117]	seawater	ambient	39±6	23.6 years	Steel pilings on pier in California
McRight [118]	aerated J13 well water pH 7.1-7.5, 6 to 8 ppm chloride.	50 70 80 90 100	401 505 531 414 320	1500 hours	Weight loss measurements were carried out on mild steel 1020. The well water was air sparged to produce the most corrosive conditions (5-6 ppm oxygen).
Merz [119]	Brine and seawater	ambient to 250	7-10000		Contains a compilation of data for carbon steel and cast iron in brine and seawater as a function of temperature and pH.
Nissing [120]	drinking water, pH 7.2 and 8.0, as f[O_2] and flow rate	ambient	14-70	3.5 years	Ring specimens were exposed to flowing tap water with oxygen concentrations in the range 0.01-4 mg l^{-1} and pH 7.2 and 8.0. The corrosion rate is constant initially then it follows a power law.
Peterson [121]	harbour seawater	ambient	120	18 months	
Reinhart [122, 123] Larrabee [124]	seawater	ambient	50-200 average ~100	0-16 years	Corrosion rate decays with time. Corrosion rate reduces with depth.
Schwarzkopf [125]	concentrated brine (26.9 wt% NaCl)	90	120	1.5 years	A cast steel tube was stored for 18 months in a heated borehole containing NaCl brine, with temperatures from 90°C to 200°C.
Shannon [126]	geothermal brines, seawater, various pHs	43	25 to 30 at pH7 ~130 at pH7	7 days	A compilation of literature results for 1 ft $second^{-1}$ flow, 60 ppb oxygen.
Simpson [127]	aerated Böttstein groundwater 0.1 mg g^{-1} O_2	80	24 52 60	700 hours 2200 hours 6200 hours	Weight loss experiments were carried out in a refreshing autoclave, so that the oxygen concentration could be maintained.

Table 2 (contd.) Carbon steel corrosion rates in aerobic, neutral conditions

Reference	Environment	Temp (°C)	Corr. rate (μm yr^{-1})	Times	Remarks
Smailos [128-131]	Q-brine	90	31-50 14 23 37 460	1 year	radiation levels of 0 1 10 100 1000 Gy hr^{-1}. Corrosion rates decreased with time.
Southwell [132]	freshwater seawater	ambient	18 64	16 years	Coupons were suspended in seawater and freshwater and the corrosion rate was monitored by weight loss. A constant corrosion rate was achieved after about 4 years (*e.g.* Figure 12).
Uhlig [10]	continuous immersion in natural seawater	ambient	25-200, average 109	up to 31 years	The reference includes a tabulation of 34 weight loss measurements from corrosion at a range of world-wide locations.
White [133]	static immersion tests Mediterranean seawater Dead Sea seawater	day: 40°C night: RT	73 14-20	103 days	

Table 3. Carbon steel corrosion rates in anaerobic, neutral conditions

Reference	Environment	Temp (°C)	Corr. rate (μm yr^{-1})	Times	Remarks
Blackwood [134]	granitic groundwater	50	initially ~2, long-term <0.1	5000 hours	The test specimens had pre-formed corrosion product films.
Diercks [43, 44]	anaerobic acid chloride solutions	20-400	10->1000		The reports contain compilations of literature results for anaerobic, acid, neutral and basic chlorides (Figure 15-Figure 17). There is an Arrhenius relationship with activation energy 32kJ mol^{-1} for the anaerobic, acid conditions (Figure 15).
Farvaque-Bera [135]	0.5M sulphate pH 0.4 to 6.0 and brines	25-90	80-154000 depending on pH and temp.	0	Instantaneous corrosion rates from polarisation curves.
Grassiani [136]	de-aerated 6% $MgCl_2$	33 41 85 90	50 244 371 452		Corrosion rates were measured using the linear polarisation technique.
Haberman [137]	high magnesium brine	90	~200	1 month	Corrosion rates were measured for ASTM 216 grade WCA mild steel using the linear polarisation technique. Arrhenius relationship for corrosion rate.
Helie [138]	de-aerated 3 g l^{-1} NaCl	90		1000 hours	Polarisation resistance was used to measure corrosion rate as a function of time. It was found that the corroded thickness, e, was given by $e=kt^{½}$, where k = 5 mm $y^{-½}$ and t = time of exposure.
Kreis [139, 140]	groundwater, distilled water, 0.8% chloride	21	<0.08 to 0.7		Hydrogen evolution measurements were used to measure the corrosion rate of iron (0.91%C) in a range of media. Corrosion rate falls with time.
Jelinek [18]	de-aerated distilled water	90	1.3 (after 43 days)	0-43 days	Hydrogen evolution experiments. Corrosion rate derived from weight loss. Variables investigated: temperature; dissolved copper concentration and pH. The results were not temperature sensitive over the range 60-316°C.

Table 3 (contd.) Carbon steel corrosion rates in anaerobic, neutral conditions

Reference	Environment	Temp (°C)	Corr. rate (μm yr^{-1})	Times	Remarks
Marsh [15]	de-aerated synthetic seawater	20 50 90	2.1-3.1 5.3-14.6 10.6-21.6	up to 425 days	Corrosion rate was measured by weight loss. It decreases to ~6 μm yr^{-1} with time. The reference also includes data for effect of radiation and results for forged, cast and low carbon steel.
Posey [141]]	4M NaCl, pH 2-7 pH7	25-200 22 50 75 100 150 200	7.6 to 12700 8.9 23 46 127 559 1270	0	Electrochemical measurements of corrosion rate in a stirred autoclave. An Arrhenius relationship exists for corrosion rate for a range of pHs.
Reda [142]	dilute $MgCl_2$/NaCl solutions (up to 0.5M $MgCl_2$ and 0.85M NaCl)	25 distilled water 0.85M NaCl 0.5$MgCl_2$	9-17 12 12 13.3	up to 1100 hours	The pH of the solutions was in the range 4.6 to 6.6. The corrosion rate was measured by weight loss. The reference also includes data on the effect of radiation.
Simpson [45, 104] and Schenck [143]	groundwater and NaCl solutions (pH 7-10) - average figures for all chloride concs. and temps.	25-80	pH 7: 2.8 pH 8.5: 1.4 pH 10: 0.3	until gas evolution rate constant, 6000 + hours	Hydrogen evolution experiments. Various types of hydrogen evolution behaviour were identified (Figure 18). The data are summarised in Figure 19 and Figure 20.
Simpson [104]	Säckingen 0.1 μg g^{-1} O_2	80	86 34	500 hours 1440 hours	Corrosion rates were derived from weight loss measurements on cast mild steel.

Table 3 (contd.) Carbon steel corrosion rates in anaerobic, neutral conditions

Reference	Environment	Temp (°C)	Corr. rate (μm yr^{-1})	Times	Remarks
Simpson [104] continued	Böttstein, Säckingen ground water, oxygen free (<0.01 μg g^{-1} O_2)	80	30-42	700 hours	
			14-16	2100 hours	
			4-6	6300 hours	
		25	1.1-1.5	2-3 days	
		50	3.2-6.5		
		80	1.5-2.5		
	$NaHCO_3/Na_2CO_3$		pH 7 8.5 10		Hydrogen evolution measurements. Steady state corrosion rates.
	0	80	0.9 0.3 0.5	2-3 days	
	80		3.8 1.5 2.5		
	800		5.0 0.5 1.0		
	8000 mg g^{-1} Cl		0.8 2.5 0.5		
Simpson [144]	Böttstein, 0 O_2	80	5-10	6170 hours	Corrosion rates were derived from weight loss measurements; the corrosion rate decreases with time. Salinity and oxygen concentration had a greater effect than temperature.
	0.1 mg/g O_2		60-68		
	Säckingen, 0 O_2		5-6		
	0.1 mg/g O_2		7-18		
Simpson [127]	anaerobic Böttstein groundwater	80	42	700 hours	Corrosion rates were determined from weight loss measurements.
			14	2200 hours	
			10	6200 hours	
Smith [145]	domestic water, pH 9	25	3	<1 hour	Corrosion rates were derived from polarisation resistance measurements
Stahl [146]	basalt groundwater	90	~70	<1 hour	Corrosion rates for 1018 steel were derived from electrochemical measurements.
Tas [147]	interstitial claywater	90	10	9 months	Initial corrosion rates are high but decline significantly with time. The equivalent corrosion rate in aerated conditions was 25 μm yr^{-1}.
Westerman [148]	$MgCl_2$ brine (6.7M Cl^-)	90	18	6 months	A216 steel weld metal.

Table 4. Carbon steel corrosion rates in aerobic, alkaline conditions

Reference	Environment	Temp (°C)	Corr. rate (μm yr^{-1})	Times	Remarks
Akolzin [47]	0.43 and 0.76 g l^{-1} $Ca(OH)_2$ (pH12 and 12.3) + Cl^-	22	0.5 to 20	0	The corrosion rates were determined by polarisation resistance measurements. Figure 23 and Figure 24 show corrosion rate as a function of time, calcium hydroxide concentration and chloride concentration.
Blackwood [149]	0.1M NaOH	30 50 80	0.1 0.4 2.3		Passive current measurements.
Byakova [150]	30% KOH	ambient	6.1	"fairly long times"	
Drazic [151]	5M KOH	ambient	30	0	The corrosion rates of iron were derived from Tafel slope extrapolation.
Hubbe [152]	NaOH / NaCl, pH 9.5 at start NaOH / NaCl, pH 7.7 at end	ambient	200	48 hours	Corrosion rates of mild steel were determined by weight loss and polarisation resistance measurement.
Lesnikova [153]	KOH pH 12 pH 13 pH 14	20	90-140 75-120 55-60	900 hours	
Schwenk [154]	0.5M $NaCO_3$ / 1M $NaHCO_3$	25	active 33 passive 3.5	up to 2500 hours	The corrosion rate of iron was measured by weight loss as function of potential.
Yasuda [48]	30% NaOH	117	4000	0	The corrosion rates of mild steel and alloy steels were measured using the linear polarisation method (Figure 25).

Table 5. Carbon steel corrosion rates in concrete

Reference	Environment	Temp (°C)	Corr. rate ($\mu m\ yr^{-1}$)	Times	Remarks
Andrade [155]	concrete ranging from dry, uncarbonated, no chloride to highly contaminated with chloride	ambient	1-1100		Linear polarisation resistance.
Andrade [156]	laboratory experiments on reinforcing bars in carbonated mortar with chlorides	ambient	<1-100	45 days	Data showed strong effect of varying relative humidity and partial immersion on corrosion rate.
Arya [75]	Cement paste with various binders, with chloride content ranging from 0 to 3%. Samples exposed to salt solution at 95% humidity.	ambient	**1% chloride** 116-348 <1 **3% chloride** 116-812 20-116	 0-40 days 40-120 days 0-70 days 70-120 days	Chloride binding and its influence on the rate of reinforcement corrosion was investigated in a range of mixes by, respectively, pore solution analysis and measuring the galvanic current in macro corrosion cells formed by embedding mild steel bars in two layers of concrete. The corrosion rates increased with increasing chloride content for all mixes due to an increase in the amount of free chloride. Anodic current densities of corrosion cells were measured.
Baccay [157]	Carbonated concrete samples. Various cement binders used containing air entraining agent and water reducing agent. 90% humidity	Varied 20-40	0.01-2.8	0-35 days	Rate of carbonation increases with temperature. Higher corrosion rate with higher temperature in OPC concrete.

Table 5 (contd.) Carbon steel corrosion rates in concrete

Reference	Environment	Temp (°C)	Corr. rate ($\mu m\ yr^{-1}$)	Times	Remarks
Cao [158]	Cement paste, containing different binders (35% BFS and 20% PFA). Cured in saturated lime, with cast in chloride and exposure to chloride solution.	ambient	2.6-41.6	3-28 days	Water to cement ratio 0.8; a high water/cement ratio. Corrosion rate measured using polarisation curves with scan rate of 17mV/sec.
Chitty [159]	ancient mortars	ambient	0.8 to 8		Examination of archaeological artefacts ranging from 80 to 1700 years old. Corrosion rate declined with age. Range of corrosion products found, including magnetite.
Flis [61]	concrete bridges	ambient	0.0812 to 350		Corrosion rates of steel rebars were measured in real structures using electrochemical techniques. The corrosion rate was found to be dependent on the potential, in a similar way to a normal polarisation curve. The corrosion rates are related to the concrete resistivity and chloride exposure (e.g. marine atmosphere, de-icing chemicals).
Gonzalez [160]	various mortars no additives with chloride and carbonation	ambient	<1 up to 100	8 days	The corrosion rate of steel rebar was measured in blocks of mortar, some of which contained added chloride, using polarisation resistance measurements. The corrosion rate depended on the chloride concentration, concrete resistivity and the percentage water saturation.

Table 5 (contd.) Carbon steel corrosion rates in concrete

Reference	Environment	Temp (°C)	Corr. rate ($\mu m\ yr^{-1}$)	Times	Remarks
Hakkarainen [161]	Concrete samples with various binders. Tests carried out in synthetic sea water and tap water.	ambient	0.016-0.05	10 months to 2 years of exposure	Cyclic polarisation curves used to obtain corrosion rate with time. No corrosion observed in samples exposed to tap water.
Hansson [63-65]	de-aerated mortar	22-43	1-7	10 months	Electrochemical measurements (Tafel slope extrapolations and polarisation resistance measurements) were used to measure corrosion rates. There is some doubt about whether the concrete was completely de-aerated. The films on the surface of the steel were cathodically reduced before the experiment.
Hauser [162]	cemented waste forms, pH 12, O_2 5 mg l^{-1}	25 50 90	< 1 2 18	12 months	Weight loss measurements were used to assess the corrosion rate of cast iron in cemented waste forms.
Lee [163]	cement paste with varied binders (PFA, BFS) exposed to saturated air	ambient	0.34-6.07	2 to 84 days	Similar corrosion rate in all samples. Rate of corrosion falls to very low values within one to two weeks.
Lysogorski [164]	Steel in simulated pore solution, wet dry cycles, short term exposure to chloride solution. Concrete samples long-term exposure, wet-dry cycle.	ambient	0-2.23 negligible	28-84 days 0-450 days	Polarisation resistance measurements were used to obtain corrosion rates.
Naish [66, 67]	various anaerobic concrete / cement mixes	ambient	0.23-1.44	up to 2.5 years	Weight loss measurements were used to measure the corrosion rates of carbon steel in cement. It was noted that the rates represented maximum values.

Table 5 (contd.). Carbon steel corrosion rates in concrete

Reference	Environment	Temp (°C)	Corr. rate ($\mu m\ yr^{-1}$)	Times	Remarks
Saito [165]	carbonated and non carbonated concrete samples exposed to various conditions: outdoors, indoors, underground, tunnel	ambient	10-25	1 year	Measurements were obtained using the potential step method and converted to corrosion current and mass loss. The calculated mass loss was compared with actual mass loss of the sample after the bars were removed from the bar. Lower corrosion rate measured in carbonated concrete compared to bare steel in water. Corrosion rate controlled by water and oxygen availability.
Tuuti [52]		ambient			Corrosion rate data were reported for real concrete structures:
	balcony slabs		50	20 years	rebars, carbonated, but no chloride
	concrete silo		200-400	25 years	salted sand had been stored in silo, chloride high, carbonated
	power line poles		50	50 years	carbonated, but no chloride
	concrete building		100-500	10 years	$CaCl_2$ added to concrete

Table 6. Carbon steel corrosion rates in anaerobic, alkaline conditions

Reference	Environment	Temp (°C)	Corr. rate ($\mu m\ yr^{-1}$)	Times	Remarks
Fujiwara [166]	artificial cement porewater, pH 12.5-13.5	35	0.005-0.01	60 days	Corrosion rate was found to increase at pH 14, due to the formation of soluble $HFeO_2^-$ species. Hydrogen was also formed under aerobic conditions when localised corrosion and acidification occurred.
Fujisawa [77]	mortar-equilibrated water pH 12 $Ca(OH)_2$ pH 12.8 synthetic groundwater + bentonite, pH 8	15 30 45 15	0.004 0.02 0.2 0.09	9,000 hours	Incubation period observed before gas generation started. The samples were not pickled initially. The incubation period was shorter at higher temperatures. Arrhenius relationship demonstrated at pH 12.6. There could have been an inhibition effect from dissolved glass. Black surface film observed. Activation energy 100 $kJ\ mol^{-1}$.
Grauer [17, 68]	de-aerated groundwaters and porewaters, and KOH, $Ca(OH)_2$, and NaOH	21	0.00007-0.7	up to 12000 hours	The reference contains a literature survey which indicates that the corrosion rate in cement is in the range 0.08 to 1 $\mu m\ yr^{-1}$. Hydrogen evolution experiments were used to measure the corrosion rate of iron wire. The corrosion rate was lowest in porewaters. Different time dependencies were observed in NaOH, KOH, $CaOH_2$ and porewaters.
Grauer [16]	sat. $Ca(OH)_2$ dilute alkali hydroxide, porewater	21	0.00015 to 0.0064	up to 13500 hours	Hydrogen evolution experiments were used to measure the corrosion rate of iron wire. The corrosion rate either decreased with time or remained constant.
Hansson [167]	$Ca(OH)_2$, pH 12.6 KOH, NaOH added in some experiments.	ambient	23-58	24 hours	Dynamic polarisation curve passive current densities were used to measure the corrosion rates. The results are probably an overestimate of the corrosion rate.

Table 6 (contd.) Carbon steel corrosion rates in anaerobic, alkaline conditions

Reference	Environment	Temp (°C)	Corr. rate (μm yr^{-1})	Times	Remarks
Kreis [139, 168]	porewater, NaOH, $Ca(OH)_2$, KOH, pH 12.5-13.2	21	<0.08		Hydrogen evolution measurements were used to measure the corrosion rate of iron (0.91%C) in a range of media. The corrosion rate depends on media. In some porewaters and groundwater corrosion rate <0.005 Ωm yr^{-1}.
Matsuda [169]	artificial cement porewater	ambient	5	up to 30 days	Hydrogen analysed by gas chromatography. Corrosion rates also measured by weight loss. Short-term measurements.
Naish [170]	various mixtures of 0.1M KOH, 0.1M NaOH, $Ca(OH)_2$ NaCl up to 10,000 ppm chloride and with application of hydrogen overpressure.	ambient, 30, 50 and 80	10 initially to <0.001 long-term		Hydrogen evolution measurements used to measure the corrosion rate of carbon steel in a range of media. The corrosion rate at 30, 50 and 80°C decreased with time (Figure 26). The presence of an existing aerobically produced corrosion product film significantly reduced the rate of hydrogen gas production.
Yasuda [48]	30% NaOH	117	1500	2 weeks	Weight loss measurements were made for a number of materials under hydrogen (Figure 25).

Table 7 **Anaerobic corrosion rates of carbon steel, derived from hydrogen generation experiments in the NSARP [69]**

Cell number	Test solution	Temp (°C)	Test duration (days)	Maximum (μm yr^{-1})	Average (μm yr^{-1})	Time for LT mean (hrs)	Mean LT (μm yr^{-1})	Total H_2 (mmol m^{-2})
5	0.1M NaOH	30	3949	3.11	0.04	>10000	0.010	68
27	0.1M NaOH	30	3821	1.21	0.11	>10000	0.098	158
14	0.1M NaOH	50	3492	5.50	0.11	>10000	0.011	~150
47	0.1M NaOH (mercury cell: no liner)	80	311	29.63	0.35	>4000	0.025	41.5
51	0.1M NaOH (mercury cell)	80	2591	23.71	0.29	>10000	0.002	376
9	0.1M NaOH + 3.5%NaCl	30	3949	1.27	0.06	>10000	0.023	91.7
28	0.1M NaOH + 3.5%NaCl	30	3821	0.69	0.057	>10000	0.044	84
15	0.1M NaOH + 3.5 % NaCl	50	3932	0.88	0.08	>10000	0.03	118.8
53	0.1M NaOH + 3.5% NaCl (Hg cell)	80	1520	20.24	0.41	>10000	0.0047	359
18	Sat. $Ca(OH)_2$	50	3494	5.07	0.037	>10000	0.003	50
24	Sat. $Ca(OH)_2$ + NaOH	30	3743	1.43	0.08	>30000	0.022	108.6
26	Sat. $Ca(OH)_2$ + NaOH	50	773	2.07	0.16	>10000	0.11	48.49
19	Sat. $Ca(OH)_2$ + 3.5%NaCl	50	1225	2.14	0.16	>10000	0.006	74.36
23	Sat. $Ca(OH)_2$ + NaOH + 3.5% NaCl	30	3743	0.87	0.08	>30000	0.027	110.2
25	Sat. $Ca(OH)_2$ + NaOH + 3.5% NaCl	50	773	1.96	0.28	>10000	0.009	84.06
37	NRVB	50	3045	3.60	0.056	>10000	0.024	65.6
39	NRVB + 20,000 ppm Cl^-	50	2591	2.35	0.065	>10000	0.010	65.2

Table 7 (contd.) Anaerobic corrosion rates of carbon steel, derived from hydrogen generation experiments in the NSARP [69]

Cell number	Test solution	Temp (°C)	Test duration (days)	Maximum (μm yr^{-1})	Average (μm yr^{-1})	Time for LT mean (hrs)	Mean LT (μm yr^{-1})	Total H_2 (mmol m^{-2})
55	As Received 0.1M NaOH	50	1037	0.28	0.022	>10000	0.001	8.94
42	Degreased 0.1M NaOH	50	817	0.11	0.08	>10000	0	25.6
41	Pre-rusted in 3.5% NaCl, 0.1M NaOH	50	2493	0.36	0	>10000	0	2.3
56	Pre-rusted in 3.5% NaCl, 0.1M NaOH	50	2100	0.71	0.21	>10000	0.404	168 [1]
43	Groundwater pH 4 (unbuffered)	50	827	5.06	0.78	>5000	0.61	247
44	Groundwater pH 7 (unbuffered)	50	856	1.85	0.43	>5000	0.35	141
49	Groundwater pH 4 (buffered)	50	2609	9.21	1.31	>10000	2.17	432 [1]
50	Groundwater pH 7 (buffered)	50	2607	5.04	0.122	>5000	0.052	123

Notes

1. The true value is in excess of this figure, because the reservoir of DBP emptied on a number of occasions due to rapid gas generation.

Table 8. Atmospheric corrosion of carbon steel

Reference	Environment	Temp (°C)	Corr. rate (μm yr^{-1})	Times	Remarks
Ambler [171]	various marine atmospheres	ambient	~10-1000	up to 12 months	There is a linear relationship between corrosion rate and salt deposition rate (Figure 27).
Blackwood [134]	anaerobic, high humidity atmosphere	50	Initially ~20, but decreasing to <0.1 after 5000 hours	up to 5000 hours.	Hydrogen evolution experiments.
Bragard [172]	various sites	ambient	typically 40	up to 10 years	The following law was found to apply: $C = At^n$, where A = weight loss, t = exposure time, and A and n are constants that depend on exposure site and steel grade.
Copson [173]	various marine atmospheres	ambient	16-1193	up to 18 years	The corrosion rate depends on the proximity to sea.
Feliu [174, 175]	various atmospheres	ambient	average 74.5, SD 113.7, min 3.2, max 743		Analyses of 324 reports in literature and fits equations to the data (see subsection 3.4).
Knotkova [176]	intermittent distilled water spray intermittent seawater spray	35	136 806	up to 30 days	Results of laboratory tests in environmental chambers.
Shastry [177]	various sites	ambient	2.5 - 10 typically	20 years	The data fit the law $\log C = \log A + B \log t$, where C = corrosion loss in micrometers, t = time in years, and A and B are constants. Values of A and B are given for various sites.
Dechema Corrosion Handbook volume 7 [7]	rural industrial sea coast	ambient	10-50 50-380 60-170	various	Typical data are given - much depends on the type of climate.

Table 9. Calibrated SMOGG corrosion parameters for carbon steel

Conditions	Acute corrosion		Chronic corrosion	
	Rate constant ($\mu m\ yr^{-1}$)	Characteristic time (yr)	Rate constant ($\mu m\ yr^{-1}$)	Characteristic time (yr)
Sat. $Ca(OH)_2$ at 30°C	0.3	1.6	0.01	~∞
Sat. $Ca(OH)_2$ at 50°C	1.5	0.2	0.005	~∞
NaOH at 30°C	1.7	0.15	0.05	3
NaOH at 50°C	0.7	0.5	0.005	~∞
NaOH at 80°C	22	0.09	0.005	~∞
NRVB at 50°C	1.0	0.25	0.005	~∞

Table 10. Stainless steel corrosion rates in aerobic, neutral conditions

Reference	Environment	Temp (°C)	Corr. rate (μm yr^{-1})	Times	Remarks
Alexander [178]	Pacific seawater	ambient	302 stainless: 18 316 stainless: 4	8 years	Weight loss experiments were carried out in tropical Pacific seawater. Most of the weight loss was due to pitting, rather than general corrosion (see Figure 35).
Little [179]	seawater	ambient	~4		The corrosion rates were measured using electrochemical techniques. The corrosion current, i_{corr} was not limited by mass transport; the corrosion rate depends on the passive current.
Juhas [180]	J-13 water	28	0.24-0.28	9000 hours	The reference gives results for weight loss measurements for 304 stainless steel in Tuff repository water. Corrosion rates decreased in the presence of radiation.
Kritsky [115]	spent nuclear fuel pond water	ambient	0.1-0.5	340 days	Corrosion rates were derived from weight loss measurements in pond water containing 2 ppm dissolved salts, pH 5-9. Up to 8 μm yr^{-1} was recorded with 12000 Gy/hr in aerated distilled water.
Morsy [83]	0.1M - 0.5M NaCl with 0.1 to 0.7M KCl additions	90	10-130	up to 10 hours	Weight loss corrosion rate measurements of a steel similar to AISI 304 increased with NaCl concentration. KCl additions were inhibitive at low concentrations but increased the corrosion rate at >0.4M KCl (Figure 36).
White [133]	static immersion tests Mediterranean seawater Dead Sea seawater	day: 40 night: ambient	 0.55 4.8	120 days	Solubility of oxygen in Dead Sea water is only 1-1.5 ml l^{-1} compared to 5.4 ml l^{-1} for normal seawater.

Table 11. Stainless steel corrosion rates in anaerobic, neutral conditions

Reference	Environment	Temp (°C)	Corr. rate (μm yr^{-1})	Times	Remarks
White [133]	Mediterranean seawater Dead Sea seawater	day: 40 night: ambient	0.9 0.8	120 days	Static immersion tests under nitrogen atmosphere.

Table 12. Stainless steel corrosion rates in aerobic, alkaline conditions

Reference	Environment	Temp (°C)	Corr. rate (μm yr^{-1})	Times	Remarks
Blackwood [149]	0.1M NaOH	30 50 80	0.06 0.18 0.82		Passive current measurements above the oxygen reduction potential. Electrochemical measurements tend to overestimate the corrosion rate.
Kearns [181]	20%-70% NaOH	93	3-9	96 hours	Weight loss measurements.
MacDonald [182]	0.3N KOH, 0.05N NaOH, 3% NaCl, pH 13.3	ambient	304: 0.3 316: 0.6	28 days	Linear polarisation resistance measurements after 28 days of cyclic wet-dry testing.
Rabald [183]	$Ca(OH)_2$ + $CaCO_3$, NaOH, NaS	50	<0.3		
Rubinshtejn [184]	1% NaOH	ambient	1-6		Exact composition of steels not checked because Russian alloys used. CrNi(Mo) steels
Scarberry [185]	50% NaOH	boiling	~1500		Weight loss experiments on 304/316 stainless steel.
Sedriks [186]	50% NaOH	boiling	~6000	10 days	Weight loss experiments.
Sorensen [187]	mortar prisms	ambient	no Cl^-: 0.01 to 0.1 + Cl^-: 1 to 100		Passive current measurements for 304 and 316.
Swandby [188]	0 - 100 wt% NaOH	0 to 400	< 25 to > 760		The corrosion rate data are shown as an iso-corrosion chart, Figure 37.
Yasuda [48]	30% NaOH	117	900	0	Electrochemical measurements of the corrosion rate for 304 and 316 are shown in Figure 25.

Table 13. Stainless steel corrosion rates in anaerobic, alkaline conditions

Reference	Environment	Temp (°C)	Corr. rate (μm yr^{-1})	Times	Remarks
Blackwood [149]	0.1M NaOH	30 50 80	0.06 0.18 0.82		Passive current measurements above the oxygen reduction potential.
Mihara [73]	pH 10 - pH 13.5		0.01		Hydrogen evolution experiments.
Naish [189]	0.1M NaOH $Ca(OH)_2$/NaOH pH 12.9	25-80	no gas detected		Hydrogen evolution experiments.
	the above + 3.5wt% Cl^-	25-80	<0.1		Weight loss; autoclave experiments.
	0.1M KOH + 10000 ppm, Cl^- under H_2 up to 10 MPa				
Sedriks [186]	50% NaOH	316	1655	14 days	Weight loss experiments.
Sharland [84]	0.1M KOH agar gel	ambient	0.4-1.6	1200 hours	Corrosion rates were derived from passive current density measurements.
Wanklyn [190]	anaerobic KOH, pH 10.7 to 11.2	270-280	surface roughening - stress corrosion main failure mode	440 hours	18/8 stainless steels
Yasuda [48]	30% NaOH	117	10-30	2 weeks	304/316. Weight loss measurement under hydrogen.

Table 14. Results of 9.5 year exposure tests for 302 and 315 stainless steels in concrete containing chloride (wt% cement); the chloride was added as $CaCl_2$ to the mix water [90], showing corrosion rates in μm yr^{-1}

% Cl in concrete	302 [1]	315 [1]
0	0.017-0.033	0.010-0.038
0.32	0.018-0.037	0.025-0.075
0.96	0.015-0.033	0.022-0.032
1.9	0.013-0.026	0.028-0.034
3.2	0.027-0.041	0.030-0.067

Notes

1. 302 composition (wt%): Cr 17.8; Ni 8.8; Mn 0.78; Mo 0.18; C 0.096; Si 0.047; N 0.02;P 0.021; S 0.023

   315 composition (wt%): Cr 17.0; Ni 10.1; Mn 1.64; Mo 1.42; C 0.056; Si 0.29; N 0.03; P 0.03; S 0.009

   cf. 316L composition (wt%): Cr 17.3; Ni 12.35; Mn 1.87; Mo 2.14; C 0.041; Si 0.46; N 0.22; P 0.03; S 0.007

Table 15. Atmospheric corrosion of stainless steel

Reference	Environment	Temp (°C)	Corr. rate (μm yr^{-1})	Times	Remarks
Alexander [178]	marine seashore	ambient	302: 2.8 316: 0	8 years	Tests were carried out in the Panama canal zone.
Baker [191]	marine atmospheres	ambient		26 years	No general corrosion. Test specimens were assessed for degree of rust, staining and pitting.
Johnson [192]	New York atmosphere marine industrial/urban	ambient	304: 0.022 304/316: <0.03 304: 0.05-2 316: 0.01	5-15 years	316 more resistant than 304.
Kearns [193]	various atmospheres	ambient	304: ~0.03-3 in industrial/urban environment	4-15 years	Corrosion rate investigated as function of alloying in a range of environments. Attack leads to surface tarnishing, corrosion rate negligible.
Dechema corrosion handbook volume 7 [7]	various atmospheres	ambient	0.05		Stainless steel hardly corroded in urban and marine atmospheres, may be some pitting. Undersides more heavily rusted than topsides.

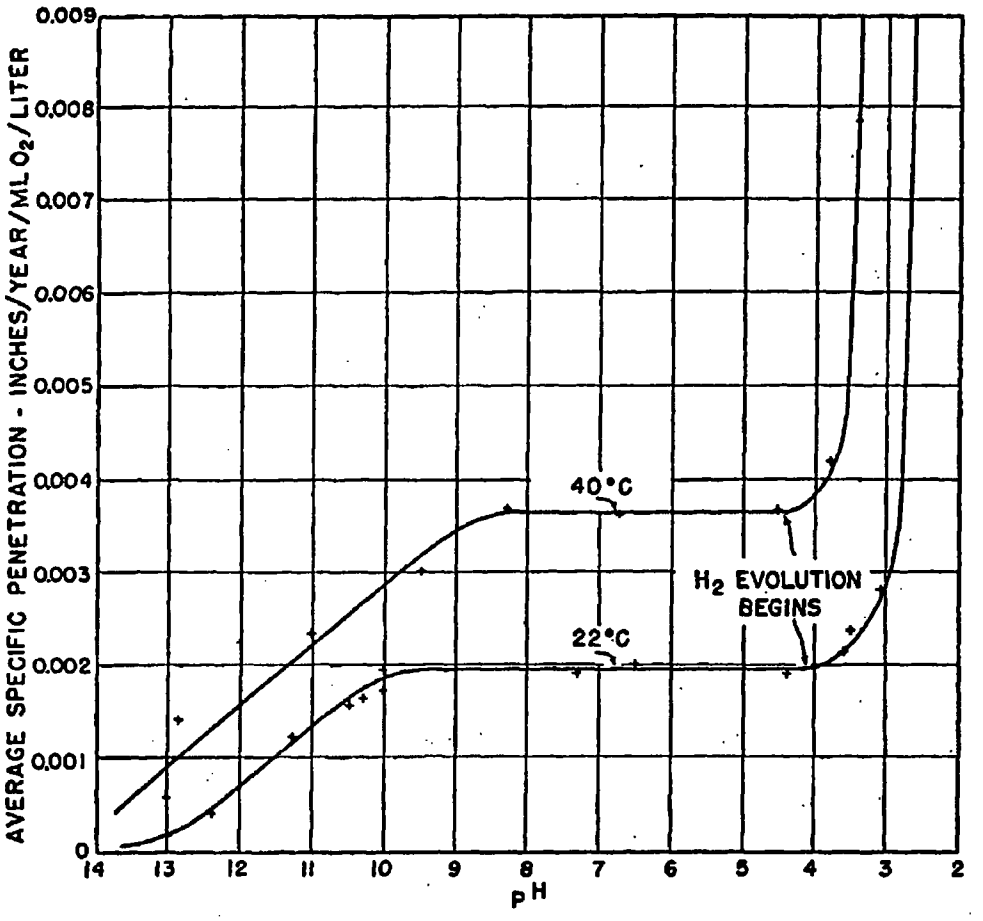

Figure 1. **Effect of pH on aerobic corrosion of mild steel [194]**

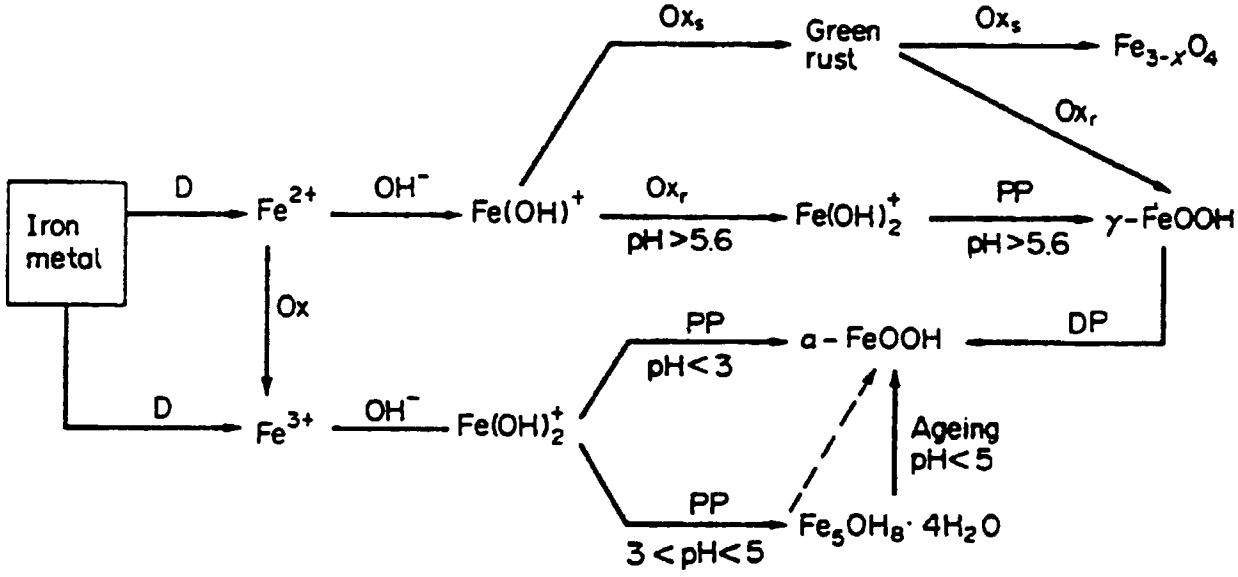

Figure 2. **A schematic diagram of the formation and transformation of the solid products of corrosion under different pH conditions at room temperature: D - dissolution; Ox - aerobic oxidation in solution; Ox_s - slow oxidation; Ox_r - rapid oxidation; PP - polymerisation-precipitation; DP - dissolution-precipitation [20]**

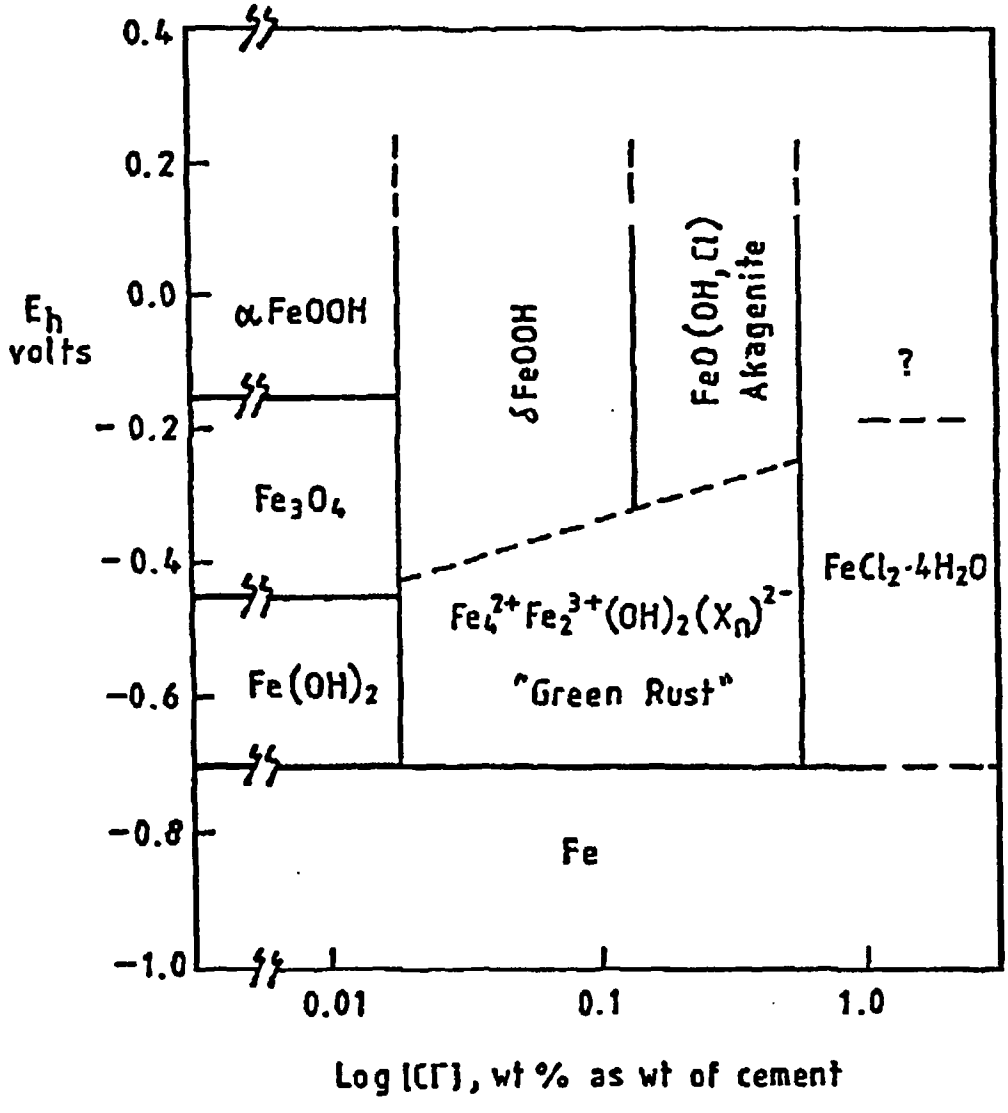

Figure 3. Eh-[Cl] stability diagram for Fe in cement at pH~12 and 20°C [25]

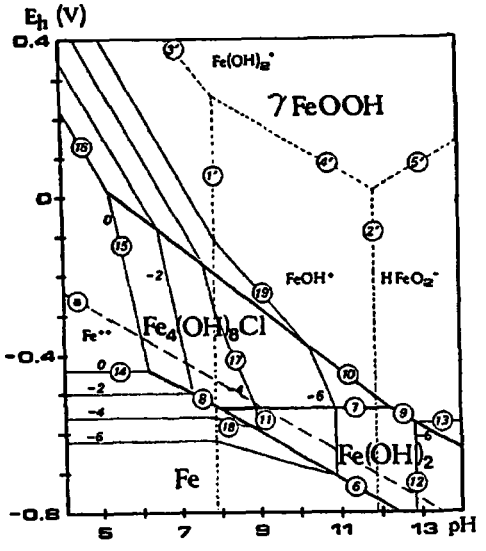

FIG. 9. The E_h–pH equilibrium diagram at 25°C and activity $[Cl^-] = 0.35$ mol l^{-1} for the system Fe–GR1–γ-FeOOH–H_2O–Cl^-. GR1 = $Fe_4(OH)_8Cl$; μ^0(GR1) = −509,500 cal mol^{-1}.

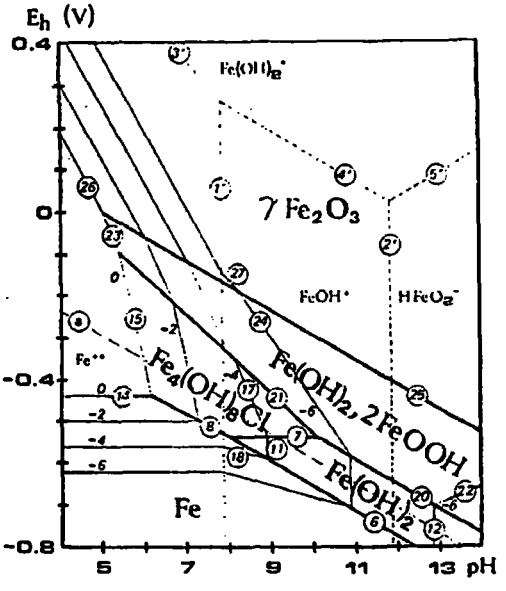

FIG. 10. The E_h–pH equilibrium diagram at 25°C and activity $[Cl^-] = 0.35$ mol l^{-1} for the system Fe–GR1–γ-Fe_2O_3–H_2O–Cl^-. GR1 = $Fe_4(OH)_8Cl$; μ^0(GR1) = −509,500 cal mol^{-1}. Hydrated magnetite, $Fe(OH)_2 \cdot 2FeOOH$, is the compound from which the final product $Fe_{3-x}O_4$ (non-stoichiometric magnetite) is obtained. The diagram is drawn for $x = 1/3$, i.e. the final product is maghemite γ-Fe_2O_3.

Figure 4. The Eh-pH equilibrium diagrams for iron in aqueous systems containing chloride at 25°C [26]

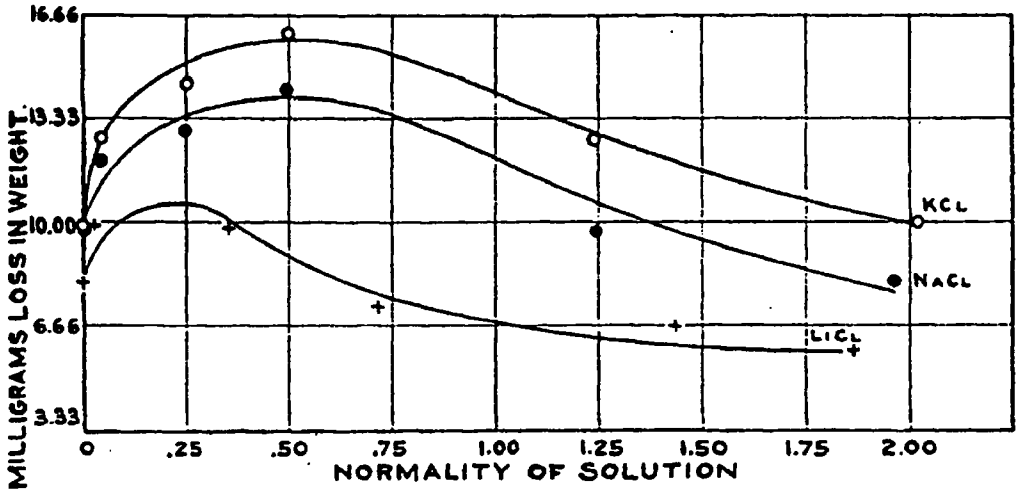

Figure 5. Corrosion rate of mild steel as a function of chloride concentration [105]

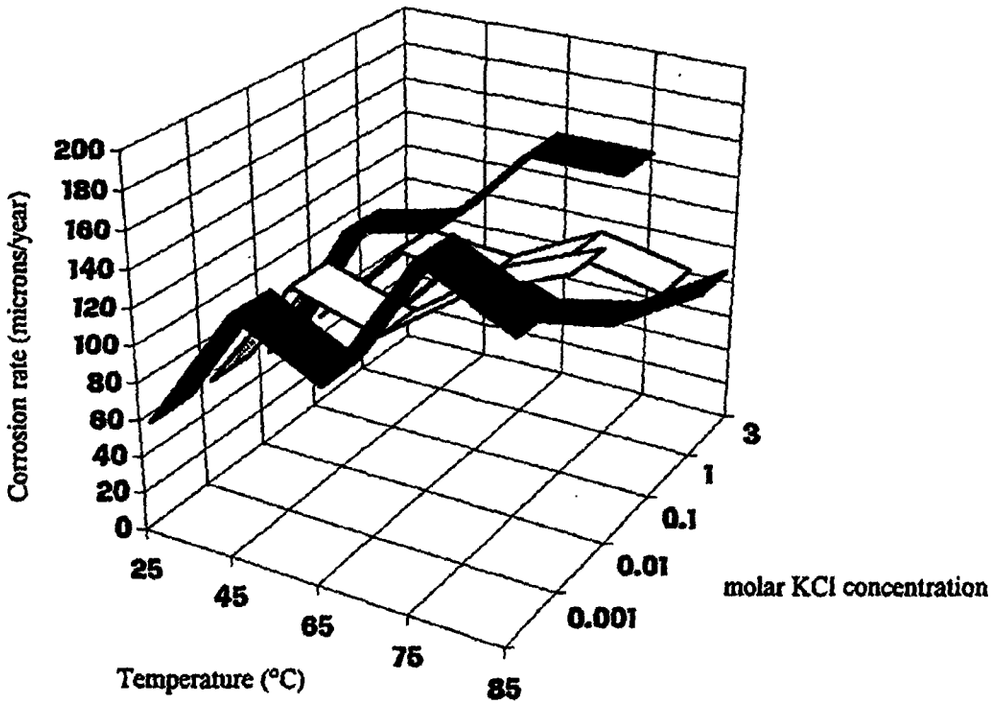

Figure 6. Corrosion of mild steel in aerobic potassium chloride solutions of different concentrations and temperatures [107]

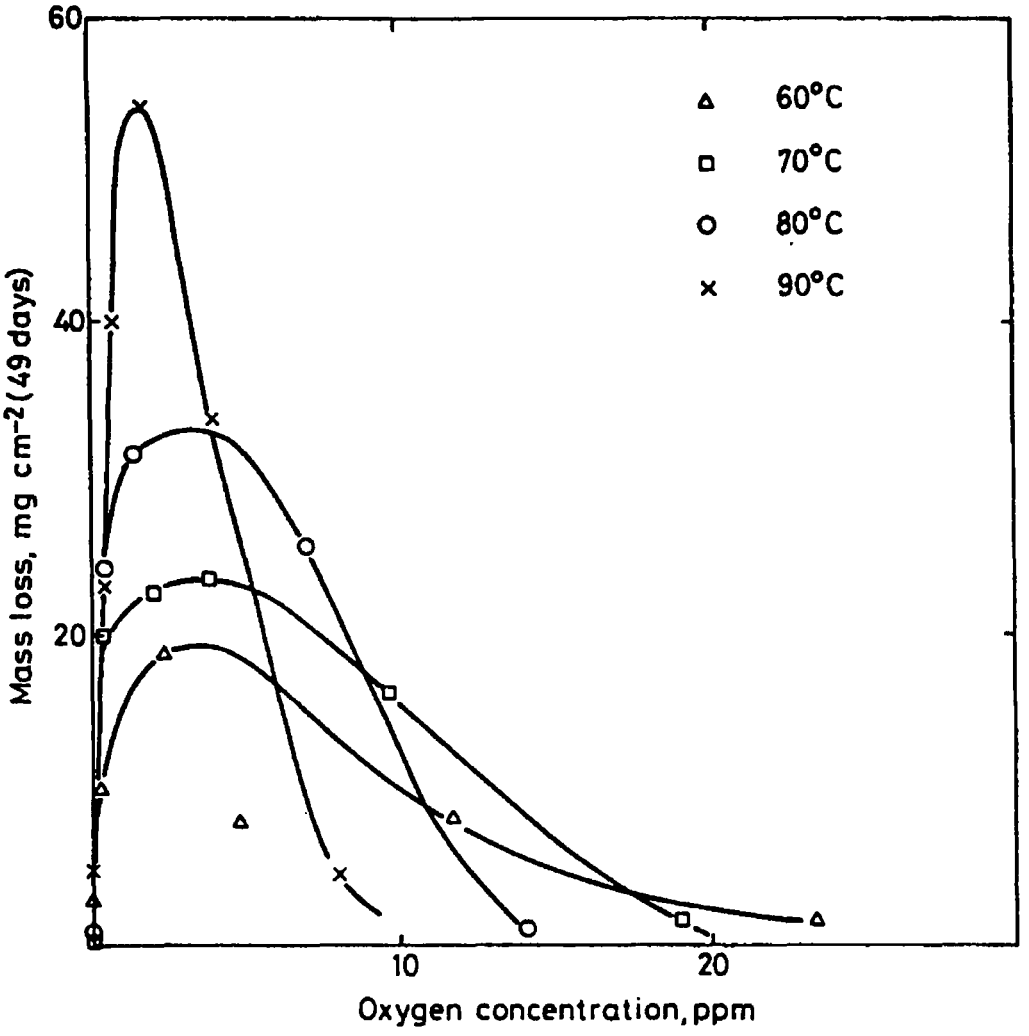

Figure 7. **Mass loss of rotating disc mild steel specimens in distilled water at varying temperature and oxygen concentration [33]**

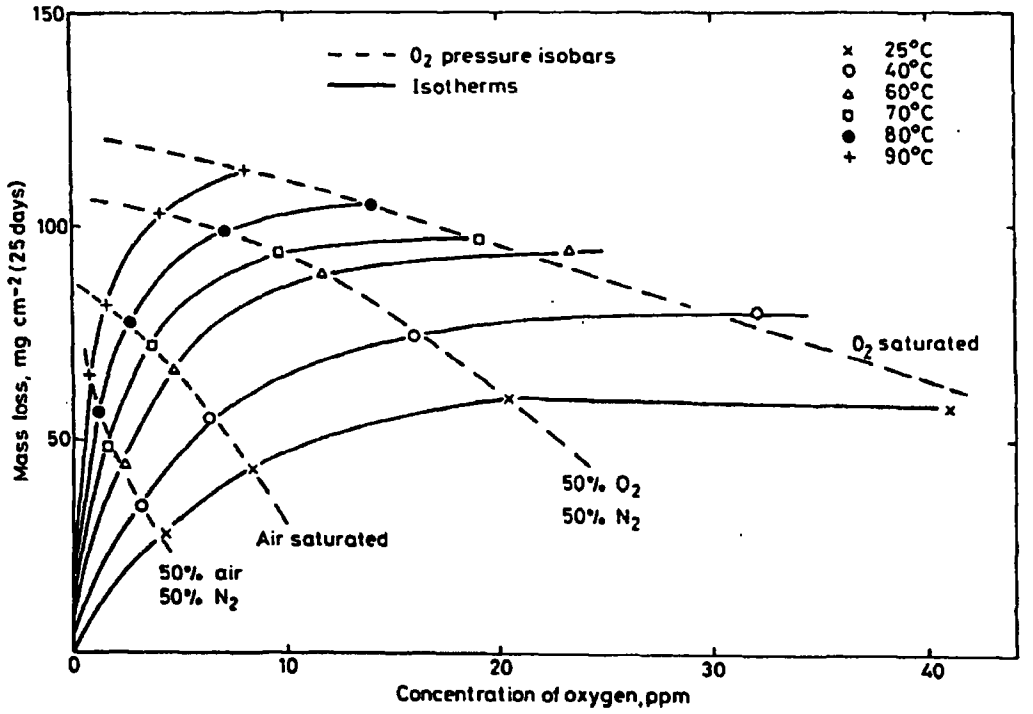

Figure 8. **Mass loss of rotating disc mild steel specimens in sodium chloride solutions (35 ppm chloride) at varying temperature and oxygen concentration [33]**

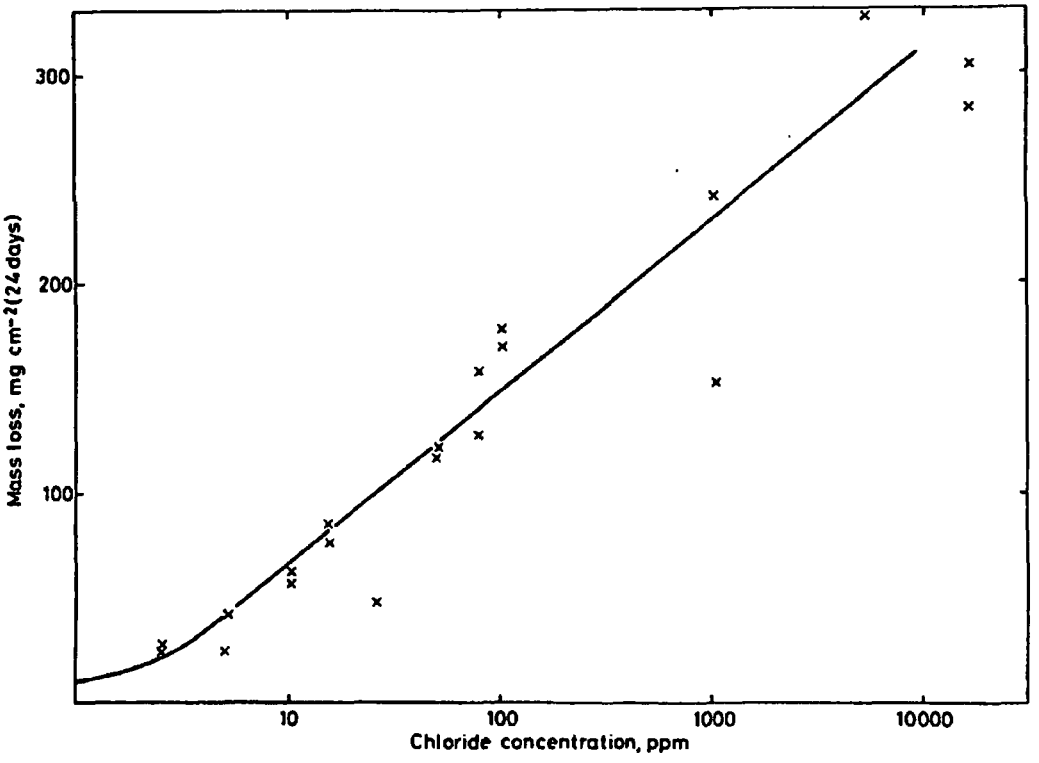

Figure 9. Mass loss of rotating disc mild steel specimens in oxygenated sodium chloride solutions at varying chloride concentration [33]

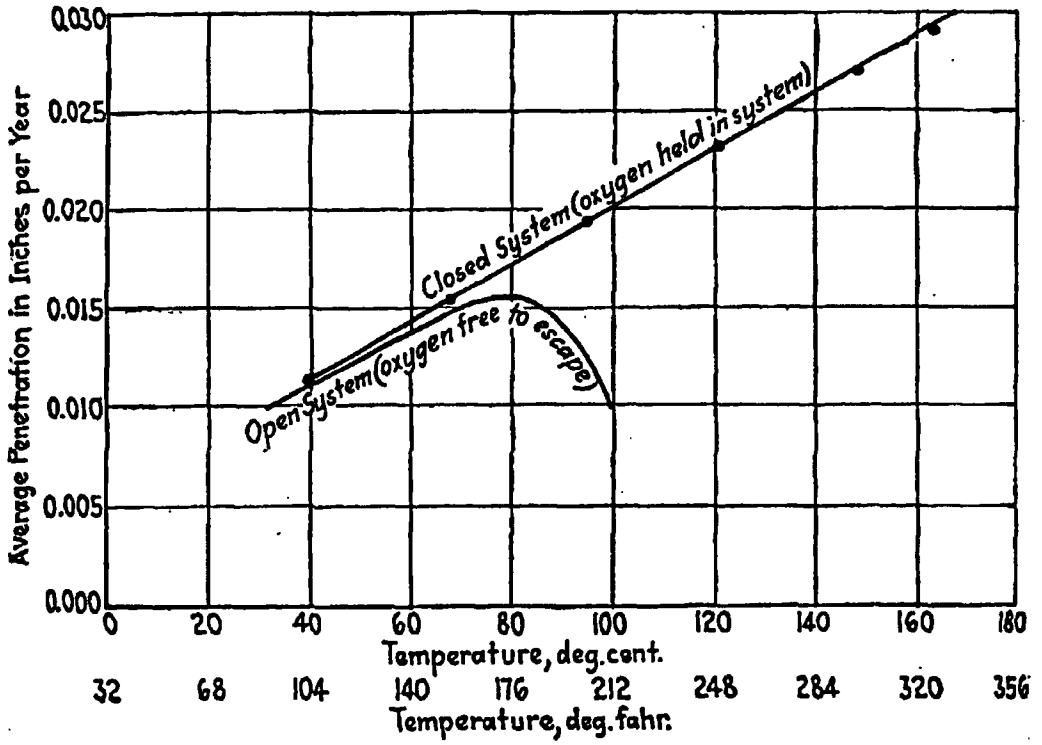

Figure 10. Effect of temperature on corrosion in water [8]

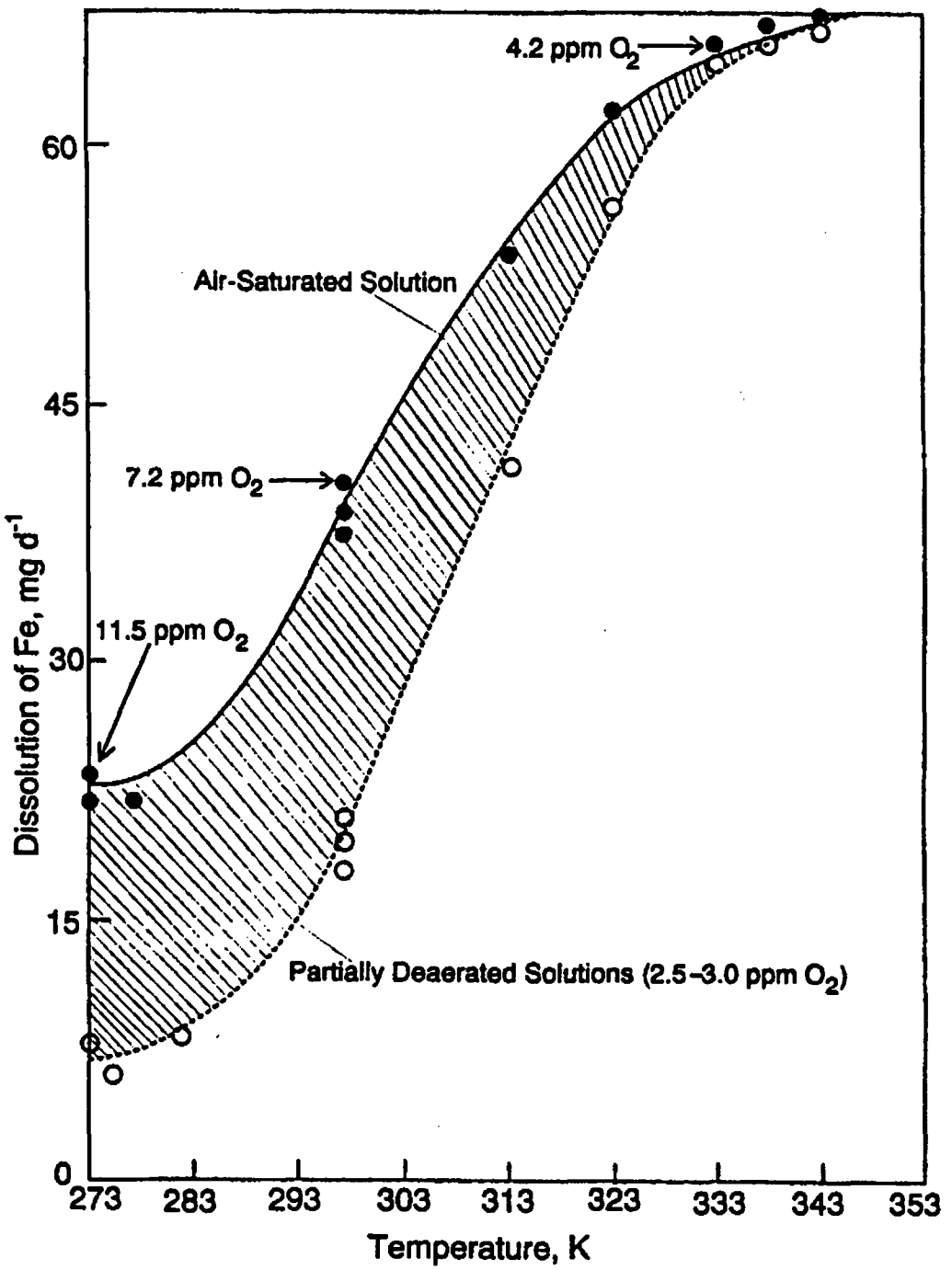

Figure 11. Dissolution of iron in 3% NaCl as a function of temperature and of dissolved oxygen. 16 hour test [111]

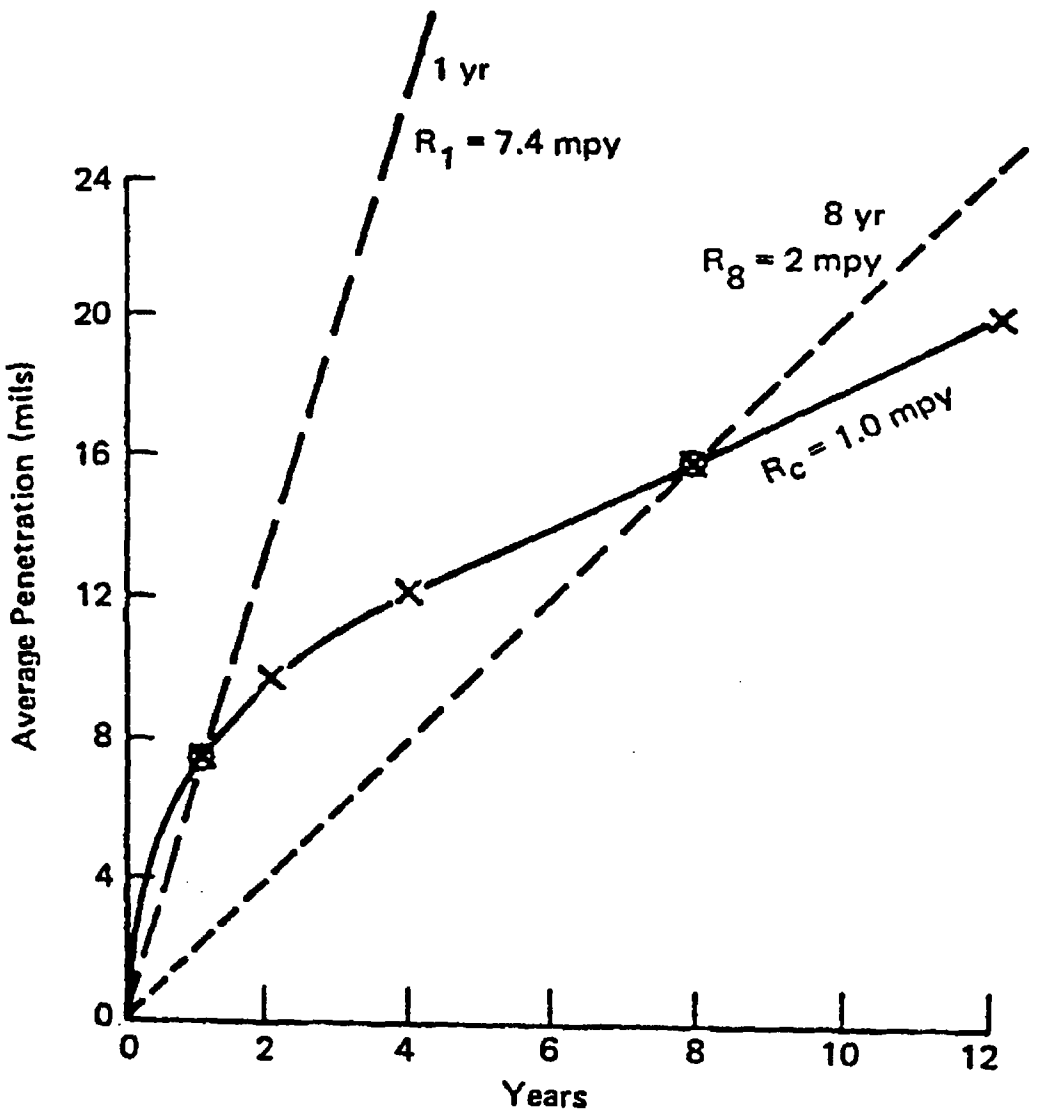

Figure 12. Typical corrosion-time curve expected for mild steel corroding underwater, showing how measured corrosion rate decreases with increasing measurement periods [132]

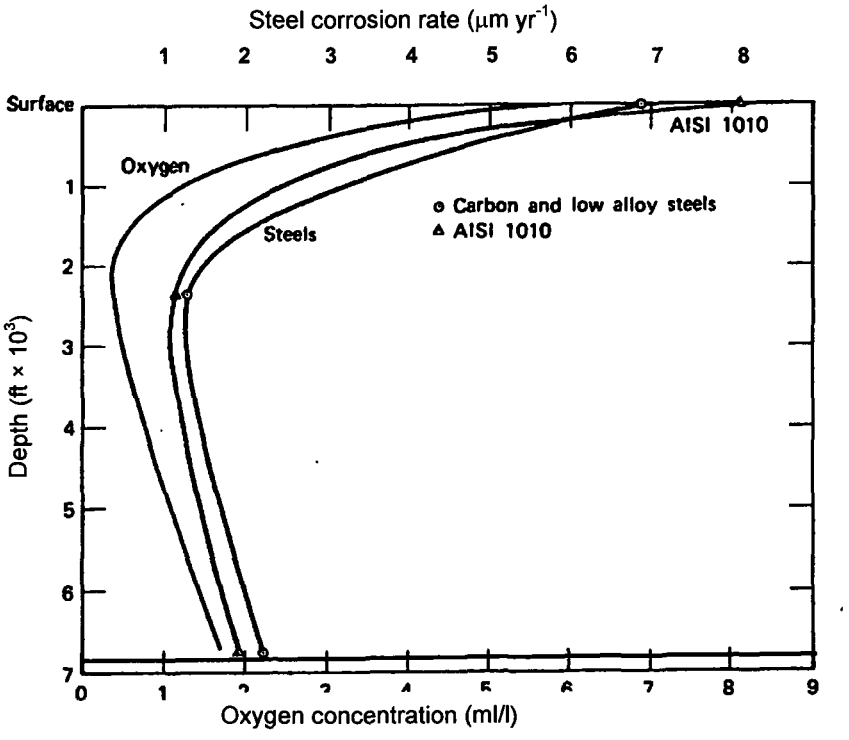

Figure 13. Corrosion of steel versus depth after 1 year of exposure [42]

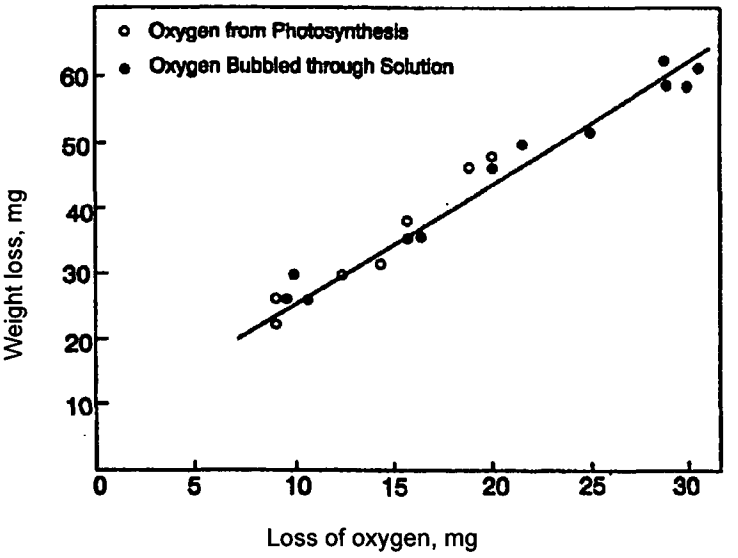

(a)

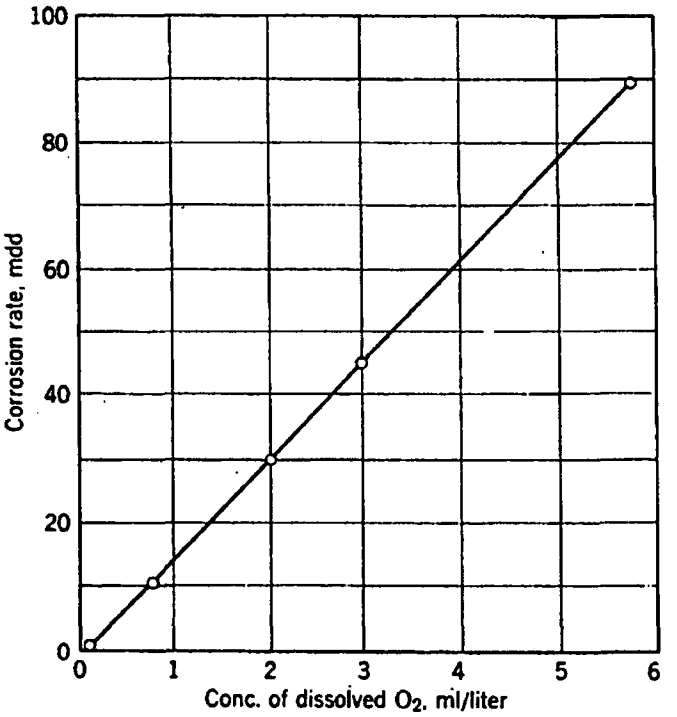

(b)

Figure 14. Effect of dissolved oxygen on corrosion rate of steel in (a) seawater [195] and (b) slowly moving water containing 165 ppm $CaCl_2$ [10]
(Note: mdd = mg dm^{-2} day^{-1})

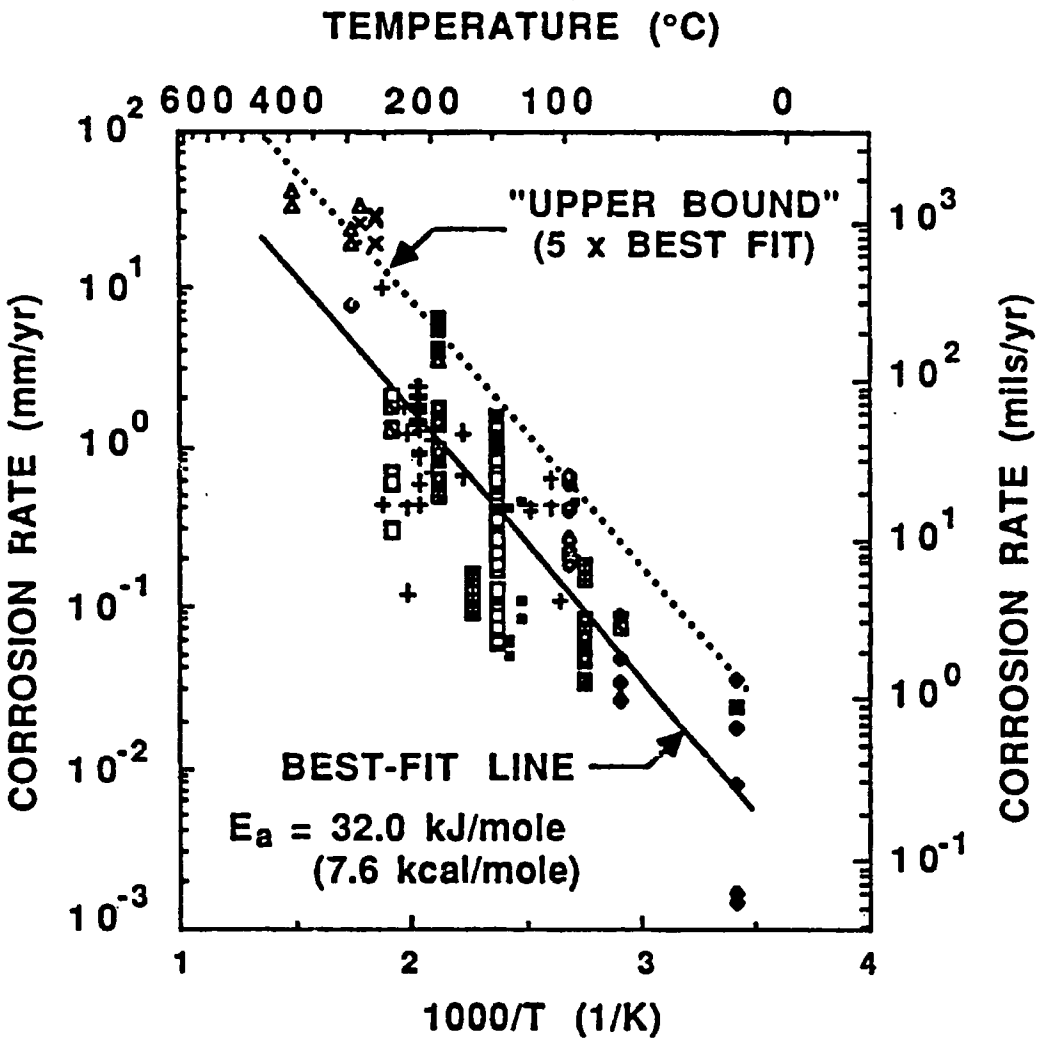

Figure 15. Corrosion rate of carbon steels in anaerobic acid chloride solutions as a function of temperature [43, 44]

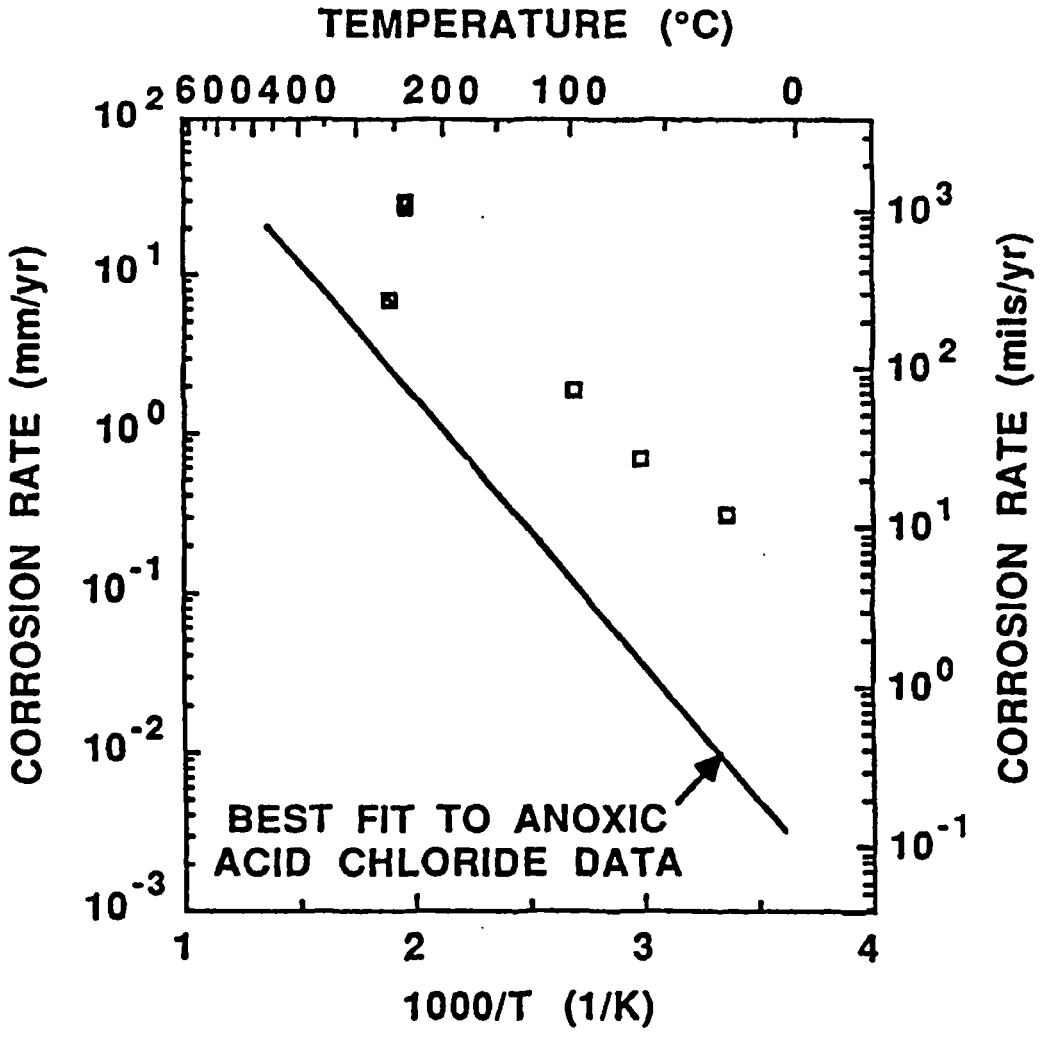

Figure 16. Corrosion rate of carbon steels in aerobic acid chloride solutions as a function of temperature [43, 44]

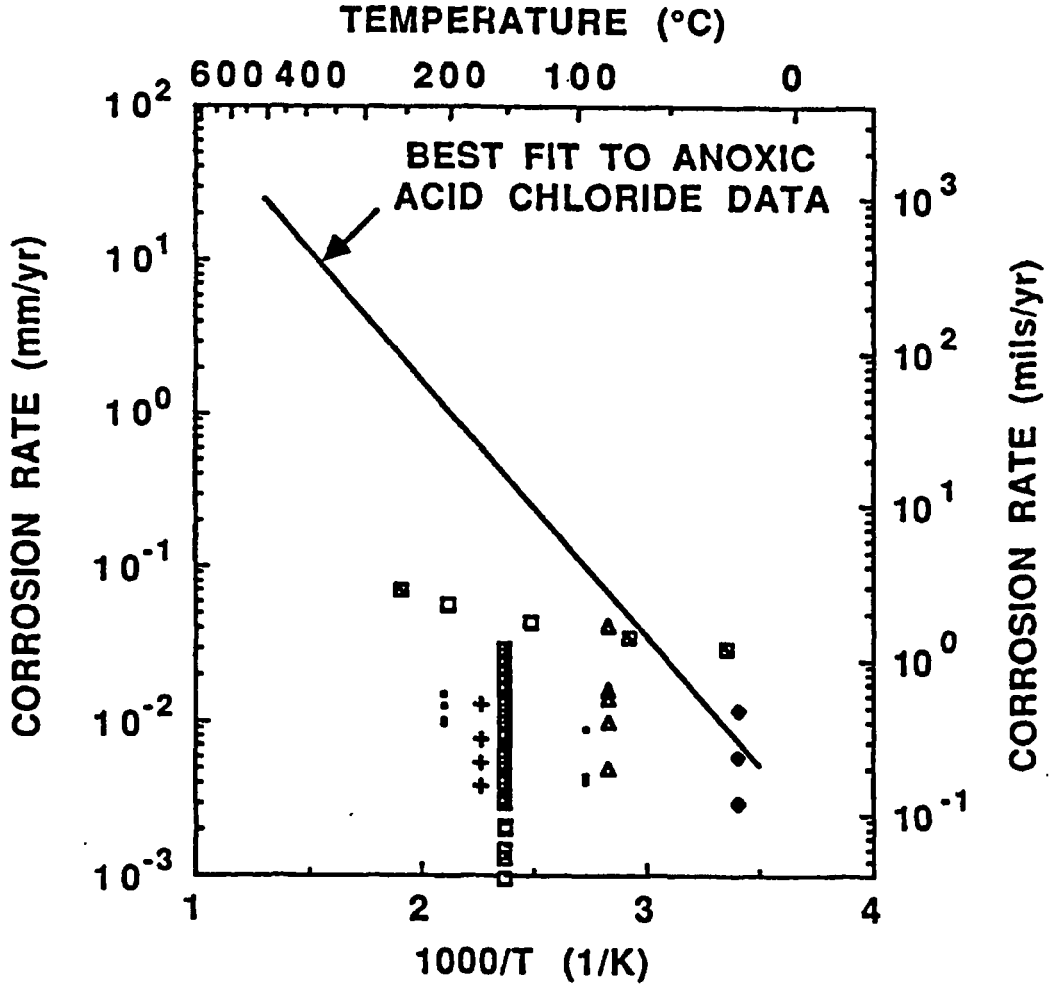

Figure 17. Comparison of corrosion rates for carbon steels in aerobic and anaerobic neutral and basic chloride solutions as a function of temperature [43, 44] (data points), and in anaerobic acid chloride solutions (best fit line)

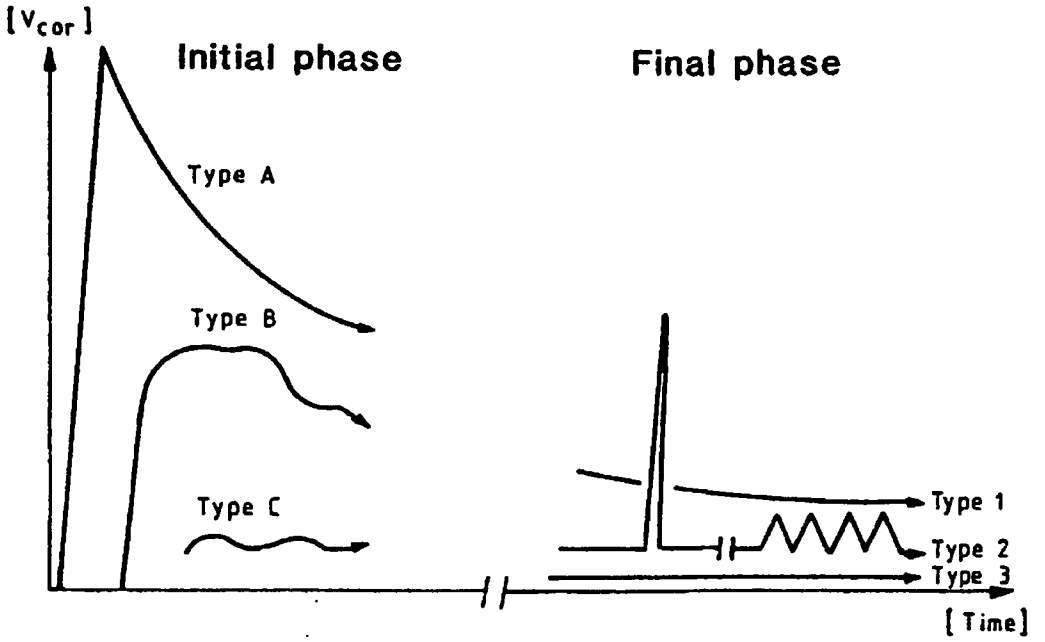

Figure 18. **Typical hydrogen evolution rate-time curves (schematic) for low carbon steel in anaerobic groundwaters, pH 7-10 [45]**

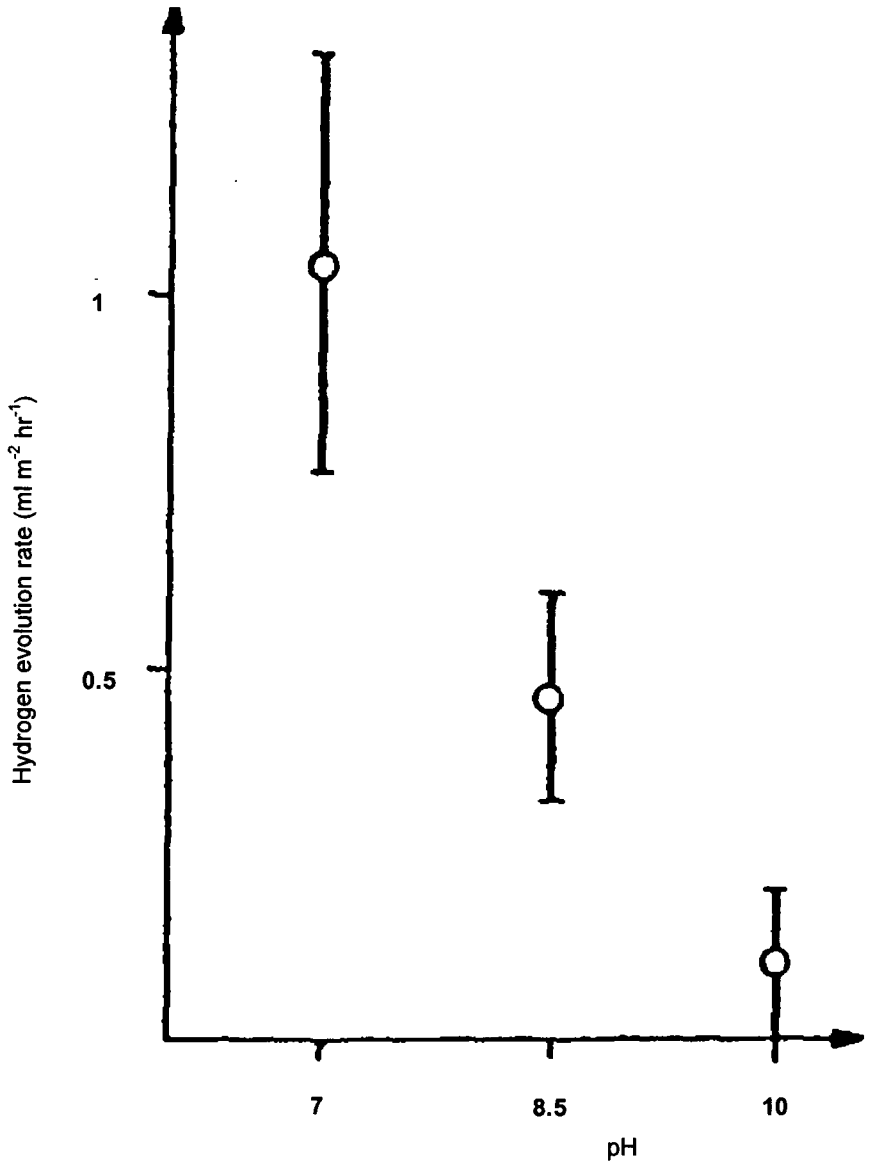

Figure 19. **Average and standard deviation of hydrogen evolution rate for low carbon steel in anaerobic groundwaters, as a function of pH for all media and temperatures [104]**

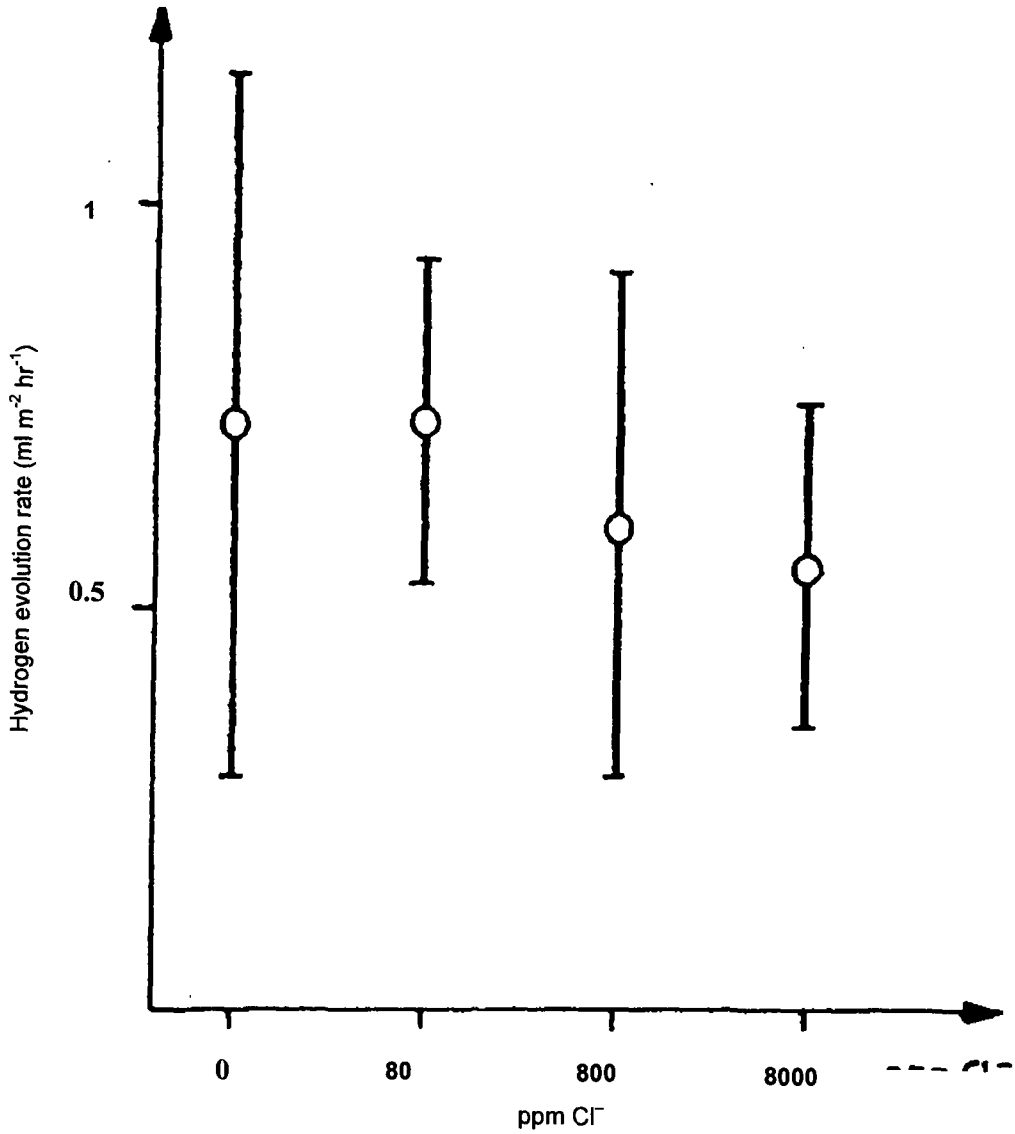

Figure 20. **Average and standard deviation of hydrogen evolution rate for low carbon steel in anaerobic groundwaters, as a function of chloride concentration for all media and temperatures [104]**

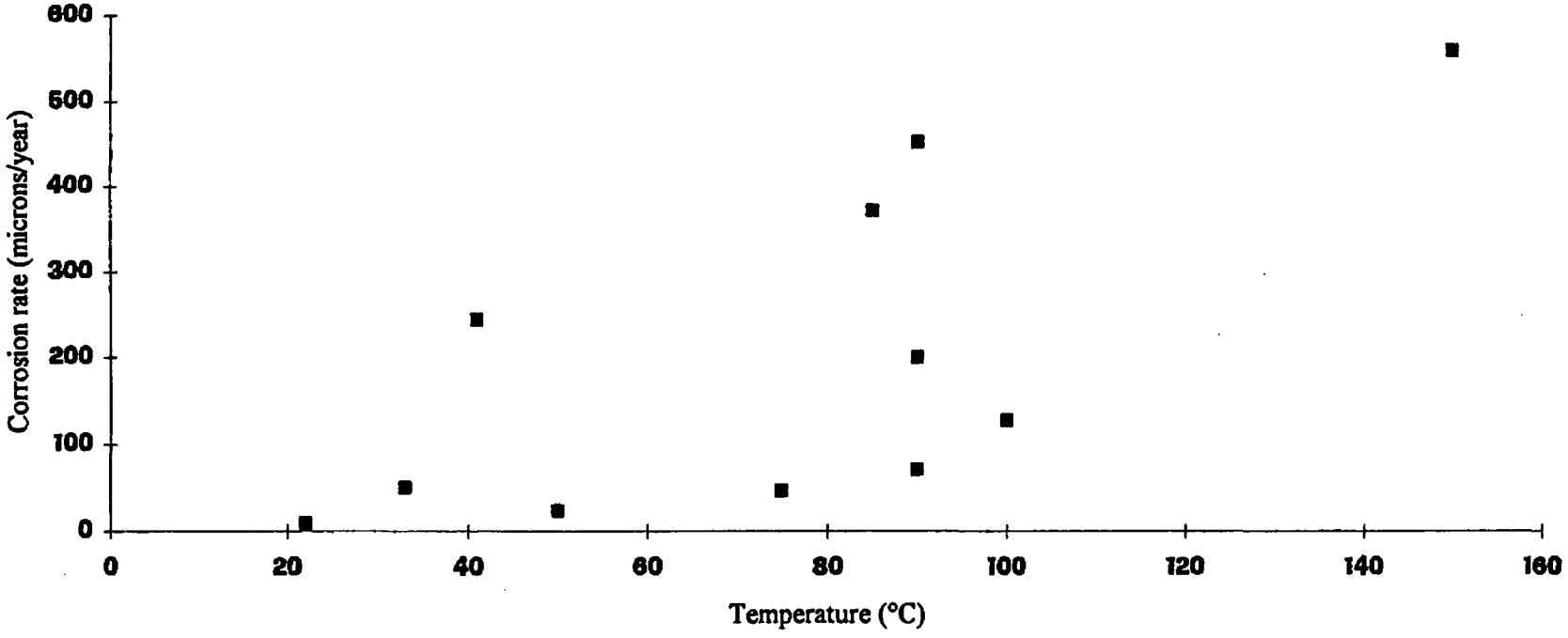

Figure 21. Instantaneous corrosion rate measurements for mild steel in anaerobic neutral solutions, as a function of temperature

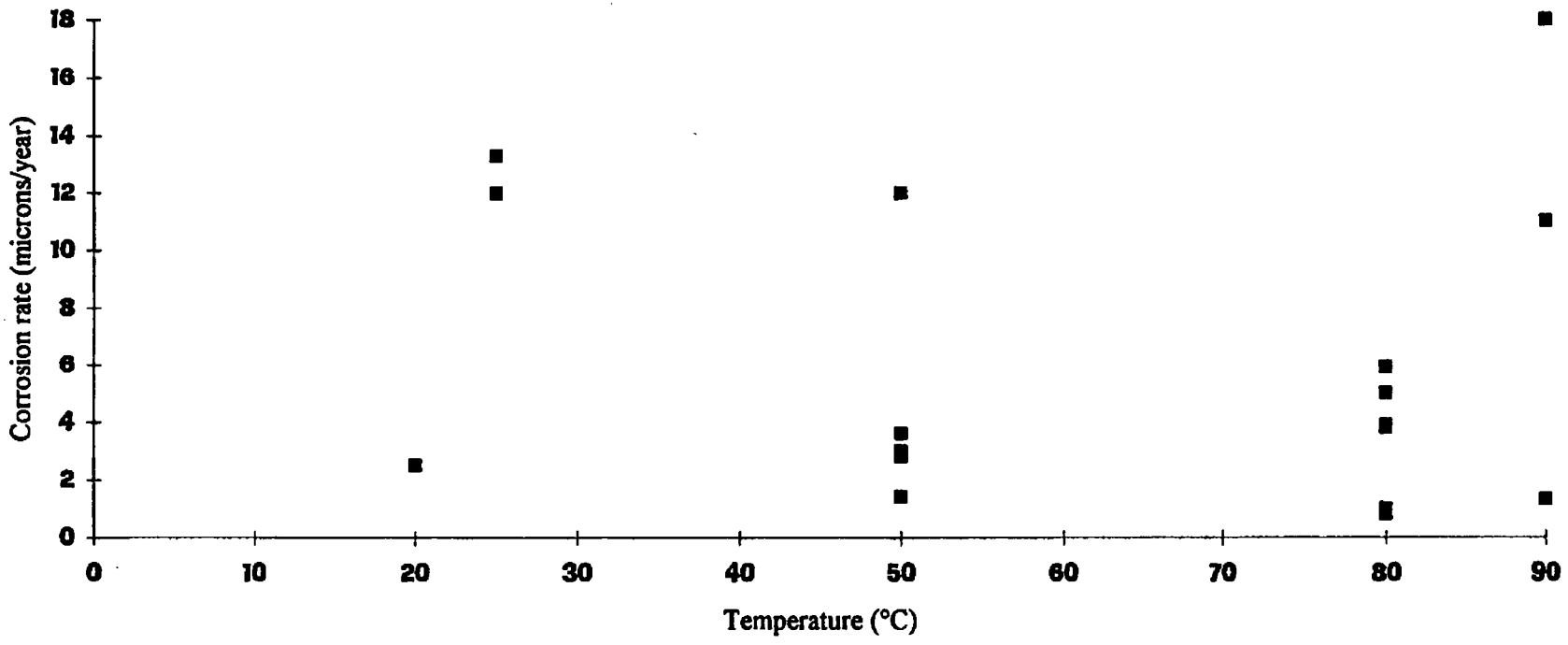

Figure 22. Integrated corrosion rate measurements for mild steel in anaerobic neutral solutions, as a function of temperature

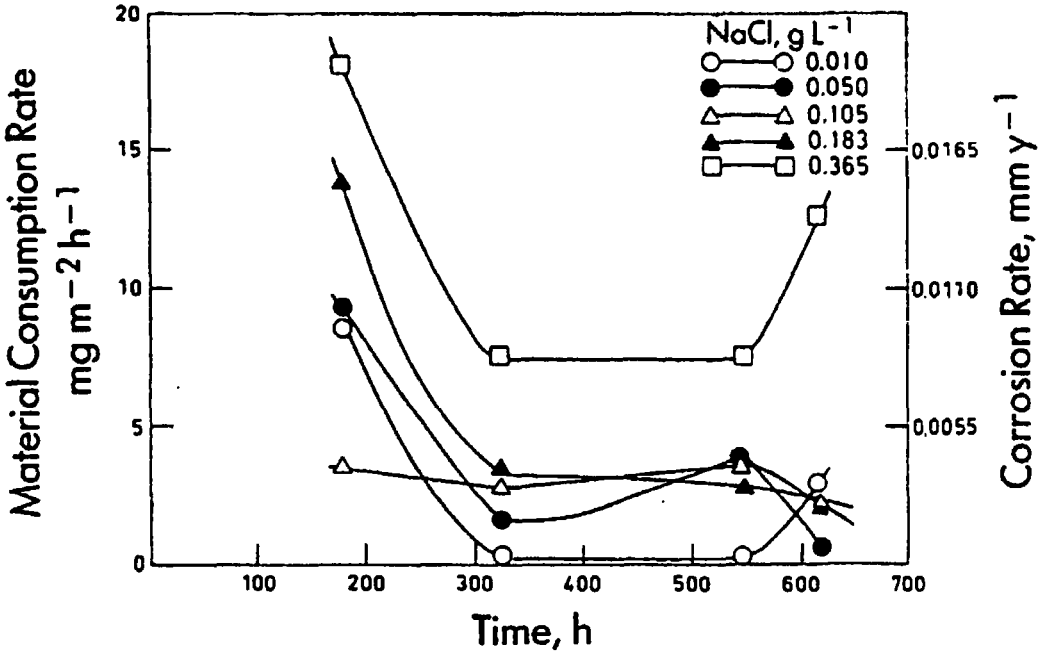

Figure 23. **Change in the corrosion rates with time of carbon steel in 0.43 g l^{-1} $Ca(OH)_2$ solution as a function of the sodium chloride content [47]**

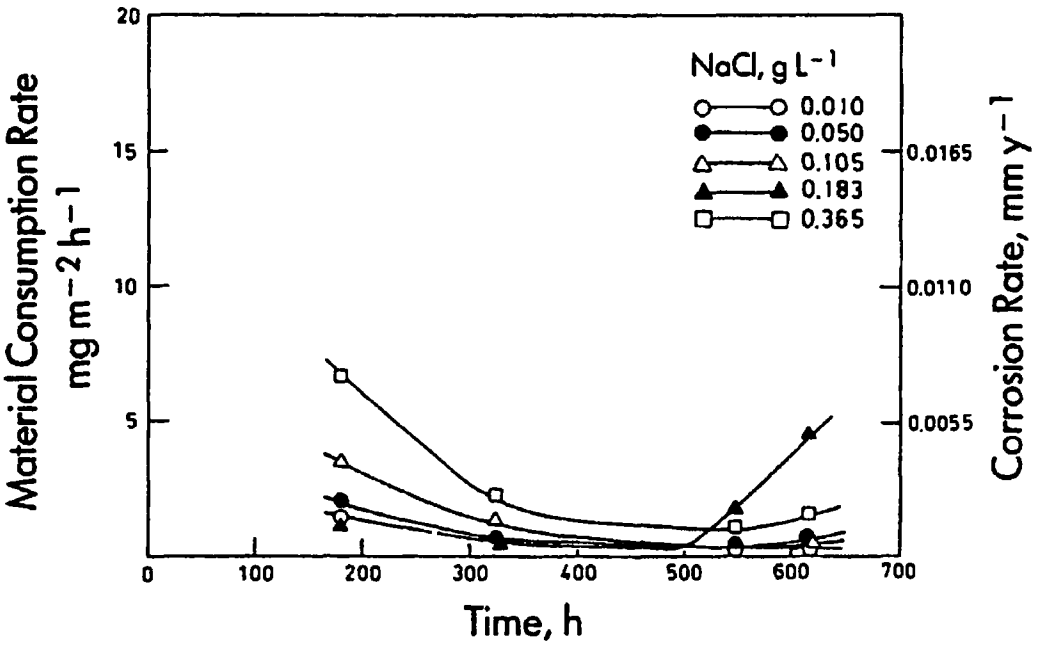

Figure 24. **Change in the corrosion rates with time of carbon steel in 0.76 g l^{-1} $Ca(OH)_2$ solution as a function of the sodium chloride content [47]**

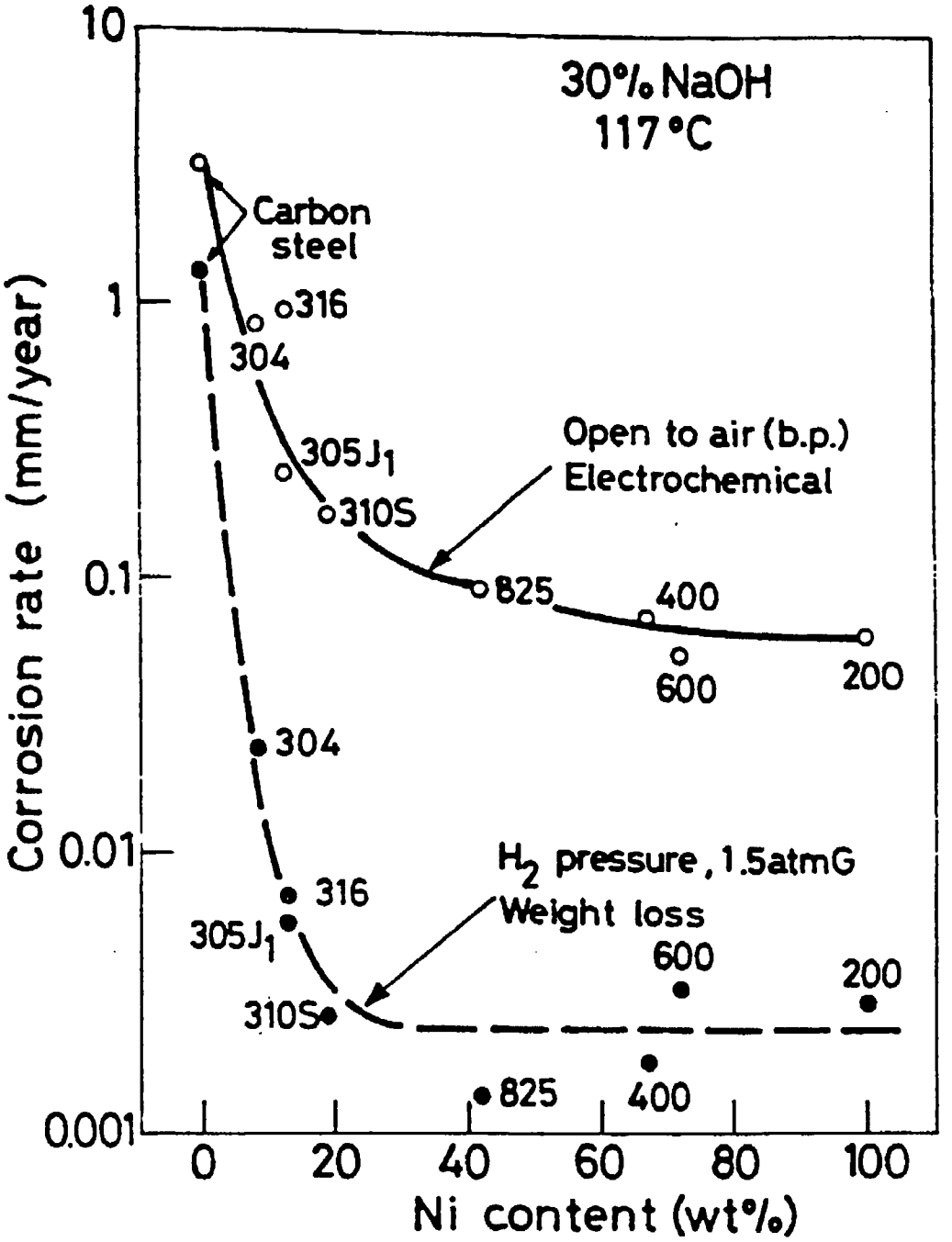

Figure 25. Corrosion rate of various materials in 30% NaOH solution as a function of the Ni content: solid line with open points - by the electrochemical technique in a solution open to the air; broken line with closed points - by weight loss measurements in a H_2 saturated solution [48]

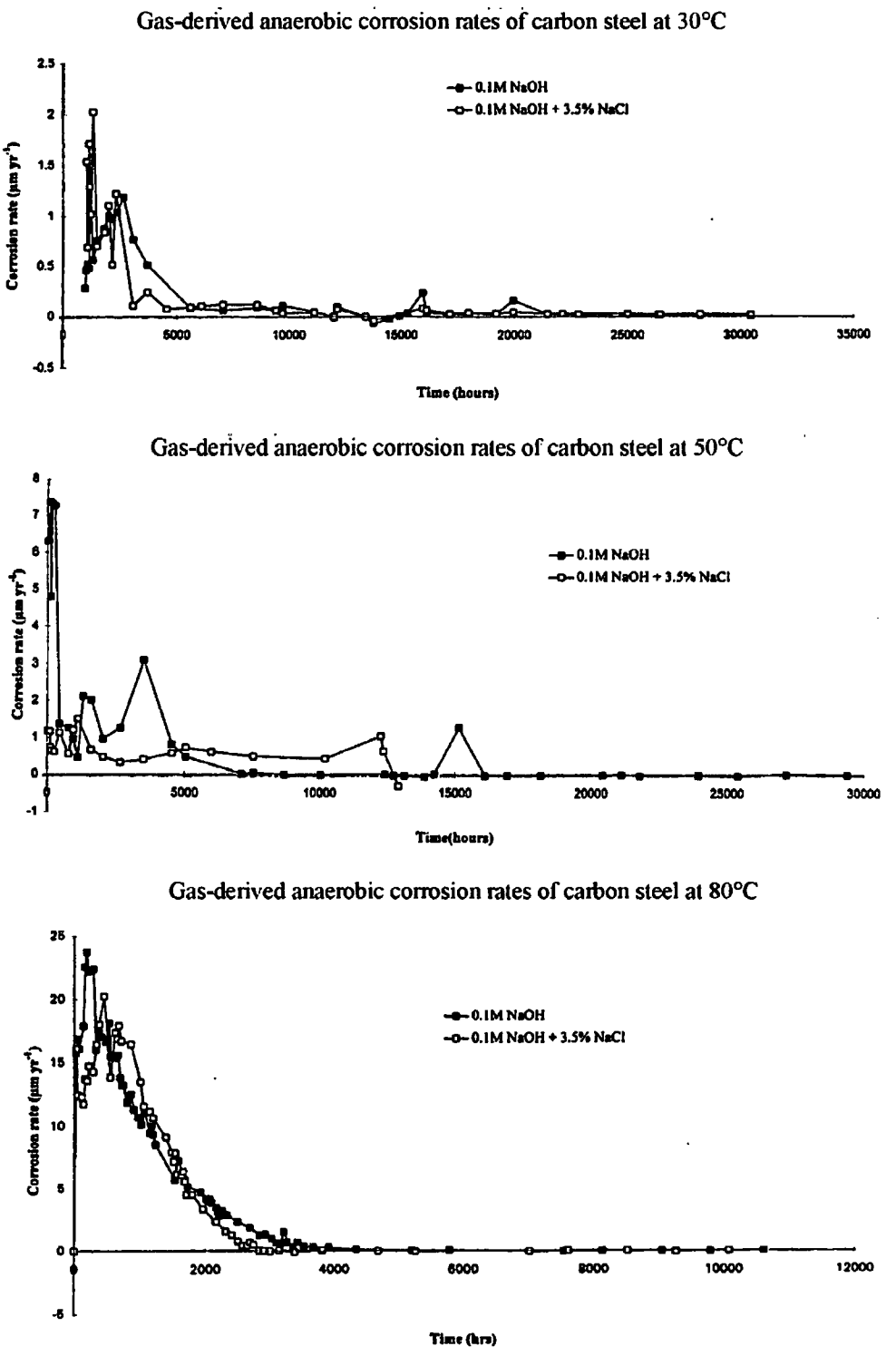

Figure 26. Gas-derived anaerobic corrosion rates for carbon steel in sodium hydroxide with and without 3.5% NaCl at 30, 50 and 80°C [170]

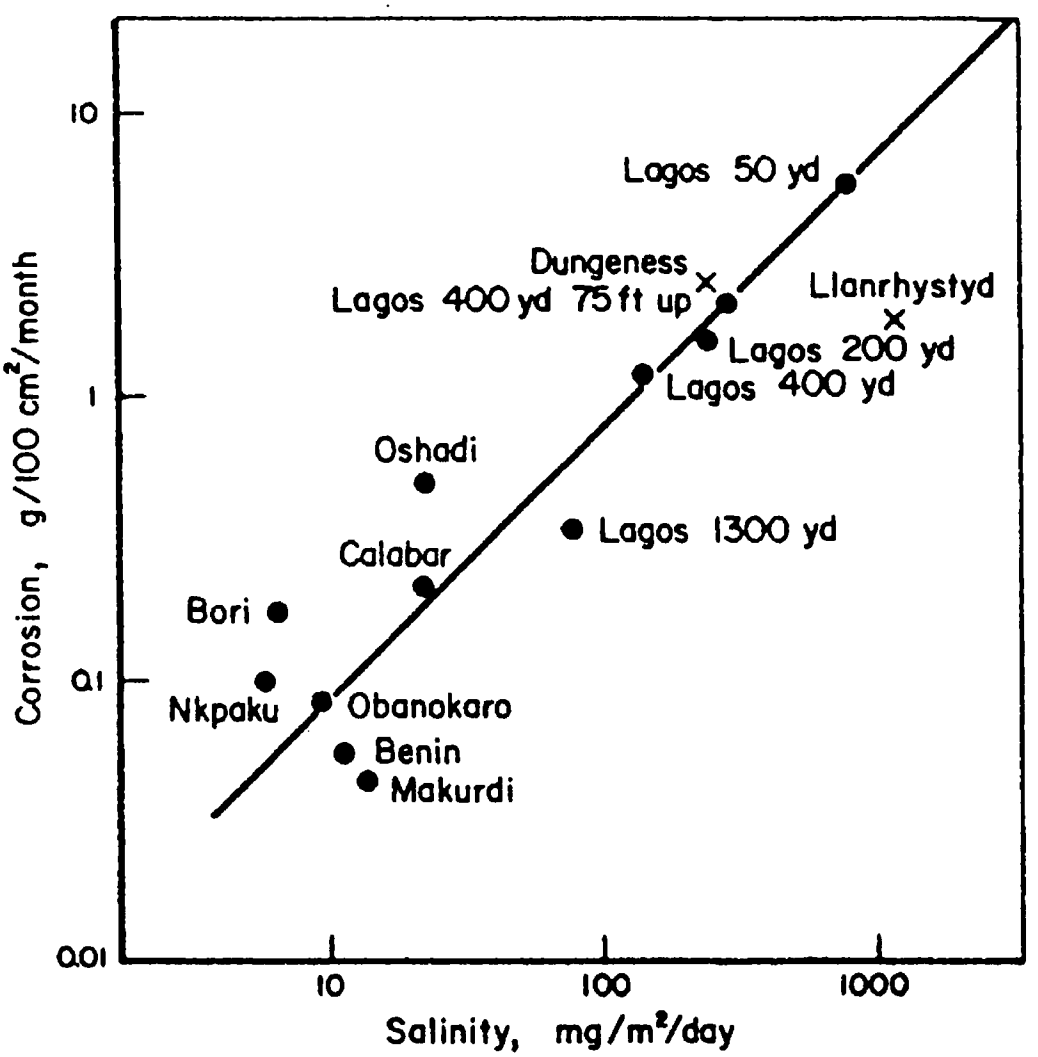

Figure 27. **Relationship between corrosion of mild steel and salinity at exposure sites in Nigeria and the United Kingdom [171]**

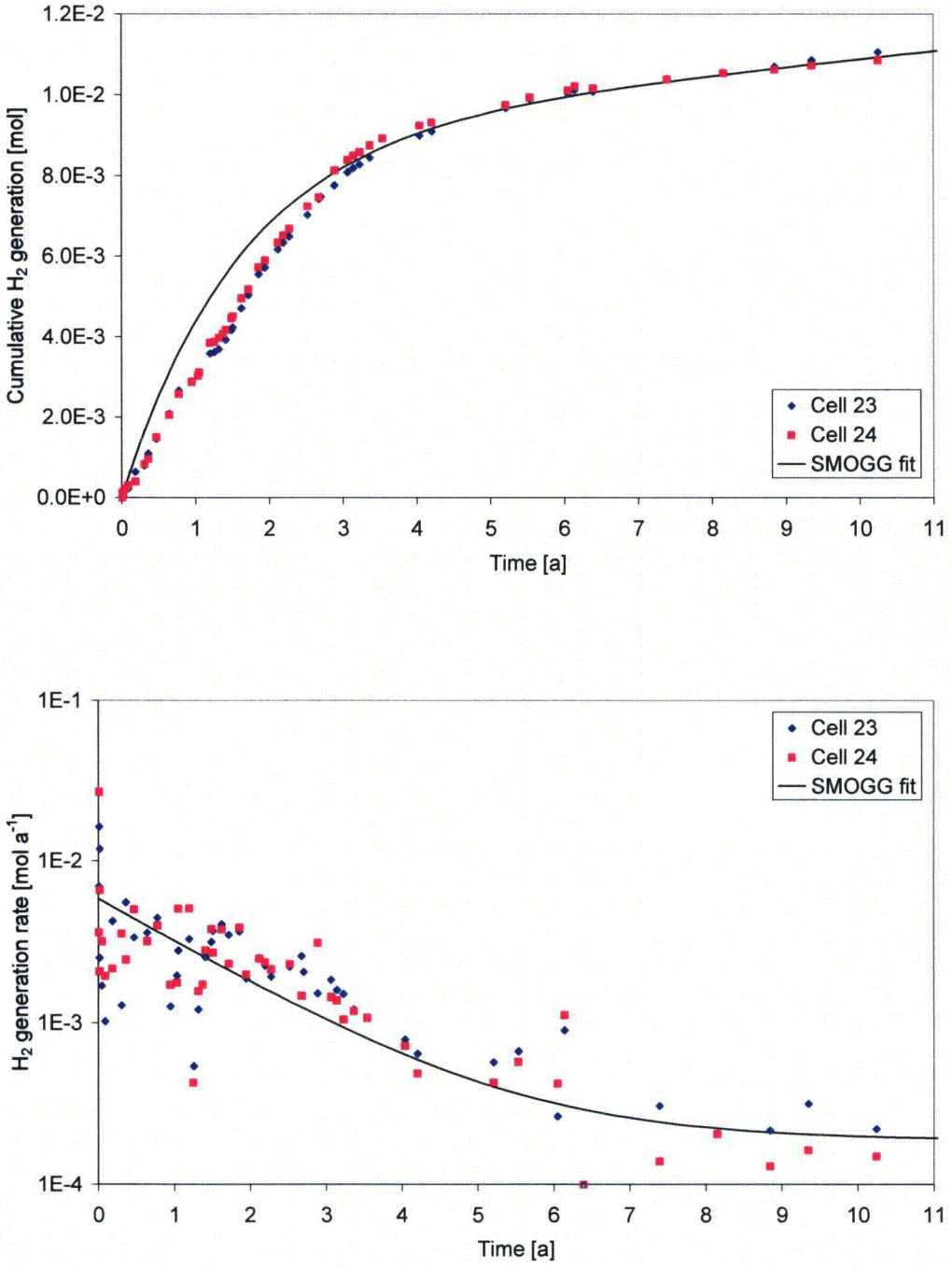

Figure 28. Comparison of gas generation results from SMOGG calibration with experimental results [69] for corrosion of carbon steel in saturated $Ca(OH)_2$ solution at 30°C (negative gas generation rates determined from experimental results are plotted as unfilled points at minimum rate for information)

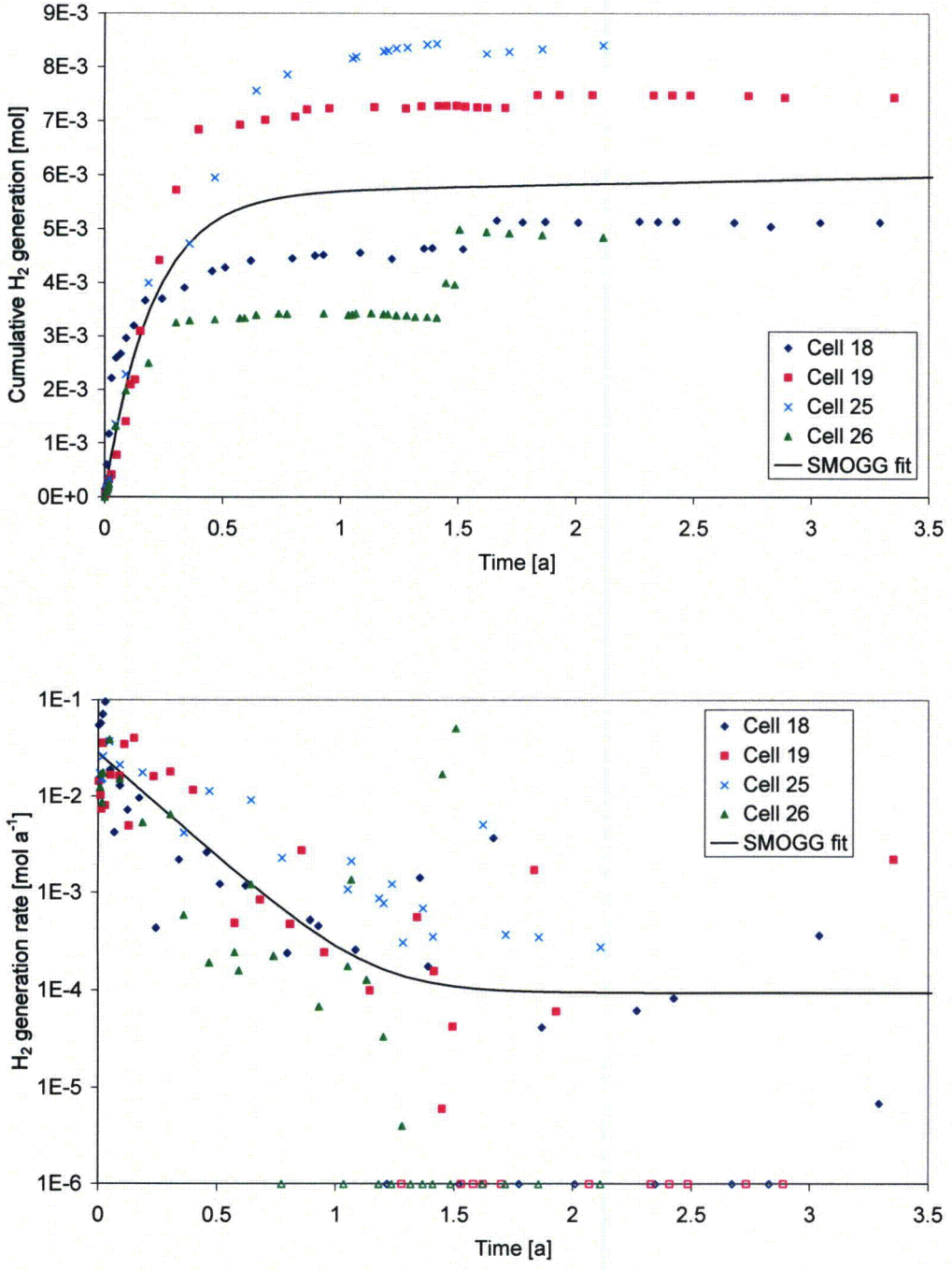

Figure 29. **Comparison of gas generation results from SMOGG calibration with experimental results [69] for corrosion of carbon steel in saturated $Ca(OH)_2$ solution at 50°C (negative gas generation rates determined from experimental results are plotted as unfilled points at minimum rate for information)**

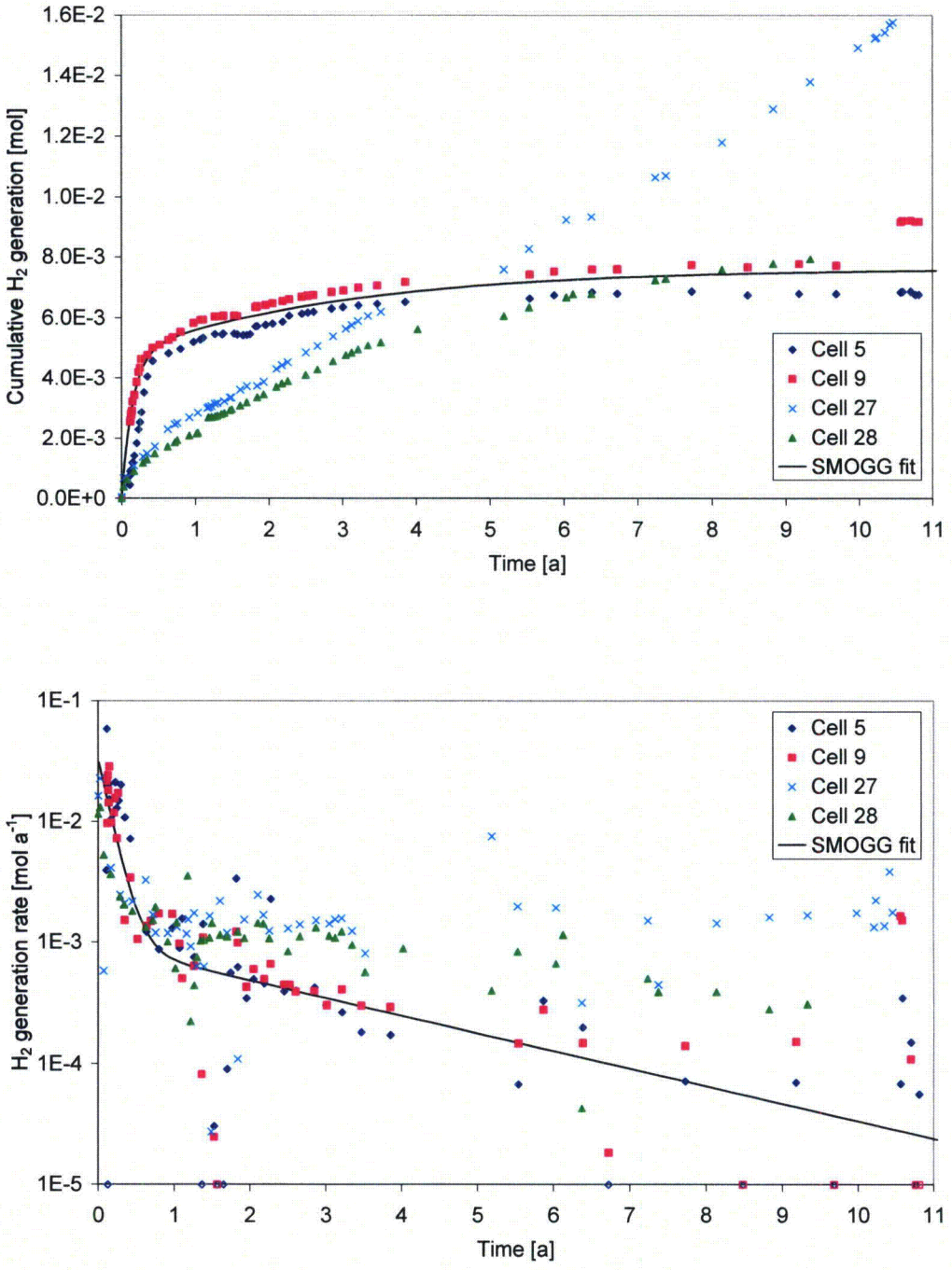

Figure 30. **Comparison of gas generation results from SMOGG calibration with experimental results [69] for corrosion of carbon steel in NaOH solution at 30°C (negative gas generation rates determined from experimental results are plotted as unfilled points at minimum rate for information)**

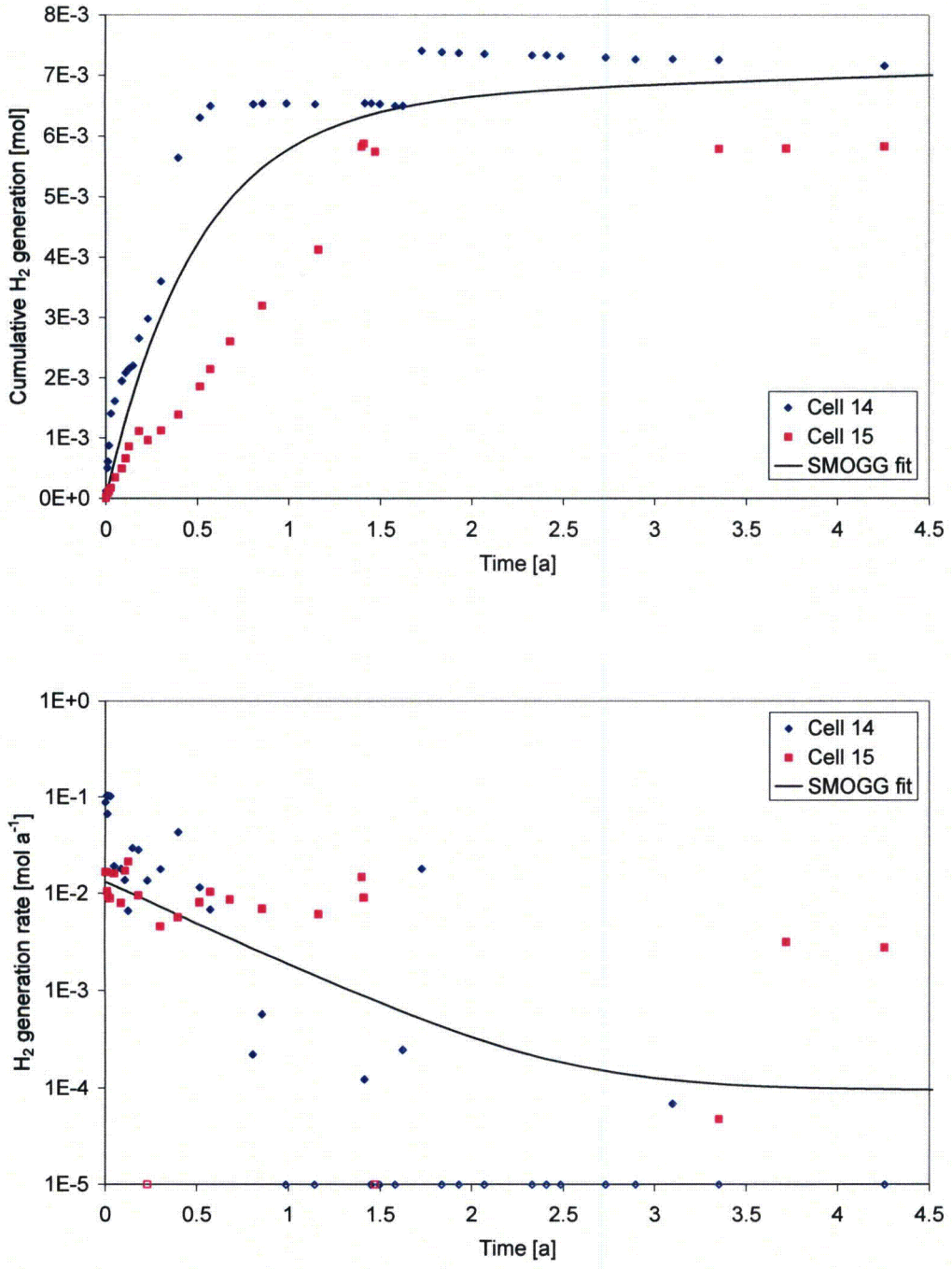

Figure 31. Comparison of gas generation results from SMOGG calibration with experimental results [69] for corrosion of carbon steel in NaOH solution at 50°C (negative gas generation rates determined from experimental results are plotted as unfilled points at minimum rate for information)

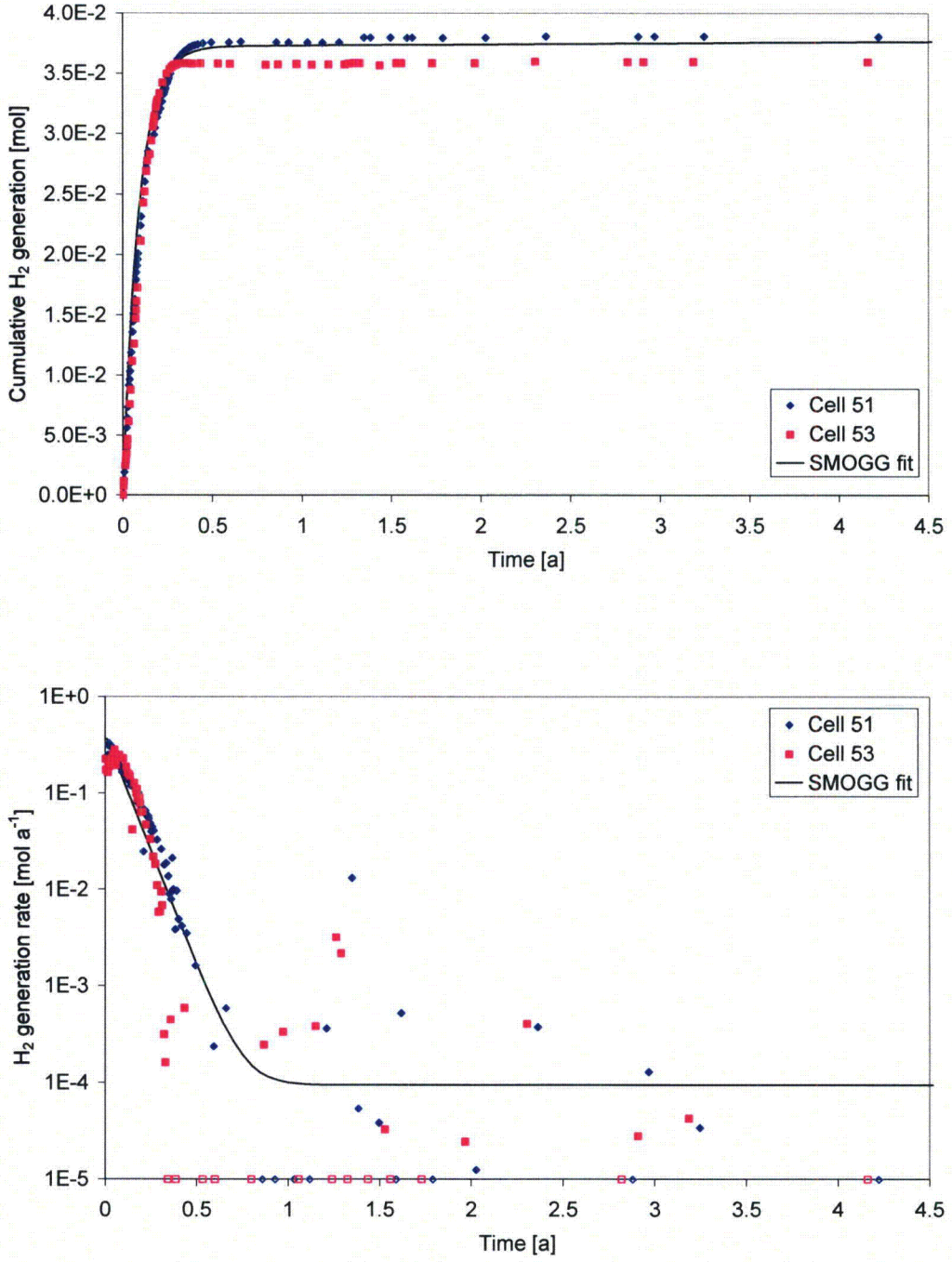

Figure 32. **Comparison of gas generation results from SMOGG calibration with experimental results [69] for corrosion of carbon steel in NaOH solution at 80°C (negative gas generation rates determined from experimental results are plotted as unfilled points at minimum rate for information)**

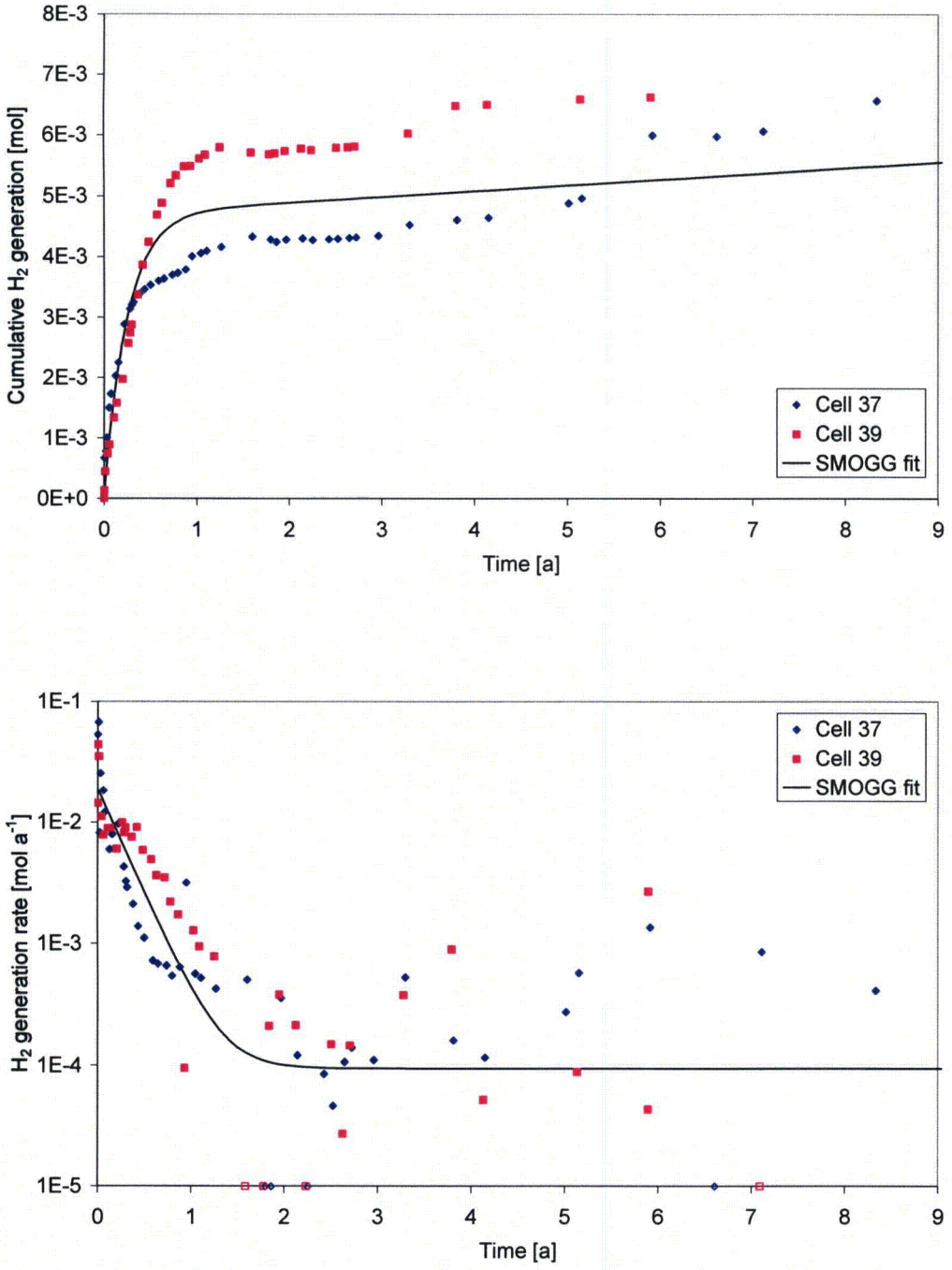

Figure 33. Comparison of gas generation results from SMOGG calibration with experimental results [69] for corrosion of carbon steel in NRVB at 50°C (negative gas generation rates determined from experimental results are plotted as unfilled points at minimum rate for information)

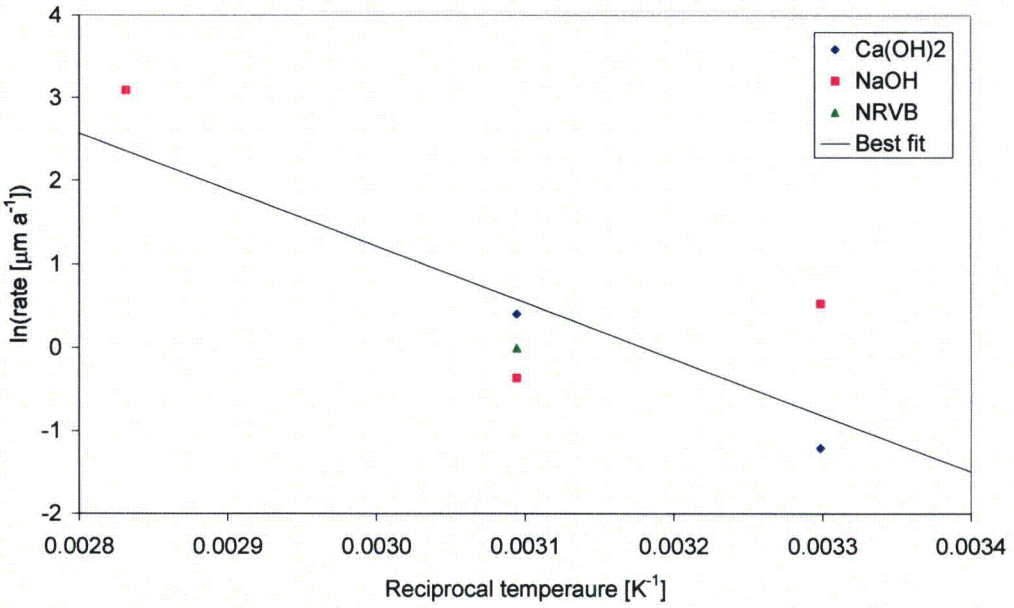

Figure 34. Examination of potential Arrhenius relationship between calibrated acute anaerobic corrosion rate constants for carbon steel and temperature

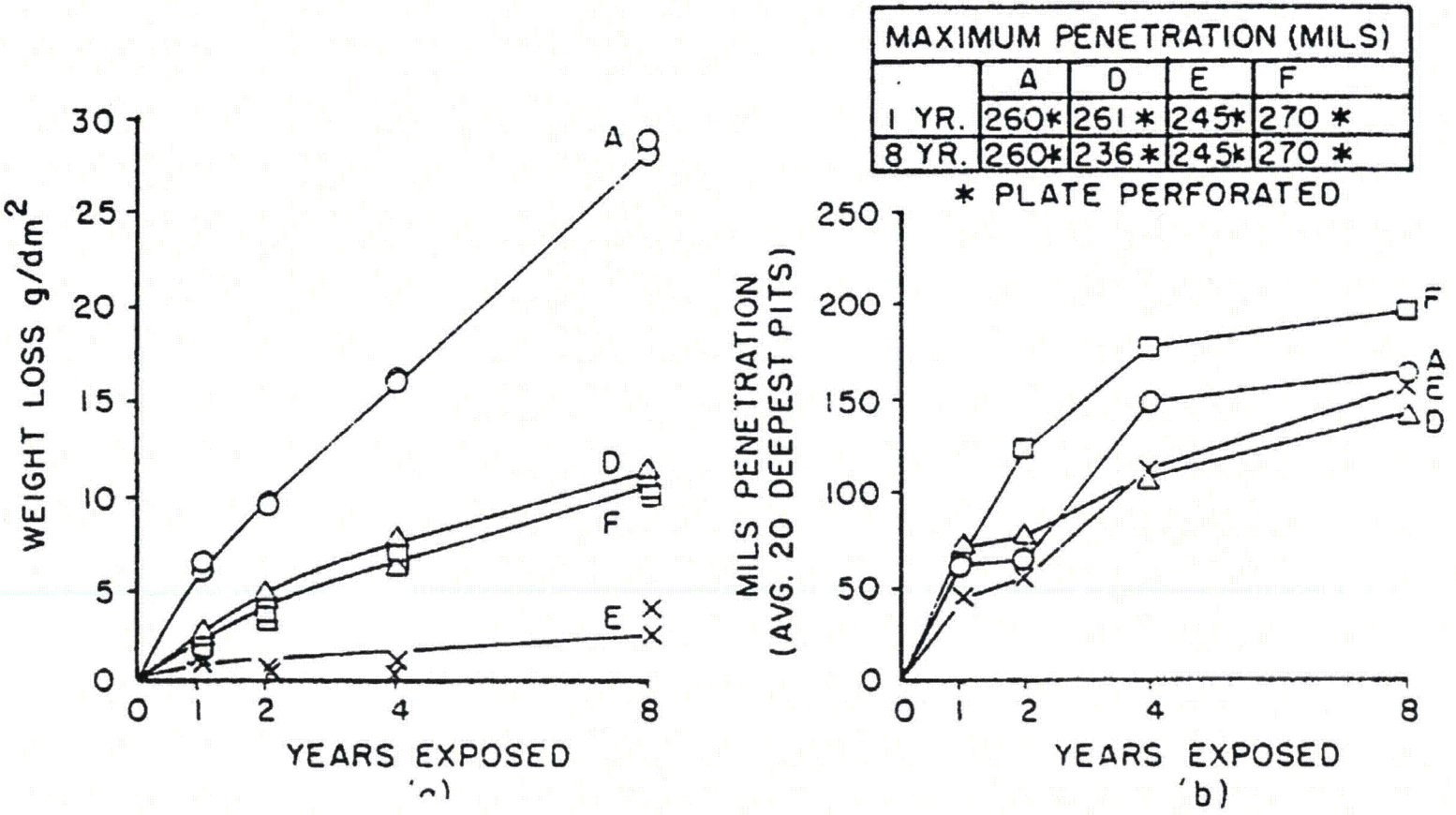

Figure 35. **Comparative corrosion rates of various stainless steel alloys continuously immersed in tropical seawater: A - type 410; D - type 302, E - type 316, F - type 321 [178]**

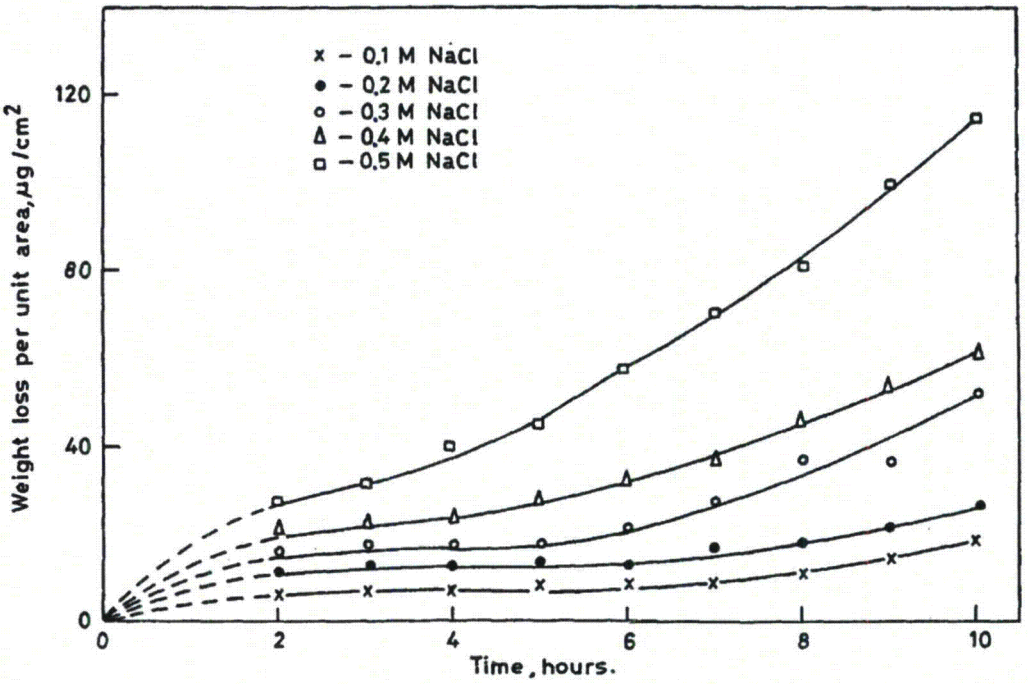

Figure 36. Effect of NaCl concentration on corrosion of stainless steel at 90°C [83]

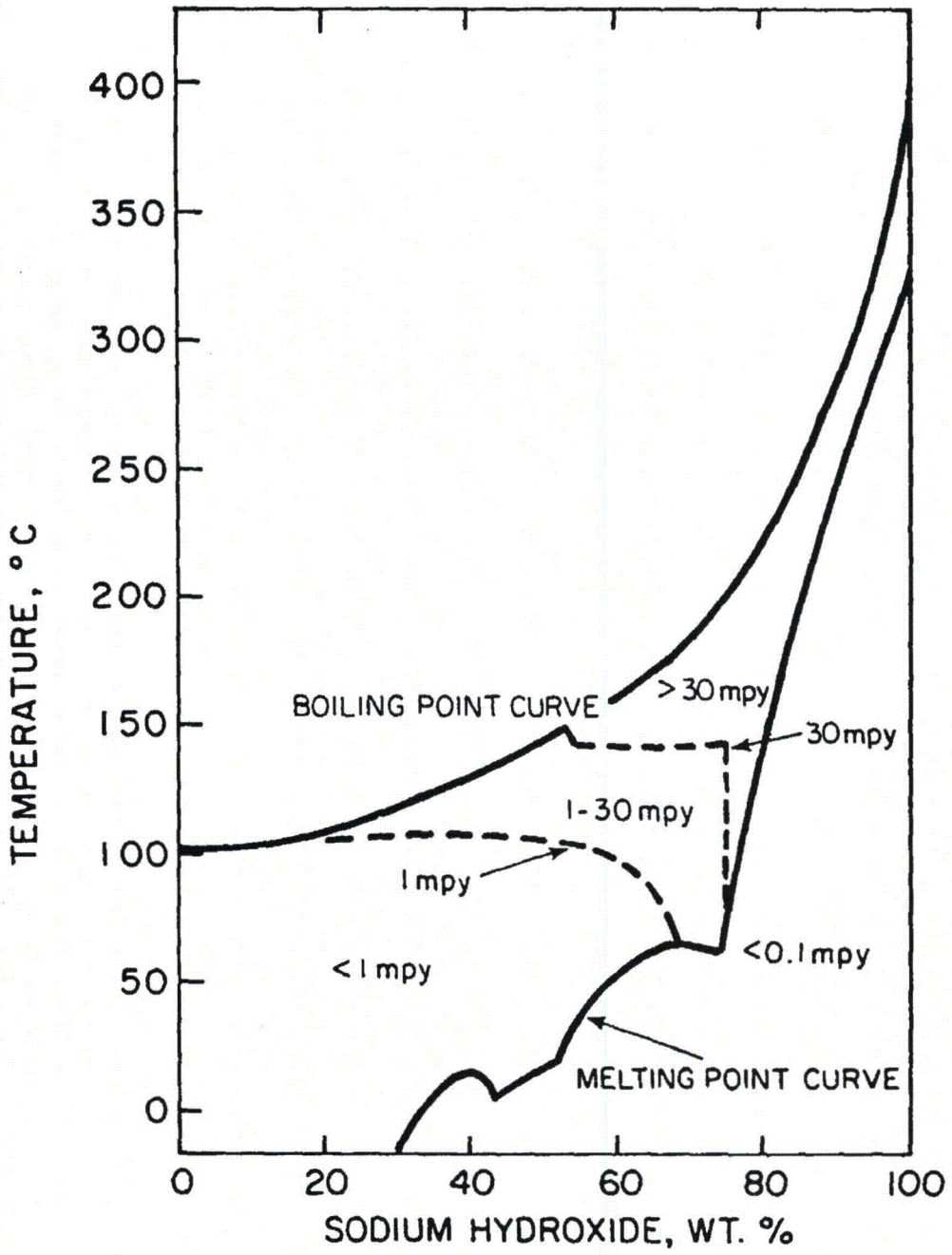

Figure 37. Iso corrosion chart for type 304 and 316 stainless steels in sodium hydroxide [188]

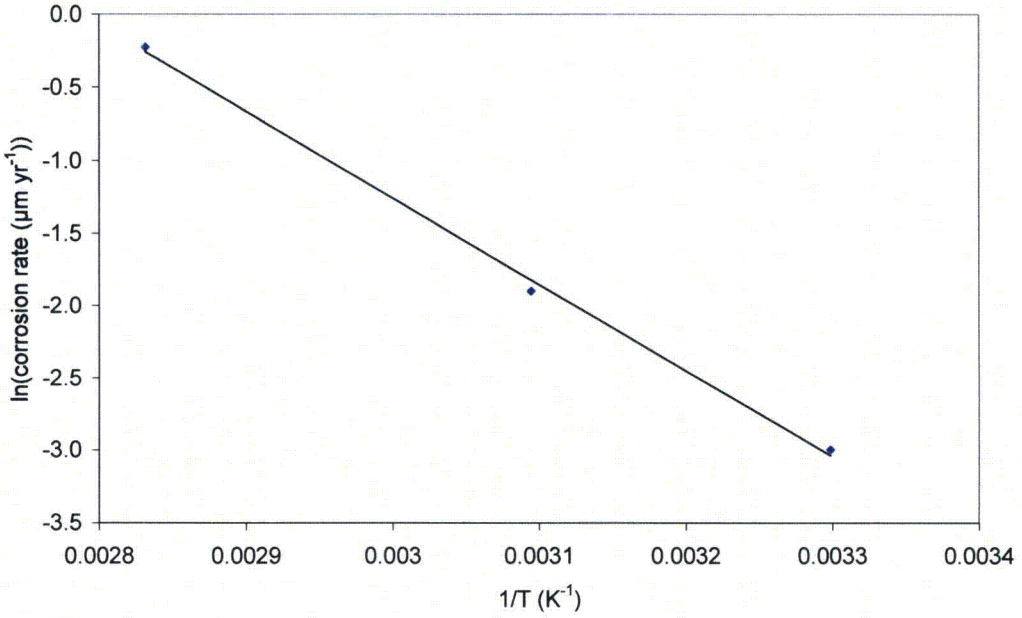

Figure 38. Fit of passive current measurements for stainless steel in simulated porewater [85] to an Arrhenius relationship